UiT The Arctic University of Norway

Faculty of Biosciences, Fisheries and Economics
Department of Arctic and Marine Biology

Melt season dynamics in a High Arctic estuarine tidal flat: A microbial perspective

Eleanor Ruth Handler

Master's thesis in Biology, BIO-3950, May 2022

Melt season dynamics in a High Arctic estuarine tidal flat: A microbial perspective

Eleanor Ruth Handler

Master's thesis in Arctic Marine Ecology and Resource Biology

Supervisors:

Amanda Poste[1,2]
Anna Vader[3]
Rolf Gradinger[1]
Maeve McGovern[1,2]

Associations
[1] Institute for Arctic and Marine Biology, UiT – The Arctic University of Norway, Tromsø, Norway
[2] Norwegian Institute of Water Research (NIVA), Oslo, Norway
[3] Department of Arctic Biology, The University Centre in Svalbard (UNIS), Svalbard, Norway

Indeed, by all standards, tidal flat ecologists appear somewhat backward: they have neither ship nor diving gear at their disposal, but walk out in rubber boots with a spade in one hand and a bucket in the other as if to collect potatoes; and when they come back from their field work, they are besmeared all over with the sticky mud and yet confess they love it.

– *Karsten Resie*, Tidal Flat Ecology

Acknowledgements

First and foremost, I would like to extend my gratitude to all of my supervisors for their support throughout this thesis. Thank you, Amanda, for giving me the opportunity to plan this project from the bottom up and for your endless enthusiasm about land-ocean interactions. I am immensely grateful to Maeve for all of the time and energy you have put into helping me become a better scientist. Thank you, Rolf, for being a voice of reason when the rest of us got carried away with unrealistic ideas. And I am so thankful for your guidance, Anna, especially in navigating the world of molecular biology.

A number of people provided crucial advice in the planning stages of this project for which I am so appreciative: Maria Jensen, Paul Renaud, Raymond Eilertsen, Josef Elster, Uta Brandt, Jan Marcin Węsławski, Tobias Vonnahme, and Sairah Malkin.

I am incredibly grateful for all of the UNIS folks who have helped me along the way. This project would not have been possible without the support of UNIS Logistics, not the least Audun Tholfsen who provided the kayak-catamaran idea. Thank you to all of the other boat drivers who tolerated my muddy sampling throughout the season: Charlotte Sandmo, Kåre Johansen, Marcos Porcires, and Mikko Syrjäsuo. Many people in the Biology Department have given me invaluable assistance: thank you especially to Stuart Thomson for all of your help around the lab and to Cheshtaa Chitkara for helping solve my many DNA-related problems. Thank you to Erwin Kers for handling many surprise issues with samples in Tromsø.

The massivest thanks are due to Sebastian Andersen. Thank you for letting me drag you into the mud (even if you would rather have kept your hands clean) and for curating the best lab playlist. There is no chance I could have done this without you.

I am so thankful for the comradery of the UNIS guest students. Thank you especially to Astrid Vikingstad, Floria Schalamon, Maria Dance, Ymke Lathouwers, Marjolein Gevers for delicious foods, endless moral support, and great adventures.

This project would not have been possible without funding from Svalbard Science Forum's Arctic Field Grant (RiS ID: 11595, PI E. Handler), the FramCenter Flagship "Fjord and Coast" grant (FreshFate; project number 132019, PI A. Poste), the Norwegian Research Council (TerrACE; project number: 268458, PI A. Poste), and the U.S.-Norway Fulbright Foundation.

And, of course, I must certainly thank my family for all their support for the past two years and the many before that.

Abstract

The substantial influx of freshwater to High Arctic coastal ecosystems influences nutrient, organic matter, and sediment dynamics, stratification, and light availability throughout the melt season. These changes shape pelagic microbial community composition and functioning, though little is known about impacts on nearshore benthic bacteria. Globally, mudflats are hotspots for biogeochemical cycling, and expected climate change driven increases in terrestrial runoff to coastal areas have highlighted a need to understand the influence these inputs from land might have on Arctic estuarine tidal flat bacteria. In this study, I investigated microbial community composition and function in an estuarine tidal flat through a full melt season, using a combined approach of metabarcoding and carbon-source utilization assays under different salinity treatments. I found that bacterial communities varied through both space and time, as environmental conditions shifted due to riverine inputs and local processes, with salinity as a key structuring gradient. Arctic freshwater bacteria demonstrated higher capacities for degrading a wider range of carbon substrates than Arctic marine microbial communities, indicating higher potential for degradation of complex terrestrially derived organic material in freshwater systems. Terrestrial and riverine taxa were transported with melt water and deposited in sediments, composing up to 60% of sequences in downstream communities. However, their unique functional capabilities appear to be inhibited by the high salinities found in subtidal mudflats, and the highest potential for utilization of terrestrially derived organic matter may be limited to areas where sediments are permeated by freshwater. With anticipated increases in riverine discharge and permafrost thaw in a warming Arctic, tidal flats will likely be more frequently inundated with freshwater and the resident bacteria will have increased access to bioavailable terrestrial organic matter, extending the region where terrestrial organic matter can be readily utilized by microbial communities further towards the sea.

Table of Contents

1 Introduction

1.1 High influence of freshwater on Arctic coastal ecosystems

The Arctic Ocean receives a substantial volume of riverine water (approximately 4,200 km^3) every summer (Haine et al. 2015). Freshwater's influence extends beyond the coastal domain, regulating circulation, sea ice formation, nutrient distributions, primary production, and more, with clear regional differences across the Arctic Ocean (Carmack et al. 2016; Solomon et al. 2021; Brown et al. 2020; Terhaar et al. 2021). Rivers act as links between terrestrial and marine systems, bridging the boundary between land and sea by contributing freshwater and terrestrial materials flushed from their catchments. In coastal systems, riverine inputs shape nutrient dynamics, organic matter availability, stratification, light availability, and temperature (Mann et al. 2016; Pavlov et al. 2019; Torskvik et al. 2019; McGovern et al. 2020). Sources of melt shift throughout the season, changing riverine biogeochemistry and the ways discharge impacts coastal systems (Nowak and Hodson 2015; Koziol et al. 2019; McGovern et al. 2020). Approximately 60% of this freshwater enters through the large Arctic rivers, (Grabs et al. 2000), and the strong influence these inputs have on the ecology of surrounding coastal areas is well documented (Macdonald and Yu 2006; Casper et al. 2015; Arashkevich et al. 2018; Pasternak et al. 2022). However, less is known about the seasonal impact of riverine inputs from small catchments, which dominate a large portion of the Arctic coastline, and contribute the other half of freshwater inputs (Kellogg et al. 2019; McGovern et al. 2020).

Riverine inputs carry with them variable quantities and qualities of terrestrially derived particulate and dissolved organic matter (Terr-OM) (Mann et al. 2016; O'Donnell et al. 2016; Kaiser et al. 2017; McGovern et al. 2020), that has traditionally been considered largely refractory (Kattner et al. 1999; Guay et al. 1999; Köhler et al. 2003; Jørgensen et al. 2015). However, recent work has identified that certain portions of this pool might be highly labile, including

that from glacial melt (Hood et al. 2009; Kellerman et al. 2021) and permafrost degradation (Vonk et al. 2013; Mann et al. 2015). Increasing glacial melt, permafrost thaw (Christiansen et al. 2005), and precipitation (Hanssen-Bauer et al. 2019; McCrystall et al. 2021) with climate change are expected to lead to higher riverine discharge (Peterson et al. 2002; McClelland et al. 2006; Haine et al. 2015; Hanssen-Bauer et al. 2019) and, potentially, a subsequent increase in influx of Terr-OM to coastal systems, although the potential future fluxes remain unclear (Parmentier et al. 2017).

Arctic rivers can carry a high volume of fine particular matter, originating from glacial erosion (Bogen and Bønsnes 2003; Overeem et al. 2017). Much of this particulate material often deposits very close to the shoreline (MacDonald 1998; Lisitzin 1999; Weslawski et al. 1999; Zajączkowski et al. 2010; Jong et al. 2020), including particulate organic matter, which can be largely permafrost derived in Arctic rivers (Guo et al. 2007; Schreiner et al. 2014; Wild et al. 2019). Dissolved organic matter can also be removed rapidly from the water column at the land-ocean interface (Kipp et al. 2020) — molecules flocculate to form aggregates or bind to inorganic sediments with salinity changes, with both processes increasing settling velocity (Sholkovitz 1976; Mulholland 1981; Meslard et al. 2018; Lasareva et al. 2019). Arctic coastal ecosystems can therefore be hotspots for burial and cycling of organic matter (Bianchi et al. 2020). With low wave action, high rates of particle deposition can create a river delta with a tidal flat (Klein 1985).

Mud flats are common coastal features across the High Arctic, where environmental limitations on vegetation growth often prevent tidal marshes from establishing (Church and Ryder 1972; Martini et al. 2019). These Arctic estuarine tidal flats house a range of invertebrate macrofauna (Weslawski et al. 1999; Churchwell et al. 2016; Churchwell et al. 2018; Martini et al. 2019) and can be important feeding grounds for migratory shorebirds (Smith and Connors 1993; Taylor et al. 2010; Brown et al. 2012; Varpe and Bårdsen 2014; Churchwell et al. 2018).

Yet Arctic nearshore environments, shaped by riverine inputs, remain understudied, both due to the traditional divisions between terrestrial and marine science and the logistical difficulties of accessing these shallow regions (Brown et al. 2011; Jong et al. 2020; Klein et al. 2021).

1.2 Estuarine tidal flats are globally important for biogeochemical cycling

Globally, tidal flats are among the most highly productive (Heip et al. 1995; Underwood and Kromkamp 1999) and widespread of coastal ecosystems (Wang et al. 2002), covering over 125,000 km^2 (Murray et al. 2019). At the interface between land and sea, their sediments often contain a combination of Terr-OM (transported through rivers), marine detritus, and organic matter (OM) from *in-situ* biological processes (Wang et al. 2002; Volkman et al., 2000; Cole et al. 2007). Microphytobenthos on the sediment surface can contribute high rates of primary

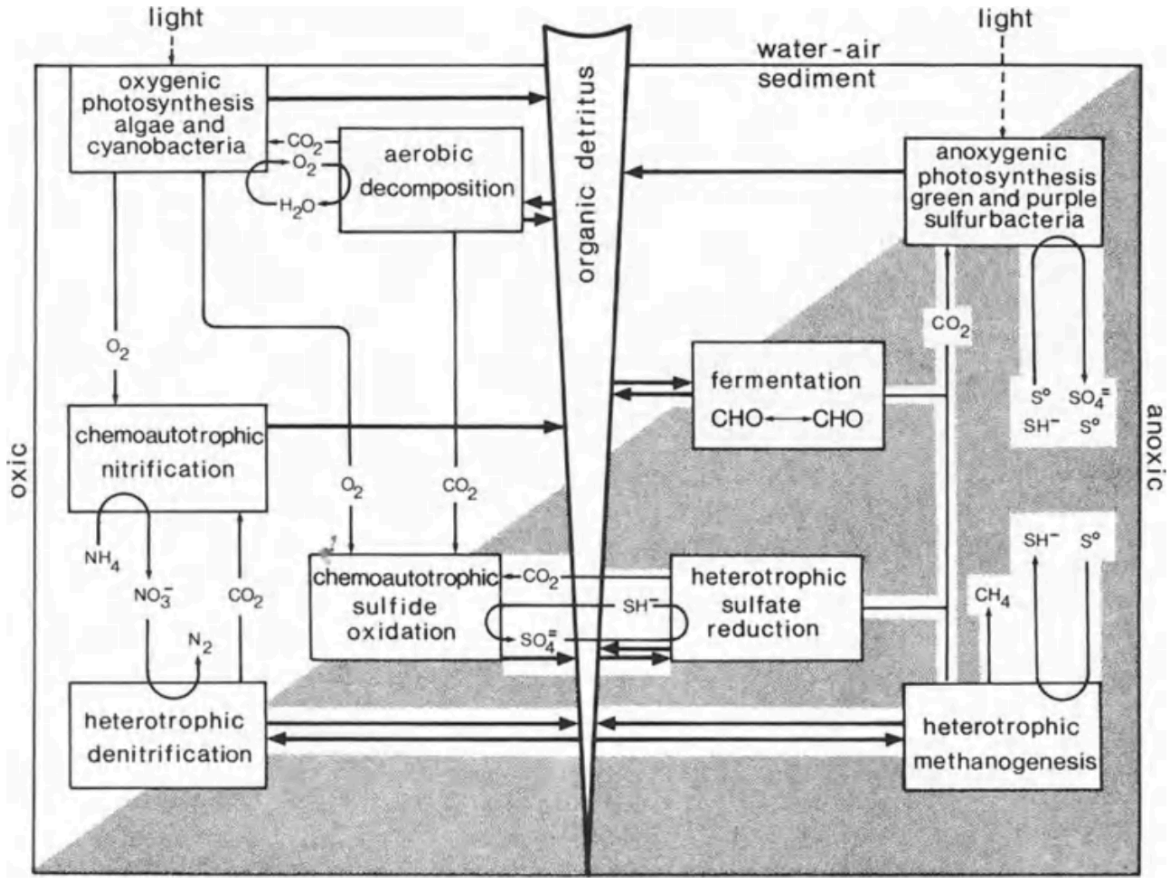

Figure 1. Diagram displaying biogeochemical processes in mudflat sediments (Reise, 1985). The dark shading denotes anaerobic processes, while the white region shows aerobic processes. The vertical wedge shows the influx of dissolved and particulate matter from above. Some microbes can exhibit different trophic modes under different conditions, contributing to multiple biogeochemical processes depending on their environment.

production to mudflats as well (Underwood and Kromkamp 1999; Paterson et al. 2003; Underwood et al. 2005; Billerbeck, 2007).

With this high input of OM and strong biogeochemical gradients in the tidally influenced sediments, tidal flats play a key role in global biogeochemical cycling, including cycling of carbon, nitrogen, and sulfur (Figure 1) (Alongi, 1998; Epstein, 1997; Jassby et al., 2002). For example, denitrification in estuarine tidal flats has been shown to reduce nitrate loading from rivers to coastal oceans (Trimmer et al., 1998; Ogilvie et al., 1997; Cabrita and Brotas, 2000). Furthermore, mineralization of OM deposited in sediments can release key nutrients for primary producers to the water column (Zou et al. 2016; Mayor et al. 2018; Mougi 2020), along with climate-active gasses, like carbon dioxide, methane, and nitrous oxide, at significant quantities for global climate budgets (Bange et al. 1994; Frankignoulle et al. 1998; Mosier et al. 1998; Mayor et al. 2018).

Bacteria are the main actors in sediment biogeochemical processes in estuarine tidal flats. They play an important role in shaping the overall ecology, with effects cascading up trophic levels — they can, for example, consume a large fraction of the available OM, in turn becoming food for protists or microfauna (Warwick et al. 1979; Kuipers et al. 1981; Schutte et al. 2019).

1.3 Environmental conditions shape sediment bacterial communities

Bacterial communities are structured by environmental conditions, especially by biogeochemical gradients (Baas-Becking, 1934; Allison and Martiny, 2008; Gilbert et al., 2012; Shade et al., 2012; Fierer 2017), and these different communities can strongly impact functional capacity (Strickland et al. 2009; Fierer et al. 2012). For example, certain taxa are more involved with the degradation of specific types of organic molecules: α-Proteobacteria are associated with consumption of amino acids, while the *Cytophaga-Flavobacterium* group is more associated with chitin, *N*-acetylglucosamine, and proteins (Cottrell and Kirchman 2000).

In tidal flat sediments, environmental gradients are both vertical, through sediment depth, and horizontal, across the surface sediments. Microbial communities show strong patterns with sediment depth, impacting functional capacity (Köpke et al. 2005; Wilms et al. 2006; Böer et al. 2009). For example, aerobic heterotrophs are responsible for high rates of OM degradation in the upper oxic zone of the sediments (Schutte et al. 2019), while denitrifiers tend to degrade matter more slowly in deeper low oxygen environments (Reise 1985).

Estuarine tidal flats can be divided laterally into three main regions with distinct environmental conditions that shape their ecology: supratidal, intertidal, and subtidal (Reineck and Singh 1973). Recent work has found that salinity differences along this tidal gradient can be an important factor for structuring microbial communities (Lv et al. 2016; Zhang et al. 2017; Zhao et al. 2019; Li et al. 2021; Niu et al. 2022), and associated grain size gradients are often correlated with bacterial abundances (Dale 1974; Schroder and Van Es 1980). Community composition can also be affected by nitrogen loading (Yan et al. 2018; Li et al. 2021; Niu et al. 2022), sulfate concentration (Zhang et al. 2017), pH (Mohapatra et al. 2021), and phosphorous concentration (Mohapatra et al. 2021). In temperate regions, changes in environmental conditions that restructure microbial communities are often connected with seasonality, including salinity (Wang et al. 2021), nitrogen availability (Guo et al. 2021), and temperature (Lv et al. 2016; Cheung et al. 2018), though shifts in community composition are not always linked to seasonality (Li et al. 2019). However, longitudinal patterns in tidal flat sediment microbial communities are generally less well understood than vertical gradients. A better understanding of the environmental factors that drive surface sediment communities, where most degradation of organic molecules occurs (Kristensen et al. 1995, Holmer 1999), is key for improving our knowledge of processes in estuarine tidal flats.

Recent research has found that the environmental impact of terrestrial inputs can shape coastal Arctic microbial communities. Community composition responds to physicochemical

changes in the water column (Han et al. 2015; Marquardt et al. 2016; Underwood et al. 2019; Thomas et al. 2020; Delpech et al. 2021) or to shifts in OM availability (Sipler et al. 2017; Paulsen et al. 2017; Müller et al. 2018c, Kellogg et al. 2019). Similar effects have been found in Arctic lake sediments, where increases in terrestrial runoff have been connected to decreases in microbial diversity and functionality (Colby et al. 2020). Furthermore, Arctic rivers can deliver allochthonous terrestrial or freshwater microbial taxa into coastal environments (Hauptmann et al. 2016; Paulsen et al. 2017; Morency et al. 2022). However, these studies have largely focused on pelagic or lacustrine environments, leaving terrestrial impacts on nearshore benthic microbial communities, which likely receive high inputs through sedimentation, an open question. Despite their importance, current understanding of the microbial communities in Arctic estuarine tidal flats and their role in biogeochemical processes is limited.

1.4 Project aims

I studied the influence of riverine inputs on surface sediment microbial communities in an Arctic estuarine tidal flat, in Adventfjorden, Svalbard from May to September. The main aim of this study was to identify how terrestrial runoff influences the structure and function of Arctic mudflat microbial community throughout the melt season. To investigate microbial community composition, I used high-throughput sequencing of the 16S rRNA gene. Functional potential was addressed through two avenues: metabolic pathway prediction from taxonomic assignment and carbon-source substrate utilization experiments. I hypothesized that riverine inputs would shape microbial communities and their functionalities either directly through delivery of riverine taxa or indirectly through changes in downstream environmental conditions. To my knowledge this study presents the highest seasonal and spatial resolution data on microbial communities in a High-Arctic estuarine mudflat.

2 Materials and Methods

2.1 Study Area

Samples were collected from May to September during the 2021 melt season in the Adventdalen and Adventfjorden system. Adventfjorden is an inner arm of the Isfjorden complex on the West coast of Spitsbergen, Svalbard. The fjord is heavily influenced by the Adventelva river and other smaller rivers throughout the melt season (Klein et al. 2021, Nowak et al. 2021, Wesławski et al. 2011, Zajaczkowski and Włodarska-Kowalczuk 2007). The braided Adventelva river is one of the largest rivers in Spitsbergen, with approximately 18% of its catchment area covered by glaciers (Ziaja 2005). A large tidal flat extends from the mouth of the river to the fjord, covering approximately 2.5 km^2, and shaped by shallow river branches. Just beyond the delta rim, the depth of the fjord rapidly increases to about 40m. Adventelva carries high sediment loads to the tidal flat and fjord, resulting in sedimentation rates in July from 10 g m^{-2} d^{-1} near the mouth to 1000 g m^{-2} d^{-1} just beyond the edge of the tidal flat, where river water slows as it enters the fjord (Weslawski 1999, Zajaczkowski and Włodarska-Kowalczuk 2007). Riverine inputs influence this estuarine ecosystem, from microbial communities in the pelagic (Delpech et al. 2021) to amphipods in the tidal flats (Skogsberg et al. 2022), though to my knowledge no studies have yet explored the bacterial communities of the tidal flats. Typically, Adventelva melts and begins flowing in late May to early June, and the river begins to freeze again in late September to early October (Nowak et al. 2021).

2.2 Sample Site Selection

To investigate the impact of riverine inputs on sediment microbial communities, four distinctly different sampling areas were established along a gradient from river to fjord in Adventelva and Adventfjorden: river, intertidal delta, subtidal delta, and inner fjord (Figure 2). The two delta stations were chosen to explore variation within the large tidal flat – one intertidal station where the sediments are exposed at low tides, exposing organisms to high variability in their physical environment, and one subtidal station where the environment was more stable but still susceptible to high influence from riverine inputs. The intertidal station was placed in an area that experiences pronounced tidal variation, based on personal communication with M.

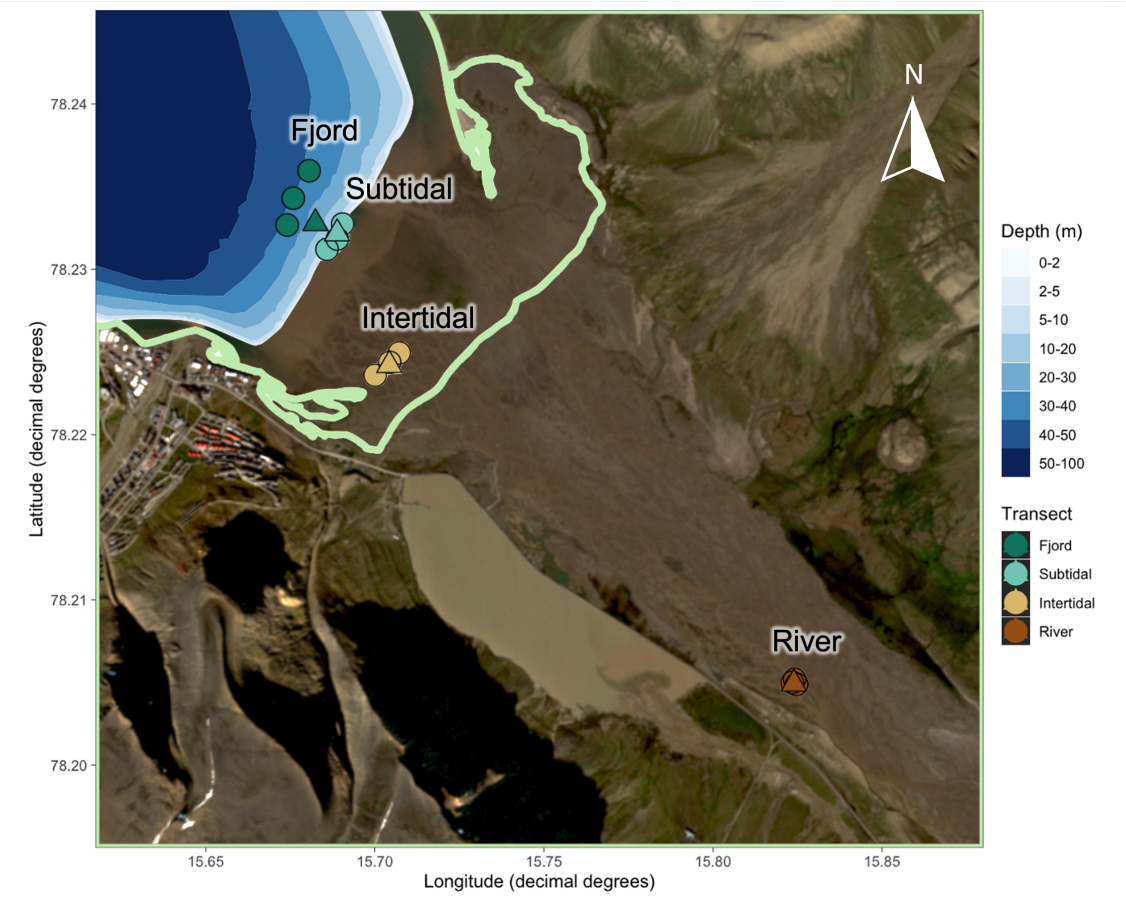

Figure 2. Map of target sampling sites within each station throughout the season. Green line demarcates medium high tide level (Norwegian Mapping Authority). Satellite image from August 14, 2021 retrieved from Sentinel EO Browser. The intertidal station was placed in a region with pronounced tidal variation based on personal communication with M. Jensen (2021). Circles denote sediment sampling stations while triangles denote adjacent water samples. High frequency *in-situ* NIVA operated sensors were located approximately 100 m upstream from the river station and 200 m towards shore from the fjord station. Exact coordinates for each month varied slightly, see Figure A1 and Table A1.

Jensen (2021), who has worked extensively on sediment transport in the region. The subtidal station was placed near the delta rim, where the water was less than 2 m deep at low tide (personal communication, M. Jensen and R. Eilertsen, 2021). The fjord station was placed approximately 200 m offshore from the bottom of a steep submerged slope, to avoid turbidity currents that cause high disturbance along the slope (personal communication, R. Eilertsen, 2021). The two endpoints (river and inner fjord) were located near NIVA-operated seasonally deployed *in-situ* sensor-based moorings. At the river station, sensors monitored conductivity, pH, temperature, turbidity, and water level, and in the inner fjord, the same variables were measured with the addition of chlorophyll-*a* fluorescence and dissolved oxygen (personal communication, A. Poste/NIVA).

Within each sampling region, I collected surface sediment samples and porewater from three sites (Figure 2). In the heterogeneous braided river and intertidal delta, sampling sites were chosen based on multiple criteria: "island" edges adjacent to river channels, fine grain size, and accessibility. With these requirements, I aimed to sample areas influenced by the river, but with higher stability and finer sediments than could be found in river channels. Fine sediments were targeted to maintain comparability with fjord and subtidal stations, where the sediments were very fine. As submerged channels continued to the subtidal region, I placed sampling sites along ridges for the subtidal station as well. In the inner fjord, sites were located in proximity to the *in-situ* sensor, near the center of the fjord.

2.3 Field Sampling

Samples were collected using three approaches to access sampling sites: walking (river stations), kayak-catamaran (intertidal stations), and small Polarcirkel research vessel (subtidal and fjord stations) (Figure 3). Samples were collected monthly from May 7, 2021 to September 14, 2021 (Table A1) — however, only the intertidal and fjord stations were sampled in May. I

sampled the intertidal station near low tide as the tide was rising, so that channels and islands were visible and sampling sites accessible with kayak catamaran to decrease the risk of getting stuck in the tidal flat. Subtidal samples were also collected during rising tide to prevent the Polarcirkel from becoming grounded.

2.3.1 River and Intertidal sampling

At river and intertidal sites, I used a 0.25 m^2 PVC frame to demarcate the sampling region (Figure 3). Sediment temperature was measured with an analog thermometer and general conditions (including cloud cover, overlying water depth, and wind speed and direction) were recorded. For all campaigns aside from May, a pre-bleached (0.5% NaOCl, 20 minutes) standard plastic spoon (15 mL) was used to collect the top 1cm of sediments in a sterile Whirl-Pak plastic bag. In May, sediment samples were collected using pre-bleached cut-tip BD Plastipak 100mL syringes (Becton Dickinson Norway AS, Oslo, Norway). Approximately 100mL of sediment was collected from each site, and a new spoon (or syringe) was used for each site. Porewater was extracted from the top centimeter of sediments with a Rhizon CSS (Rhizosphere

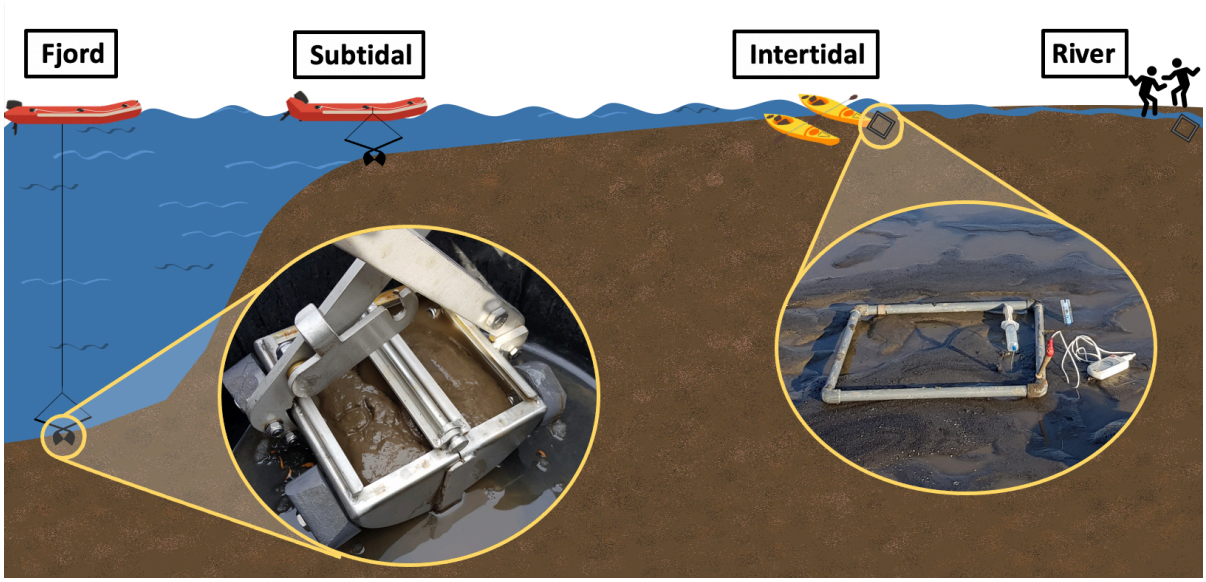

Figure 3. Diagram illustrating sampling collection. Two distinct approaches were used — sediment samples in the fjord and subtidal regions were collected from a Polarcirkel with a 0.025m^2 van Veen grab with two removable windows while intertidal and river sampling sites were marked with a PVC frame on the sediment surface.

Research, Wageningen, The Netherlands), with a new Rhizon used for each site. Approximately 30 to 100mL of porewater was collected from each station in a BD Plastipak 60mL acid washed (15% HCl by volume, 24 hours) plastic syringe (Becton Dickinson Norway AS, Oslo, Norway) and stored in acid-washed and burned (4.5h, 450ºC) brown glass bottles.

One adjacent water sample was collected from each station, using a clean plastic bucket to collect surface water. The sampled water was prefiltered using a 200µm mesh to remove large grazers. Water temperature was measured *in-situ* with an analog thermometer. Salinity, conductivity, and pH were measured either in the field or immediately upon return to UNIS using a multiparameter meter (HI 9829, Hanna Instruments, USA). The pH sensor was calibrated prior to every sampling campaign. All sediment and water samples were kept cool and dark until further processing at UNIS, within eight hours of collection.

2.3.2 Subtidal and Fjord sampling

At all replicate sites for the subtidal and fjord stations, I collected surface sediment samples using a 0.025 m^2 van Veen grab with two removable windows (Figure 3). The top 1 cm of sediments was collected through the windows on the grab. If sufficient sediment material was in the grab, one side was used for sediment collection while the other was used for porewater extraction. If the grab did not contain enough sediment, the first replicate was collected for sediments and a second grab was used for porewater extraction. To allow for longer porewater extraction with continued use of the grab, an intact portion of the top layer of sediments was transferred to an acid-washed plastic container. Sediments and porewater were collected and stored in the same manner as at river and intertidal stations and processed within eight hours.

Adjacent water samples were also collected — from the surface with a clean plastic bucket for the subtidal and from just above the seabed with a 7L Niskin bottle for the fjord — and processed the water in the same manner as above.

2.4 Sample processing

Utensils for splitting sediment samples were pre-bleached (0.5% NaOCl for 20 minutes) between sampling days. All bottles for water sample storage were acid washed prior to use (15% by volume HCl for at least 8 hours), and glass bottles were also pre-combusted to remove organic matter (450ºC for 4.5 hours).

The sediments in each Whirl-Pak were homogenized with a metal spoon, split with the spoon and a spatula into subsamples, and preserved for analyses. Both utensils were sprayed with ethanol and burned between each sample. For DNA extraction, 3 subsamples were frozen at -80ºC in sterile 2 mL cryo vials. For photopigment concentrations, one subsample was frozen at -80ºC. Pre-weighed bottles of known volume were filled with sediment and frozen at -20ºC for bulk density, porosity, grain size, and loss on ignition measurements. For one site from each station, subsamples were stored in the dark at 4ºC for Biolog EcoPlate™ inoculation.

As the nominal pore size of the Rhizon CSS is 0.18 μm, porewater was not additionally filtered upon return from the field. Subsamples, approximately 5-20 mL, for characterization of chromophoric dissolved organic matter (cDOM) in porewater were stored in acid-washed, pre-combusted glass bottles. Porewater samples for analysis of dissolved inorganic nutrient concentrations were preserved with 4N H_2SO_4 (1% final concentration by volume) and stored in acid-washed, pre-combusted glass bottles. Silicate concentrations were expected to be sufficiently high that potential contamination from storage in glass bottles would be negligible. All porewater samples were stored at 4ºC in the dark until analysis.

Adjacent water samples for analysis of dissolved inorganic nutrients (nitrate and nitrite, phosphate, silicate, and ammonia) were filtered through pre-combusted glass fiber filters (Whatman GF/F, nominal pore size 0.7 μm), preserved with 4N H_2SO_4 (1% by volume), and stored in 100 mL acid-washed HDPE bottles in the same manner as porewater. To determine concentration of suspended particulate matter (SPM) in the water column, water was filtered

through pre-combusted, pre-weighed 47 mm GF/F filters until coloration appeared on the filter, approximately 300 – 1500 mL depending on SPM concentration. Filters were stored at -20ºC in the dark prior to analysis.

2.5 Laboratory Analyses

2.5.1 Sediment characteristics

Porosity was calculated using a wet-dry method (Zaborska et al. 2008). Frozen bottles filled with sediments of known volume were thawed and weighed (A0204 DeltaRange, Mettler Toledo, Columbus, OH). Sediments were then dried in an oven (OMH 180, Thermo Scientific, Waltham, MA) at 60ºC for seven days, until all water had evaporated, and then were reweighed. Density of porewater was calculated based on temperature (5ºC as sediments were stored in a fridge prior to splitting) and salinity (see method below) according to the UNESCO International Equation of State of Seawater (UNESCO, 1980). Organic content of sediments was determined through loss on ignition (LOI). Pre-weighed dry sediments were burned at 450ºC in a muffle furnace (Nabertherm GmbH, Lilienthal, Germany) for five hours and reweighed (Morata et al. 2020). 450ºC was chosen to balance the need to limit release of carbonates and structural water in clays at higher temperatures with the need for temperatures high enough to oxidize recalcitrant OM (Sutherland 1998; Wang et al. 2011). Grain size distributions were determined by wet sieving through mesh sizes of 2 mm, 1 mm, 500 µm, 250 µm, 125 µm, and 63 µm (Bale and Kenny, 2005).

2.5.2 Pigment concentrations

Following extraction with acetone for 24 h, sediment chlorophyll-*a* (chl-*a*) and phaeopigment concentrations were measured fluorometrically. Fluorescence was measured with a Turner 10-AU fluorometer (Turner Designs, USA) calibrated with pure algal chl-*a* (Sigma-

Aldrich, Oslo, Norway). Samples were then acidified with 2-3 drops of 10% HCl, and fluorescence was read again. Chl-*a* and phaeopigment concentrations were calculated according to Parsons (1984).

2.5.3 cDOM

To characterize the chromophoric dissolved OM (cDOM) in porewater and adjacent water, absorbance was measured with 1 nm resolution from 200 to 900 nm with a Shimadzu UV-1900 UV-Vis spectrophotometer (Shimadzu Corporation, Tokyo, Japan). A 1 cm path-length quartz cuvette was used for most porewater samples because of low sample volumes and higher expected DOM content. Absorbance was measured four to seven days following sample collection, and absorbance values were blank corrected with MilliQ water. Absorbance spectra were processed according to McGovern et al. (2020) to calculate the absorbance coefficient at 254 nm (a proxy for DOM concentration), spectral slopes from 275-295 nm and 350-400 nm and the ratio between them (inverse proxies for molecular weight) (Hansen et al. 2016). The ratio between the absorbance coefficients at 250 and 365 nm (E2/E3) was also calculated for an additional inverse proxy for molecular weight (De Haan and De Boer 1987).

2.5.4 Physicochemical water characteristics

Remaining porewater from cDOM analysis was stored in acid-washed and burned sealed glass bottles for up to six months prior to salinity measurements. Due to low volumes, porewater salinity was measured using a salinity refractometer (Magnum Media Salinity 10ATC), calibrated with deionized water. Concentrations of inorganic nutrients in adjacent water samples and porewater samples were measured at the Norwegian Institute for Water Research (NIVA, Oslo, Norway) using inductively coupled plasma mass spectrometry (Kaste et al. 2022). Filters for SPM from adjacent water samples were dried in an oven (OMH 180, Thermo

Scientific, Waltham, MA) for a minimum of one hour at 105ºC (or until the mass had stabilized within 0.5 mg) and weighed (A0204 DeltaRange, Mettler Toledo, Columbus, OH). Filters were then burned in a muffle oven for one hour at 450ºC and reweighed to determine organic content through loss on ignition (Walch 2021).

2.5.5 Microbial Community Structure and Function

DNA Extraction and Sequencing

Microbial DNA was extracted from 0.4 to 1.6 g wet weight of sediment using the PowerSoil® DNA Isolation Kit (MO BIO Laboratories Inc., Carlsbad, CA USA) following kit instructions. Extraction blanks (MilliQ water) were included with each extraction batch. PCR tests using bacterial primers 515F (Parada et al. 2016) and 806R (Apprill et al. 2015) were performed following each extraction for quality control — amplification was never observed in extraction blanks. Library preparation, including PCR amplification, and sequencing (Illumina MiSeq 2x300 bp paired-end V3 chemistry) were performed by the Integrated Microbiome Resource (IMR, Dalhousie University in Halifax, Nova Scotia, Canada) using standard protocols (Comeau et al. 2017). Sequences in the V3-V4 region of the 16S rRNA gene were amplified using primers 341F (CCTACGGGNGGCWGCAG) and 805R (GACTACHVGGGTATCTAATCC) (Illumina / Klindworth 2012). 54 samples, three replicate sites from each station for the sampled months, and five extraction blanks were sequenced.

Biolog EcoPlates

Biolog EcoPlates™ (Biolog Inc., Hayward, CA) were used to assess potential microbial community functions (Garland and Mills 1991; Insam 1997). EcoPlates are 96-well microtiter plates that contain three replicates of 31 different carbon sources (Table A2), chosen to differentiate between community-level physiological profiles (Insam 1997), and three blank wells

with no substrate. All non-blank wells also contain a tetrazolium salt that turns purple with cellular respiration in the well, i.e., when bacteria metabolize the provided carbon substrate (Garland and Mills 1991). The intensity of color scales with the degree of respiration in the wells.

Following each sampling event from June through September, one replicate site sample from each station was used to inoculate plates within eight hours of sample collection (Table A3). Water for sediment suspensions was first filtered through 0.2 µm polycarbonate syringe filters to remove all organisms. I used two water sources: river water from Adventelva (collected during the main sampling campaign) and filtered seawater from Adventfjorden (taken from the UNIS lab sea water supply, with an intake pipe at approximately 30m depth). The filtered seawater was analyzed for dissolved inorganic nutrients in the same manner as for adjacent water samples[1]. To simulate brackish water, a 1:3 mix of seawater to river water was made. Through a two-step dilution process, 1.8 mL of sediment was diluted 1:272 with one of these water types (Table 1). Different water for suspensions was used for the same sediments to investigate microbial activity throughout the tidal cycle.

Each well was inoculated with 140 µL of sediment suspension and the absorbance of each well at 590 nm was recorded immediately with a Multiskan GO spectrophotometer (Thermo Fisher Scientific, USA). Inoculated plates were incubated in the dark at 10ºC in a Termaks cooling incubator (Nino Labinteriör AB, Kungsbacka, Sweden).

Table 1. Treatments for sediment suspensions used to inoculate plates for June through September samples.

Station	**Salinity of suspension water**		
	Fresh	*Brackish*	*Marine*
River	X		
Intertidal	X	X	X
Subtidal	X	X	X
Fjord			X

[1] The water collected from the seawater intake pipe at UNIS generally had higher nutrient concentrations than did deep fjord water and was consistent throughout the season (Figure A3). It had similar ammonium concentration as river water (medians 1.3 and 1.1 µmol L^{-1}), higher nitrate/nitrite (13.2, 8.0 µmol L^{-1}), higher phosphate (0.29, 0.06 µmol L^{-1}), and lower silicate (16, 61 µmol L^{-1}).

10ºC was chosen after initial testing to balance faster metabolic rates at higher temperatures with greater substrate usage at lower temperatures. The absorbance of each well at 590 nm was then recorded daily for 14 days to determine community substrate utilization.

In May, fjord and intertidal sediments were used to inoculate EcoPlates, each suspended with corresponding filtered adjacent water. Plates were incubated at 4ºC, and results from the fjord sediments plate were used for comparison, but not included in formal analysis. The intertidal plate was excluded due to high salinity adjacent water (Figure A2).

2.6 Data Processing and Analysis

All processing of DNA sequences and EcoPlate absorbances and statical analyses were performed within the R framework (v4.1.0, R Core Team), using RStudio (RStudio Team). The *tidyverse* package was used throughout processing and analyses (Wickham et al. 2019).

2.6.1 DNA Sequence Processing

I received demultiplexed sequences from IMR. Primers were first clipped using cutadapt (v3.7, Martin 2011), with a maximum error rate of 0.1. Sequences without primer sequences were discarded. Sequences were then processed with DADA2 (Callahan et al. 2016), using a pipeline modified after Pearman et al. (2021). Forward reads were truncated to 253 bp while reverse reads were truncated to 189 bp. The maximum numbers of "expected errors" allowed were two and five, accounting for differences in quality between the forward and reverse reads, respectively. Sequences with a quality score of 2 or less were discarded. Sequences were dereplicated for each sample and error rates for forward and reverse reads were learned with the first 10^8 bp. This parametric error matrix was used to infer amplicon sequence variants (ASVs) from the dereplicated reads, using the "pseudo-pool" option within DADA2 to reduce impact of different read numbers on diversity (Kleine Bardenhorst et al. 2022). Forward and

reverse reads were merged with a minimum overlap of 12 bp and no mismatches allowed. Chimeric sequences were removed with the *removeBimeraDenovo* DADA2 function using the "consensus" method.

Taxonomy of the resulting ASVs was assigned using the RDP Naive Bayesian Classifier algorithm (Wang et al. 2007) against the SILVA SSU nonredundant (v 138.1) reference database (Quast et al. 2013), with a minimum bootstrap of 70. ASVs classified as eukaryotes, chloroplasts, or mitochondria were removed, and the results were combined to form a *phyloseq* object (McMurdie and Holmes 2013), which was used for further processing. Contaminants were identified from sequencing of extraction blanks and removed from the dataset using the prevalence method in the *decontam* package (Davis et al. 2018). Only one contaminant was identified, and it was only found in three samples at very low abundances: June-Subtidal-x (0.01%), June-River-y (0.02%), and July-Fjord-z (0.02%). Finally, only ASVs with more than one sequence in more than two samples were kept, removing 3.7% of reads retained up to that step (Table A4). Samples with fewer than 3000 reads were not used for downstream analyses, removing one May intertidal sample and one July subtidal sample.

2.6.2 Biolog EcoPlate Data Processing

Absorbance values at 590 nm were adjusted for blanks and initial readings of each well according to Sofo and Ricciuti (2019). For each timepoint, the mean absorbance of the three blank wells was subtracted from all other wells on the same plate. Then, the first absorbance measurement for each well (already blank adjusted) was subtracted from the blank-adjusted absorbances for each timepoint to get the OD_i (optical development at time i). Negative OD_i values were set to 0. The area under the curve (AUTC) for each substrate on each plate was calculated using OD_i values. AUTC condenses several kinetic measures into one metric —it is highly correlated with lag times, rates of substrate use, and maximum OD values (Preston-

Mafham et al. 2002). It was calculated with the trapezoidal rule, using all readings of OD: $\text{AUTC} = \sum_{i=1}^{N} \frac{OD_i + OD_{i-1}}{t_i - t_{i-1}}$, where N is the number of absorbance readings and t is the time when absorbance was measured (Hackett and Griffiths 1997).

For each plate, I calculated four metrics to estimate diversity of substrate use: substrate richness, average well color development (AWCD), Shannon's diversity index, and Simpson's diversity index. With an OD_i greater than 0.250, wells were considered purple, i.e., the bacterial community was able to use that substrate (Garland 1996, Kenarova et al. 2014, Jałowiecki et al. 2016, Sofo and Ricciuti 2019). Furthermore, substrates were only considered utilized by the community if at least two of the three replicate wells on a plate turned purple. Substrate richness was measured as the number of substrates used on a plate at the final time point (day 14). AWCD provides a metric of the development of the plate. AWCD was calculated by taking the mean OD_i of all wells across each plate (excluding blanks) at the final time point. Shannon's and Simpson's diversity indices were calculated according to Zak et al. (1994).

2.6.3 Statistical Analysis

To investigate spatial and seasonal trends in environmental conditions across samples, principal component analysis (PCA) was performed on scaled environmental variables. All ordinations were made using the *vegan* package (Oksanen et al. 2020).

To evaluate alpha diversity, the community matrix rarefied to 4130, the lowest number of reads in any sample, using the packages *phyloseq* (McMurdie and Holmes 2013) and *microbiome* (Lahti et al. 2017-2020). Alpha diversity estimators (number of ASVs, Chao1 (Chao 1984), Abundance-based Coverage Estimator (ACE) (Chao and Lee 1992), Shannon's and Inverse Simpson's diversity indices and Pielou's evenness index) were calculated for each sample with rarefied, non-normalized, and standardized (proportions by sample multiplied by median read count) datasets using *phyloseq*.

Shared ASVs between stations were evaluated on the rarefied dataset, using the package *MicrobiotaProcess* (Xu and Yu 2021) and plotted with the package *VennDiagram* (Chen 2021). The proportion of riverine taxa in each non-river sample was found by first identifying all ASVs that had been found at relative abundance greater than 0.05% in any river sample. The relative abundance of those taxa was then calculated for all other samples.

For investigations of beta diversity between samples, community dataset was transformed to proportions and treated as compositional (Gloor et al. 2017). The community matrix was Chi-square transformed and Euclidean distances were calculated using the *vegan* package. Hierarchical cluster analysis was performed on the distance matrix, using Ward's (1963) clustering criterion. Other ordinations and hierarchical clustering based on non-normalized, standardized, rarefied, Hellinger transformed, and clr-transformed data using Bray-Curtis dissimilarity or Euclidean distances showed similar patterns.

Abundant genera in each cluster were identified by grouping ASVs by genus and calculating means of proportional abundances within each cluster. Indicator taxa for each cluster were determined with Dufrêne-Legendre Indicator Values, using the multipatt function of the *indicspecies* package (De Cáceres and Legendre 2009) with 999 permutations. Only ASVs with an indicator value > 0.7 and a p-value ≤ 0.001 were considered significant indicators. Indicator ASVs were considered highly abundant if they had a relative abundance of at least 0.5% within their cluster. The taxonomic composition of highly abundant indicators was examined.

To identify potential community functions from the taxonomic assignments, I used Tax4Fun (Aßhauer et al. 2015) to predict both KEGG Ortholog (KO) and KEGG metabolic pathway reference profiles. The KEGG pathway matrix was curated to remove functions irrelevant to bacterial communities and used in the same manner as the community dataset to explore differences between samples. Targeted functions were investigated with either the metabolic pathways or with KO genes or enzymes related to functions of interest (Table A5).

I used variance partitioning (Borcard et al. 1992) with testing by permutation (999) to quantify the contributions of station and month to variation in community composition. Canonical correspondence analysis (CCA) was used to examine the relationships between environmental variables and microbial community structure. Environmental variables were z-scaled and grouped by sediment characteristics, porewater chemistry, and indicators of OM quality (Table 2). Constraining variables within each group were selected using supervised forward and reverse model selection with the ordistep function in *vegan*. I chose to focus on large and small fractions for grain size, rather than the intermediates, and chl-*a* rather than phaeopigment concentrations. Selected variables from each group were then combined to a single model which was similarly evaluated. Significance of each variable was subsequently tested with a permutation test (n=999). Multicollinearity of variables, tested using vif.cca in the *vegan* package after ordination, showed low rates of collinearity in the final model. Spearman correlations of indicator taxa abundance with the same environmental variables were calculated with the function rcorr in the *Hmisc* package (Harrell 2021).

Table 2. Groupings of environmental variables. Bold variables were included in the final CCA.

Sediment characteristics	**Porewater chemistry**	**Indicators of OM quality**
Porosity	**Salinity**	**Chlorophyll-*a* concentration**
Grain size fractions:	Nitrate and nitrite	Phaeopigment concentration
<63 µm	Phosphate	**Percent phaeopigments**
63-125 µm	Silicate	**cDOM abs coefficient 254**
125-250 µm	Ammonium	cDOM E2 / E3
>250 µm		**cDOM slope 350-400**
LOI percent		cDOM slope 275-295
		cDOM slope ratio

PCA, created and plotted with *PCAtools* (Blighe and Lun 2021), based on mean AUTC for each substrate on the Biolog EcoPlates was used to investigate similarities in community-level physiological profiles between stations, months, and suspension water. Variance partitioning with *vegan* was performed to evaluate the role of suspension water as opposed to sediment sampling location.

Plots were created with the *ggplot2* package (Wickham 2016). Maps were made with the *PlotSvalbard* package (Vihtarki 2020). Due to low sample size, to test for differences between groups, for diversity metrics, proportions of riverine taxa in other samples, environmental variables, and EcoPlate results, I used the Kruskal-Wallis rank sum test (Kruskal and Wallis 1952) with Dunn's post-hoc test (Dunn 1964), with p-values corrected using the Benjamini and Hochberg (1995) method.

3 Results

3.1 Seasonal dynamics

Data from the NIVA operated *in-situ* inner fjord and river sensors (unpublished data provided by A. Poste/NIVA) were used to provide high-frequency seasonal context but were not included in formal analysis in the current study (Figure A4B and C).

During the May field sampling campaign, Adventelva remained completely frozen. High chl-a content throughout Adventfjorden (Andersen in press), indicated the presence of a spring phytoplankton bloom. Adjacent water collected from a channel in the intertidal flat at low tide had very high salinity (38.7 PSU, Figure A2), suggesting it may have originated through brine drainage from the ice foot.

Ice covering Adventelva and the upper tidal flat melted and the river began to open on May 30, fully flowing by June 1 (Andersen in press). Throughout the melt season, river water was characterized by high concentrations of suspended particulate matter (SPM) (median 219 mg L^{-1}), low salinity (0.1 PSU), and high concentrations of silicate and nitrate/nitrite (61 and 8 µmol L^{-1}) (Figures A2, A3). Pulses of high river flow with high turbidity were detected by the in-situ sensor in the river, predominantly in July and August (Figure A4B). Throughout the melt season, surface water from the intertidal and subtidal was generally very similar to river water. A sediment plume or freshwater lens was detected in the surface of the inner fjord from June through August (Andersen in press). Though this lens was often quite shallow (<1 m), it occasionally extended deeper in the inner fjord, and low salinities were detected by the *in-situ* inner fjord sensor at 2 m depth throughout the first two weeks of July, along with a spike in chlorophyll fluorescence (Figure A4C). After a series of cold days prior to the September campaign (Figure A4A), water level and SPM concentration in the river substantially decreased (15 mg/L). Following a warm period in late September, the river refroze in early October.

3.2 Environmental context

In general, biogeochemical characteristics of sediments and porewater suggested similarities between the river and the intertidal stations and the fjord and subtidal stations (Figure 4). All variables measured varied between stations and across months, though they exhibited different trends. Measured sediment temperatures ranged from 0.5 to 8.6 ºC, with fjord sediments consistently coldest and July and August as the warmest months. While oxygen concentration was not explicitly measured, I neither saw nor smelled evidence of anoxic conditions in any of the sampled surface sediments.

Sediments were generally finer in the fjord and subtidal and coarser in the river and intertidal (Figure A5). The silt and clay percentage of sediment by dry weight generally increased

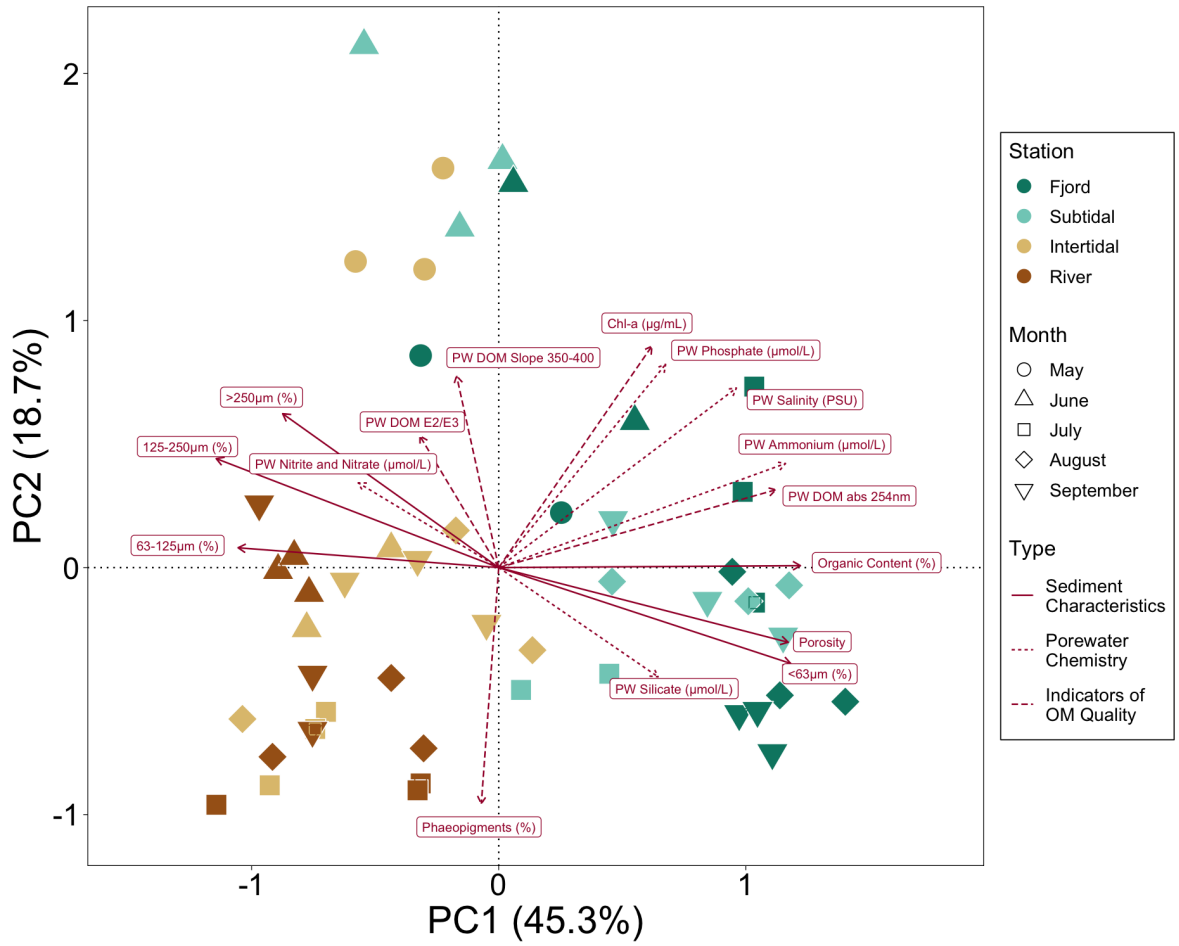

Figure 4. Principal component analysis on z-scaled environmental data. Highly skewed variables (chl-*a* concentration, inorganic nutrient concentrations, and sediment grain size fractions 125-250µm and >250µm) were natural log-transformed prior to z-scaling to increase normality. Each point is one sample. Colors represent station and shape shows month. Different line types on loading arrows display groupings of environmental variables.

throughout the melt season in the fjord (median June 71% - September 98%), subtidal (46-95%), and intertidal (31-61%) while in the river it increased until August (46-69%) and then decreased sharply in September (36%). Organic content and porosity both followed similar patterns as the proportion of silt and clay (Figure A6), and the two were highly correlated with one another (Spearman's rho = 0.73, $p<0.001$). Porosity ranged from 41% (intertidal in May) to 77% (fjord in August), while organic content values ranged from 0.7% to 6.8%.

Porewater chemistry showed further distinctions among stations and months. Porewater salinity was near 0 PSU in the river throughout the season and the intertidal from June and July (median 1.5 PSU). In May, intertidal porewater salinity was hypersaline (44.5 PSU), while it was brackish in August and September (6.5 PSU). Subtidal and fjord porewater salinity was 'marine' (37.5 PSU), except in July when the median subtidal porewater salinity was 19.5 PSU. The concentrations of most inorganic nutrients in porewater did not show pronounced seasonal variation (Figure A3). Phosphate and ammonium concentrations followed similar patterns as porewater salinity, respectively ranging from medians of 0.1 μmol L^{-1} and 1 μmol L^{-1} in the river to 0.4 μmol L^{-1} and 71 μmol L^{-1} in the fjord. Concentrations of both were generally higher in porewater than in corresponding adjacent water. Porewater nitrate concentrations ranged widely (0.07 μmol L^{-1} to 38.9 μmol L^{-1}) and did not show clear seasonal nor spatial patterns. In all stations but the fjord, adjacent water generally had higher nitrate concentrations than did porewater. Across all samples, silicate concentrations in porewater were similar to silicate concentrations in river water (medians 60 and 61 μmol L^{-1}). As silicate concentrations in subtidal and fjord adjacent water samples were much lower (16 and 2 μmol L^{-1}) (Figure A3), porewater generally had higher silicate concentrations than did adjacent water in these regions.

Indicators of OM quality showed strong seasonal and spatial patterns. Chl-*a* concentrations ranged widely (0.035 – 15 μg mL^{-1}), with generally higher proportions of phaeopigments in sediments with lower chl-*a* concentrations (Figure A7A and B). Chl-*a* concentrations were

consistently lowest and phaeopigment proportions high in the river (medians 1.3 µg mL^{-1} and 60%), while they varied seasonally in other stations. The highest chl-*a* concentrations were found in fjord sediments in June and July (5.6 µg mL^{-1}), with fairly low ratios of phaeopigments (28%). cDOM absorbance coefficients at 254 nm were high in the fjord (11) and low in the river and intertidal (3 and 5), with more seasonal variation in the subtidal (Figure A7C). The subtidal shifted from low values in June and July (5) to higher values in August and September (13). E2/E3 ratios of cDOM absorption were high in May (9.2), both in the fjord and intertidal. Throughout the melt-season, E2/E3 ratios were generally highest in the subtidal (9.4), with lower values from the river (7.2), intertidal (5.3), to fjord (3.6). cDOM absorption slopes from 275 to 295 nm and 350 to 400 nm followed the same pattern as E2/E3 ratios.

3.3 Community Composition

3.3.1 Alpha diversity

Following processing of sequences and reads, including removal of singletons, a total of 7,131 ASVs (amplicon sequence variants) were identified across all samples. Bacterial diversity varied somewhat between stations. Estimated richness (Chao1) was higher in fjord and subtidal sediments than in river and intertidal sediments (Figure 5, Kruskal-Wallis test (KW): $p = 0.047$). However, observed richness (number of ASVs), evenness, and Shannon's diversity index were not significantly different between stations, (Figure 5, KW: $p = 0.48$, 0.84, 0.84). With all stations considered together, no patterns appear across months, however within stations, some seasonal patterns exist, especially low diversity in the fjord in June. Similar patterns for richness (observed, Chao1, and ACE), diversity (Shannon's and Inverse Simpson's), and evenness (Pielou's) metrics were found when they were calculated with the rarefied, non-normalized, and standardized datasets (Figure A8).

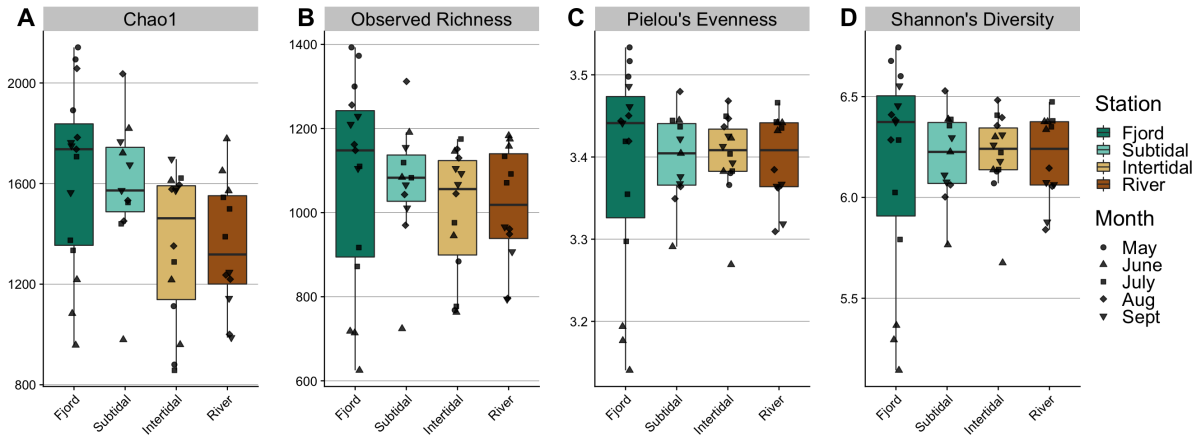

Figure 5. Boxplots displaying alpha diversity metrics for the four stations and five sampling campaigns. Individual samples are shown with black points, where shape denotes sampling month. All indices were computed on the rarefied dataset to remove bias from differing reads per sample. Richness was calculated as **(A)** Chao1, **(B)** observed richness (number of prokaryotic ASVs), **(C)** Pielou's evenness index, and **(D)** Shannon's diversity index. ACE followed similar patterns for richness, and Inverse Simpson's followed the same trends as Shannon's (Figure A8). Only Chao1 showed statistically significant differences between stations (KW: p=0.047).

3.3.2 Taxonomic composition

Gammaproteobacteria was the most represented class in all stations with mean relative read abundance across all samples 40±6% (Figure 6). Fjord, subtidal, and intertidal communities were also dominated by Bacteroidia (means 30, 29, and 17% respectively), though these were much less prominent in riverine sediments (8%). Desulfuromonadia displayed a similar pattern (7, 7, 4 and 0.7%), while Alphaproteobacteria had a similar read abundance of 8±3% across all samples. Both Actinobacteria and KD4-96 (a clade within Chloroflexi) had higher read abundances in the river and intertidal than the subtidal and fjord (1.1 vs. 6.5% and 0.4 vs. 3%, respectively). In general, I found strong similarities between communities within the three replicates collected at each station, each month.

Across the whole season, the fjord had the highest number of unique ASVs (1312) (Figure A9). The subtidal had the least with 249, and the intertidal and river had 432 and 468 unique ASVs respectively. 2473 ASVs were found in at least three of the stations, and 83% of the 2733 riverine ASVs were also found in other stations, especially in the intertidal (71%) as compared with the subtidal (58%) and fjord (43%).

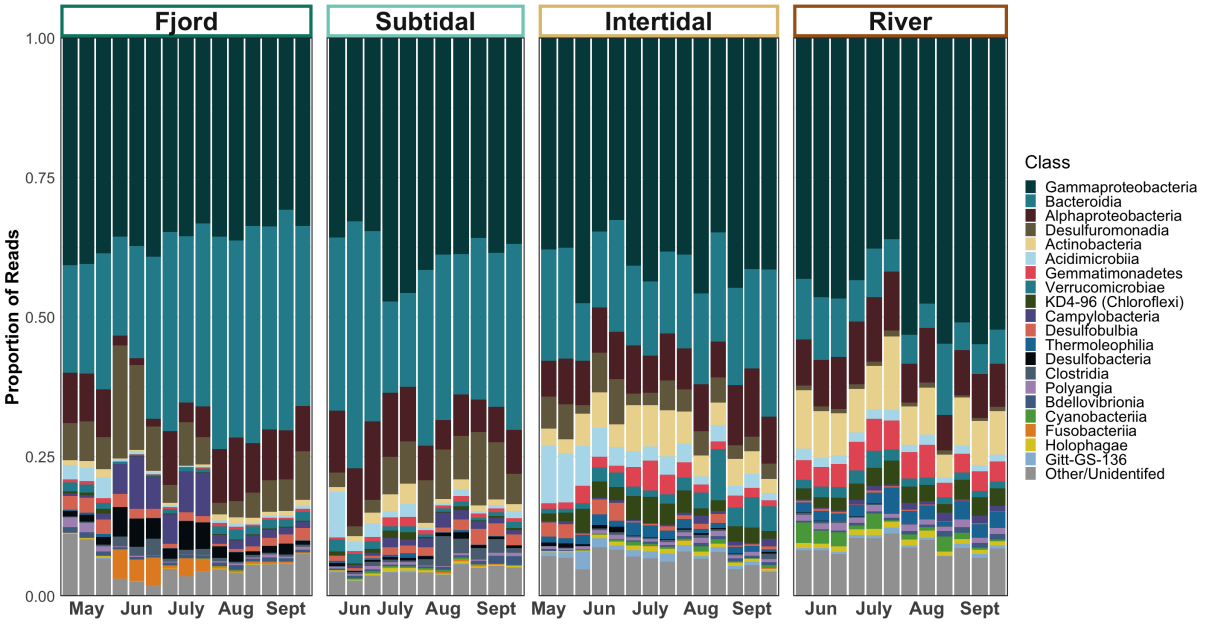

Figure 6. Stacked barplot displaying proportions of reads within the most represented bacterial classes. The top 20 most represented are displayed here, ordered by their overall proportional abundance across all samples. Samples are separated by sampling station and ordered by month within each station.

3.3.3 Seasonal and Spatial Variation in Bacterial Community Structure

Microbial community composition in sediments was significantly correlated with both station and sampling month, based on permutation tests ($p = 0.001$). Results of variance partitioning on canonical-correspondence analysis (Figure A10) showed that station individually accounted for 26% of community variation and month individually accounted for 12%, with no variation explained by both factors (all proportions were significant at $p=0.001$).

Results of hierarchical clustering on community composition showed two distinct groups, separating marine and freshwater communities (Figure 7A). Low porewater salinity and cDOM absorbance at 254 nm distinguished freshwater from marine conditions (Figure 7B, Dunn's post-hoc test (D): $p < 0.01$). These groups were further divided into five clusters, which were named based on physical and temporal characteristics of their environments: *Riverine, Melt-Influenced, Pre-Melt, Late-Marine,* and *Post-Bloom.* The two clusters within the freshwater group, *Riverine* and *Melt-Influenced*, were further characterized by coarse, compacted sediments with relatively low values for porosity, sediment organic content, and ammonium and

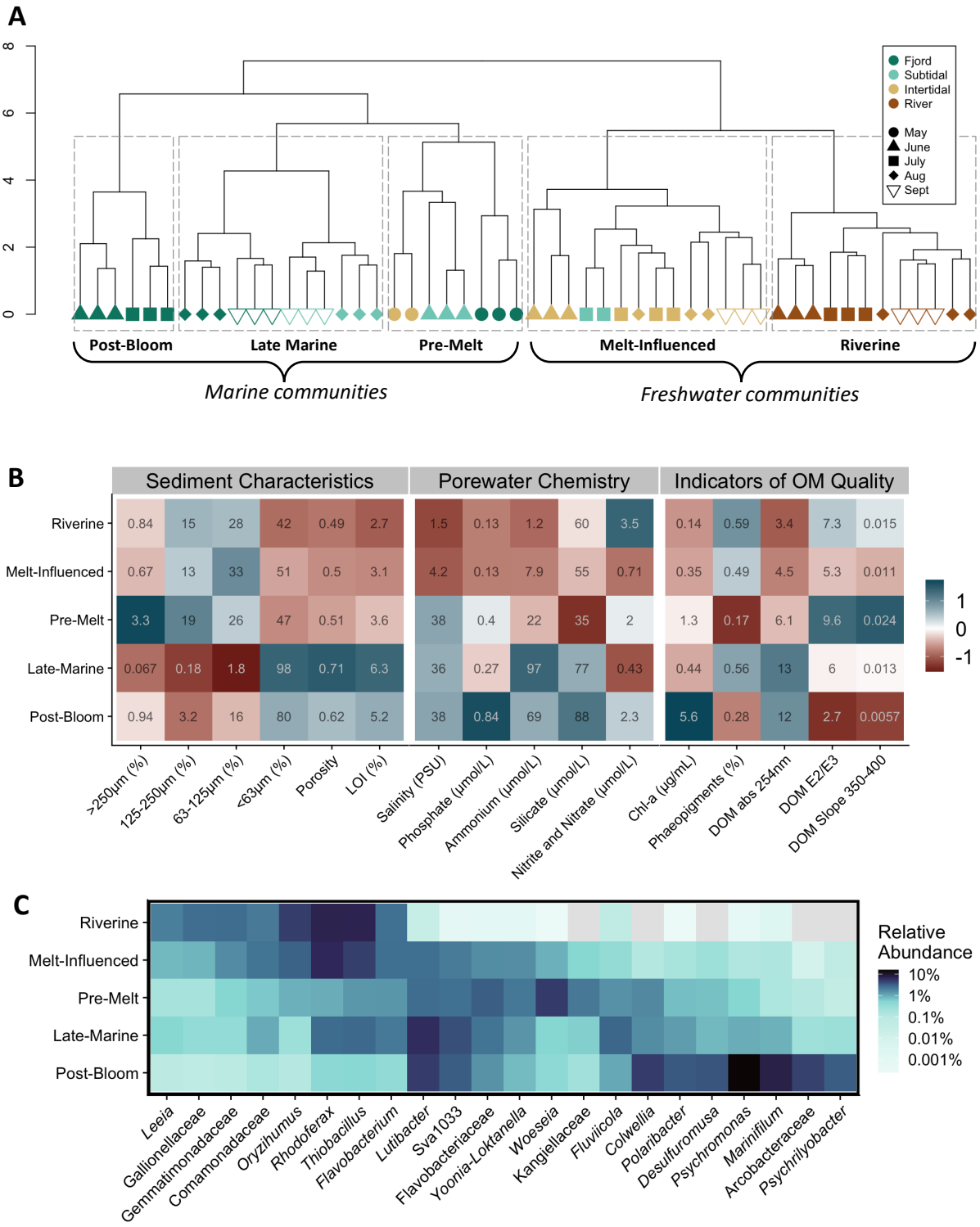

Figure 7. (A) Hierarchical clustering of microbial communities, using Ward's clustering criterion on chi-squared distances between samples. **(B)** Heatmap displaying medians of z-scaled environmental variables for each cluster. Text within fields show unscaled medians. Blue indicates relatively high values while red indicates relatively low values. Kruskal-Wallis tests showed significant differences between clusters for all environmental variables ($p < 0.01$) except for porewater nitrate and nitrite and porewater silicate. See appendix for results of Dunn's post-hoc tests for pairwise comparisons (Tables A6-8). **(C)** Heatmap showing mean relative abundance of abundant genera (defined as contributing > 2% of the total reads in any cluster) from each cluster, colored on a log-scale for increased resolution. Light blue indicates low relative abundance while dark purple indicates high relative abundance. Light grey tiles indicate no reads.

phosphate concentrations. The *Riverine* cluster included all river communities, and the *Melt-Influenced* cluster included all intertidal communities, aside from May, and July subtidal communities. The only significant differences between the two freshwater clusters were higher cDOM E2/E3 ratios in the *Riverine* cluster and higher salinity in the *Melt-Influenced* cluster (D: $p = 0.03$, 0.02). Though not statistically significant, chl-*a* concentrations were also higher and phaeopigments lower in the *Melt-Influenced* cluster than the *Riverine* cluster.

Within the marine group, I identified three clusters: *Pre-Melt*, *Late-Marine*, and *Post-Bloom*. All three were characterized by high porewater salinity. The *Pre-Melt* cluster, with all May and June subtidal communities, was similar in sediment characteristics to the freshwater clusters, but had higher cDOM E2/3 ratios than the *Melt-Season* (D: $p = 0.001$), and higher cDOM slope 350-400nm, and ammonium and phosphate concentrations than both freshwater clusters (D: $p < 0.02$). The *Late-Marine* and *Post-Bloom* clusters exhibited different sediment characteristics from the other clusters, with finer grains and higher LOI and porosity (Tables A6-8). They also had high concentrations of ammonium and silicate and high cDOM absorbance at 254 nm. The *Late-Marine* cluster included fjord and subtidal communities from August and September. The *Post-Bloom* cluster, with fjord communities from June and July, was distinct from all others but the *Pre-Melt* in its extremely high chl-*a* concentrations (D: $p < 0.01$).

The most abundant genera in *Riverine* communities were *Rhodoferax* (mean read abundance 7%), *Thiobacillus* (7%), *Oryzihumus* (5%), and unidentified genera from Gemmatimonadaceae (3%) and Gallionellaceae (3%) (Figure 7C). Indicator taxa analysis identified distinctions between the clusters. The fifteen taxa that were found to characterize *Riverine* communities were largely from the taxonomic groups mentioned above, with additional Gammaproteobacteria (*Arenimonas*, *Sulfurirhabdus*, *Methylotenera*, *Leeia*), *Parablastomonas*, and *Sulfuricurvum*. Nearly the same abundant genera were found in the *Melt-Influenced* cluster, but with *Lutibacter* (3%) and *Flavobacterium* (3%) replacing the Gemmatimonadaceae and

Gallionellaceae genera. Eight abundant indicator taxa for the *Melt-Influenced* cluset were identified within the genera *Rhodoferax*, *Lutibacter*, *Luteolibacter*, *Pseudorhodobacter*, and *Sphingorhabdus*. In the *Late-Marine* cluster, *Lutibacter* (6%), *Thiobacillus* (3%), *Rhodoferax* (3%), *Fluviicola* (3%) and the unidentified genus Sva1033 (Desulfuromonadales, 4%) were abundant. Abundant indicator taxa included a wide range of genera, many not among the most represented overall: *Lutibacter*, OM60(NOR5) clade, *Flavobacterium*, *Motiliproteus*, SAR11 Clade Ia, *Colwellia*, and *Oleispira*. The *Pre-Melt* and *Post-Bloom* clusters had the least similar abundant genera to the other clusters. In the *Post-Bloom* communities, the most abundant genera were *Psychromonas* (16%), *Marinifilum* (8%), *Colwellia* (5%), *Lutibacter* (5%), and an unidentified genus of Arcobacteraceae (5%). This cluster had the largest number of abundant indicator taxa (20), out of which eight were strains of *Psychromonas* and seven were members of the other four most abundant genera. Others represented taxa included *Polaribacter*, *Desulfofrigus*, *Geopsychrobacter*, and *Psychrilyobacter*. The most abundant genera in the *Pre-Melt* communities were *Woeseia* (5%), an unidentified genus of Flavobacteriaceae (3%), *Lutibacter* (3%), an unidentified genus of Sva1033 (3%), and *Yoonia-Loktanella* (2%). Only six indicator taxa were identified in the *Pre-Melt*, members of *Woesia*, *Maribacter*, *Maritimimonas*, and *Muriicola*.

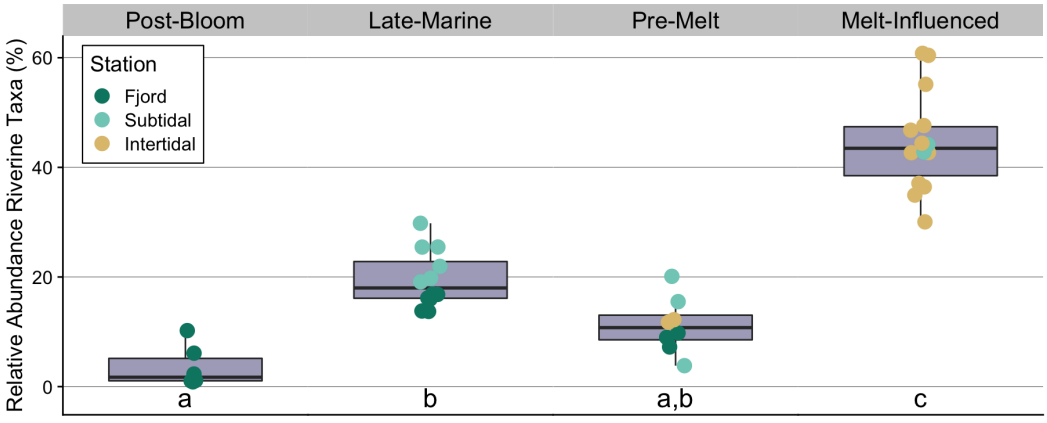

Figure 8. Boxplot depicting proportional abundance of riverine taxa in other community clusters. Riverine taxa were identified as ASVs with at least 0.05% relative abundance in any river sample. Points are individual samples, colored by sampling location. Kruskal-Wallis test showed significant differences between clusters ($p < 0.001$), lowercase letters along the x-axis indicate significant differences between clusters (D: $p < 0.01$).

The proportion of riverine taxa (i.e. ASVs with at least 0.05% relative abundance in any river sample) varied between the clusters (Figure 8). *Melt-Influenced* communities had the highest relative abundance of riverine taxa (median 44%), followed by *Late-Marine* communities (18%), and *Pre-Melt* communities (11%). The lowest relative abundance of riverine taxa was found in *Post-Bloom* communities (2%).

3.3.4 Community composition confers differences in potential function

Potential community functions inferred from taxonomic assignments showed clear distinctions between the freshwater and marine communities (Figure 9, see also Figure A11). Marine communities generally had higher potential capabilities for metabolism of more bioavailable molecules, including glycolysis and metabolisms of fructose and galactose, and *Pre-Melt* and *Late-Marine* communities' functional potentials were very similar. Freshwater communities had higher potential capacity for degradation of more recalcitrant compounds including aromatics, like naphthalene and xylene, and polycyclic aromatic hydrocarbons. Predicted capacities for photosynthesis, sulfate reduction, and nitrogen fixation tended to be higher in

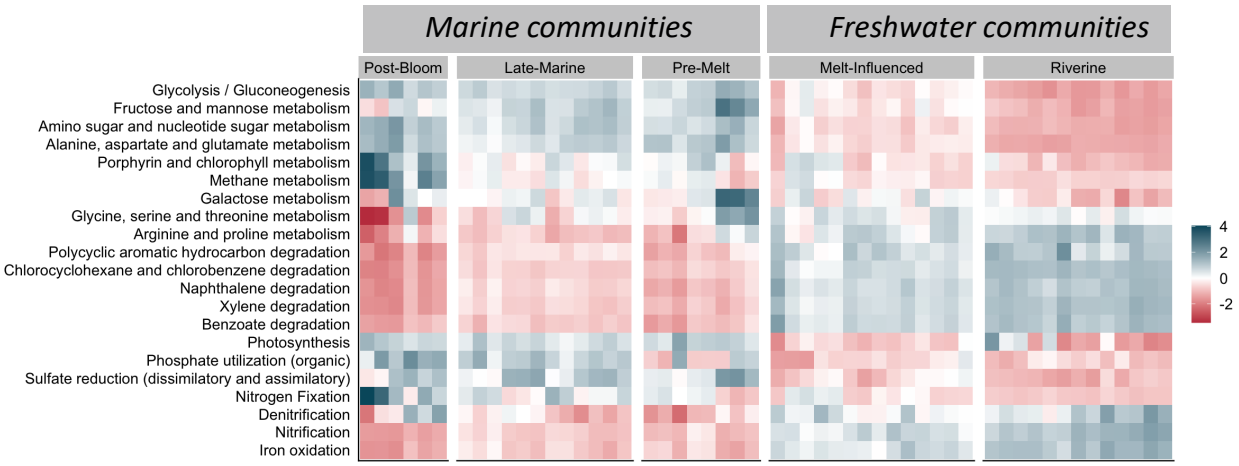

Figure 9. Heatmap displaying differential abundances of selected potential metabolic and biogeochemical functional capacities predicted with Tax4Fun based on taxonomic assignment. Potential functions were z-scaled for comparison across samples, and samples are grouped by cluster. Blue indicates a relatively high abundance while red indicates a relatively low abundance. See Appendix for full results of metabolic and degradation pathways (Figure A12).

marine communities, while freshwater communities had higher potential for denitrification, nitrification, and iron oxidation. Organic phosphate utilization potential was generally higher in marine communities, although *Pre-Melt* communities did not exhibit this pattern.

3.3.5 Environmental drivers of community composition

Variables that played a significant role in shaping community composition were determined with permutation testing on a canonical correspondence analysis (CCA) model (Figure 10, Table 3). Porewater salinity, sediment chl-*a* concentrations, porosity, the percentage of

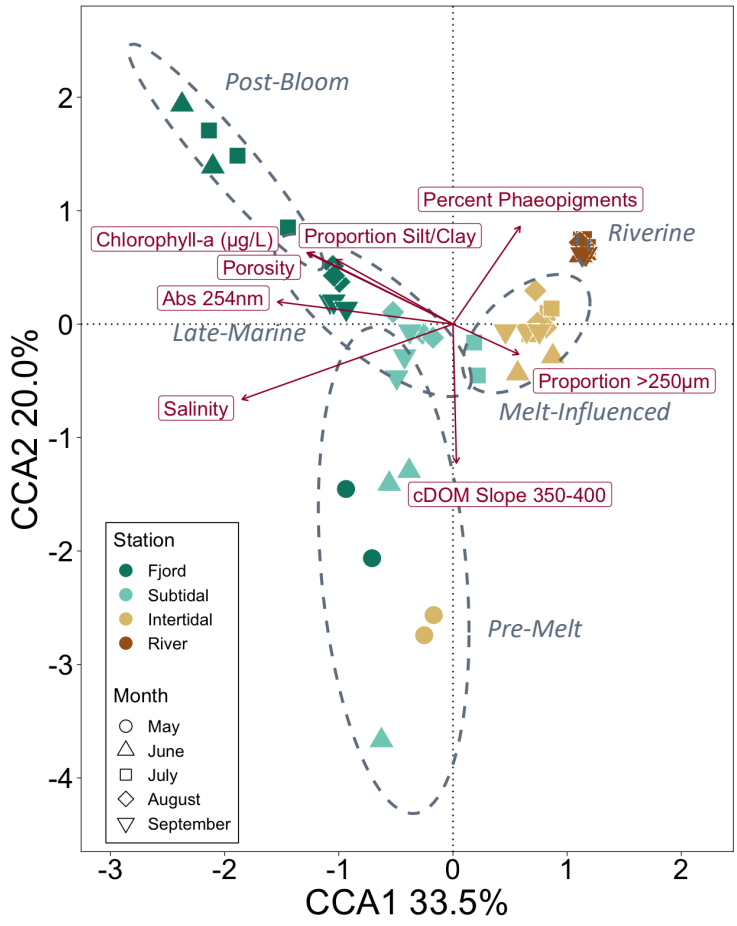

Figure 10. CCA with community composition and environmental variables. Points are samples, colored by station and shaped by month. Community composition was transformed to proportions and environmental variables were z-scaled before ordination. Dashed circles represent 95% confidence intervals for clusters from hierarchical clustering analysis, labeled in grey text. Three samples ("5-Fjord-y", "6-Fjord-y", and "6-Intertidal-y") were not included due to missing environmental data from low porewater volumes.

Table 3. Summary statistics of CCA.

Summary of CCA	Inertia	Proportion
Total	4.01	100%
Constrained	1.83	45.7%
Unconstrained	2.18	54.3%

Table 4. Results of permutations tests (n=999) to test significance of terms included in the CCA and variance inflation factor (VIF) for each term.

Variable	χ^2	F	*p*	VIF
Salinity	0.57	10.5	0.001	3.2
Chl-a	0.34	6.2	0.001	1.6
Porosity	0.32	5.9	0.001	4.3
Phaeo (%)	0.17	3.2	0.001	2.0
Silt and clay (%)	0.15	2.7	0.001	3.9
DOM slope 350-400	0.095	1.7	0.026	1.4
DOM abs 254nm	0.097	1.8	0.020	3.9
Coarse grains (%)	0.090	1.6	0.077	1.6

phaeopigments, and the sediment fraction of silt and clay were all highly significant ($p = 0.001$, Table 4). The cDOM spectral slope from 350-400 nm and absorbance at 254 nm were also significant ($p = 0.026$ and 0.02). The high F-value of the porewater salinity model suggests that porewater salinity accounts for a large degree of variation between microbial communities, and communities accordingly separated along a salinity gradient from river to fjord on the first axis of the CCA (Figure 10). The gradient along the first axis was also correlated with other physicochemical variables including sediment porosity, the proportion of silt and clay in sediments, and the proportion of coarse material in sediments. Sediment chl-*a* concentration was also highly correlated with the first axis. The arrangement of communities from different stations along this gradient suggests that these environmental variables are important for shaping communities' differences from river to fjord. The *Pre-Melt* cluster separates from other communities along the second axis, suggesting these communities are associated with lower proportions of phaeopigments in the sediment and higher E2/E3 ratios. Similar results were found with RDA on Hellinger-transformed and clr-transformed community data (Figure A13).

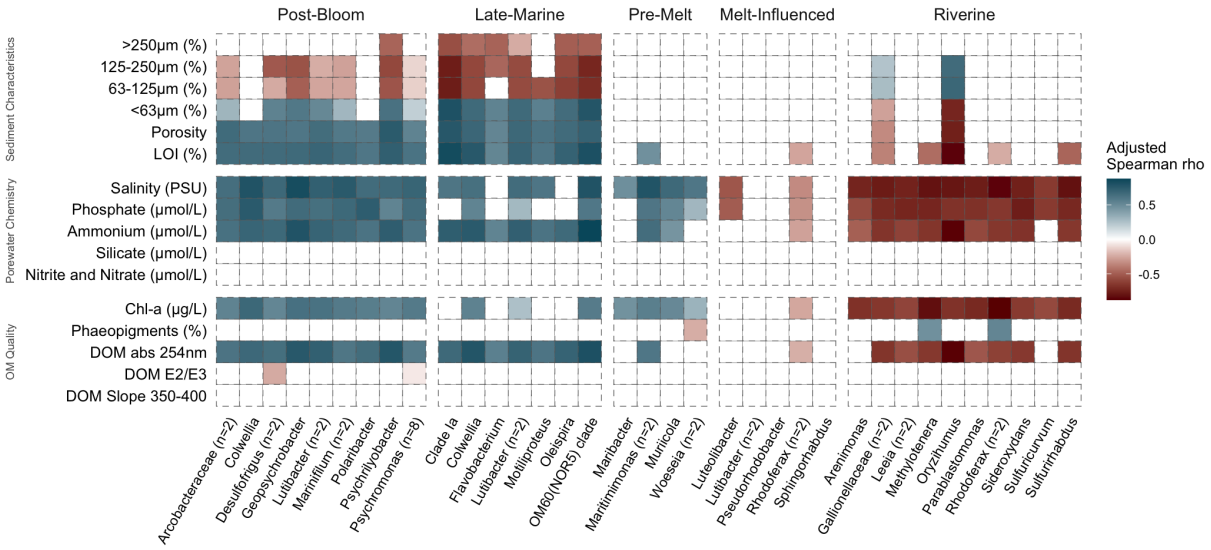

Figure 11. Spearman rank correlation of indicator taxa abundance with environmental variables. Only correlations with an adjusted p-value (Benjamini & Hochberg, 1995) of less than 0.05 are displayed. Indicator taxa were collapsed by genus — mean spearman rank correlation is displayed is multiple ASVs were members of the same genus, indicated in the axis text. Blue indicates positive correlations while red indicates negative correlations.

Correlations of relative abundance of indicator taxa with environmental variables showed similar patterns, mirroring seasonal and spatial patterns in environmental characteristics (Figure 11). Porewater salinity was highly correlated with most indicator taxa, separating marine from freshwater organisms. Sediment characteristics seemed most important for *Late-Marine* and *Post-Bloom* indicator taxa, reflecting the fine grains, high porosity, and high organic content characteristic of their environments. Chl-*a* and phosphate concentrations were positively correlated with *Post-Bloom* and *Pre-Melt* indicator taxa, while negatively correlated with riverine indicators. Similarly, cDOM absorbance coefficient at 254nm and ammonium concentration were positively correlated with *Post-Bloom* and *Late-Marine* taxa, and negatively correlated with riverine taxa. Indicators of *Melt-Influenced* communities showed very few significant correlations, perhaps due to intermediate values for most environmental variables in these samples.

3.4 Carbon substrate utilization depends on suspension water

Microbial communities used between a minimum of two (July intertidal with marine water) to a maximum of 27 substrates on each plate (June subtidal and intertidal and August river and intertidal, all with river water) (Figure 12). Most communities, regardless of suspension water, used all available polymers (glycogen, Tween 40, Tween 80, and **α**-cyclodextrin) and certain carbohydrates, including D-cellobiose, D-mannitol, N-acetyl-D-glucosamine, **α**-D-lactose, and **β**-methyl-D-glucoside. There was little seasonal change in carbon substrate utilization throughout the melt season. Furthermore, in May prior to river melt, fjord sediments suspended in marine water (incubated at 4ºC rather than 10ºC) showed similar patterns in substrate use to the marine suspensions throughout the melt-season (Figure A14).

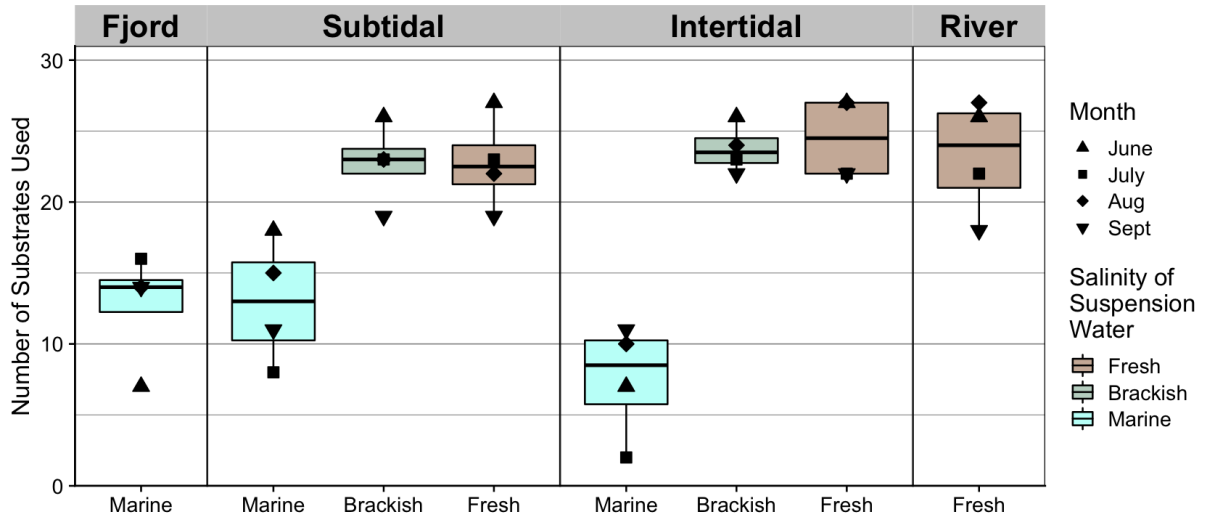

Figure 12. Boxplot showing the number of substrates used in Biolog EcoPlates. Plates are grouped by sediment sampling location and type of water used for sediment suspensions. Black points represent single plates, with shape depicting the sampling month. Kruskal-Wallis test showed significant differences between salinity treatments ($p < 0.0001$), with Dunn's post-hoc test showing no difference between fresh and brackish suspensions while both were different from marine ($p < 0.001$).

Across all stations and all months, microbial communities were capable of utilizing a larger number of substrates when suspended in fresh or brackish water (medians 22.5 and 23 substrates used) than when suspended in marine water (median 11 substrates used, D: $p < 0.001$). Similar patterns were observed using average well color development (AWCD), Shannon's diversity index, and Inverse Simpson's diversity index (Figure A15).

Certain substrates were used consistently by communities suspended in fresh or brackish water but not by communities suspended in marine water, regardless of sediment origin (Figure A14). These included three of the five available amino acids (L-arginine, L-asparagine, and L-serine), four of eight carboxylic acids (D-galacturonic acid, D-glucosaminic acid, itaconic acid, and γ-hydroxybutyric acid), one of two amines (putrescine), one of two phenolic compounds (4-hydroxy benzoic acid), and only two of ten carbohydrates (D-xylose and i-erythritol). Only one substrate, threonine, was used more often in marine suspensions, and then only by fjord communities.

Microbial communities suspended in fresh or brackish water used a similar number of substrates, regardless of station (Figure 12). However, communities suspended in marine water showed a difference in number of substrates used based on station, with more substrates used by fjord and subtidal communities (medians 14 and 13) than by intertidal communities (8.5). When suspended in marine water, intertidal communities utilized D-cellobiose, Tween 80, and N-Acetyl-D-Glucosamine less consistently than subtidal and fjord communities suspended in marine water did (Figure A14).

Principal component analysis based on AUTC for each substrate showed a high degree of similarity of substrate use within type of suspension water and little separation based on sampling station (Figure A16). This finding was confirmed with variance partitioning where 40% of the variance was explained by suspension water, 2% by station, and 16% by both. The one clear exception was within brackish water suspensions, where the intertidal and subtidal communities' substrate use was separated along PC2, correlating with higher AUTC for D-cellobiose, α-cyclodextrin, and glycogen in subtidal brackish water suspensions.

4 Discussion

This study aimed to identify the ways in which terrestrial runoff influences the structure and function of Arctic mudflat microbial communities throughout the melt season. My results suggest that riverine discharge strongly influences environmental conditions across the tidal flat, and microbial communities are in turn shaped by a combination of riverine and local processes. Freshwater inflow is also a direct source of riverine and terrestrial taxa to downstream communities, and these taxa exhibit unique functional capacities not widely found in the Arctic marine system. Changes in microbial communities can lead to feedbacks in biogeochemical cycling on local and global scales, though the degree to which predicted functions are realized requires further investigation.

4.1 Direct impact of melt water influx through downstream transport of allochthonous taxa

Taxa previously found in the permafrost active layer, glacial systems, or acid mine drainage were identified in all riverine communities, suggesting a high degree of connectivity between the catchment and riverine sediments. While many of the abundant genera in the *Riverine* communities have previously been found in Adventelva and other Arctic freshwater systems (e.g. *Rhodoferax, Thiobacillus*, *Oryzihumus,* and Gallionellaceae from Kosek et al. 2019; Kohler et al. 2020; Delpech et al. 2021; Morency et al. 2022), Gemmatimonadaceae and *Oryzihumus* are more frequently associated with terrestrial soil systems (DeBruyn et al. 2011; Kim et al. 2017; Kim et al. 2018; Semenova et al. 2021), including Arctic tundra and particularly the active layer of Svalbard permafrost (Kim et al. 2014; Semenova et al. 2021; Loganathachetti et al. 2022). As the non-glaciated area of Adventdalen is covered by 90% permafrost (Humlum et al. 2003), these taxa may have been transported to the river from active layer soils. Acidobacteria are well documented members of Arctic tundra soils (Chu et al. 2010;

Männistö et al. 2013), including in the active layer of Svalbard permafrost (Schostag et al. 2015; Xue et al. 2020). It was therefore unexpected to find such low abundances in this study, though low Acidobacteria abundances have also been reported in other Svalbard freshwater systems (Wang et al. 2016; Kosek et al. 2019). Many abundant indicator taxa for my *Riverine* communities have previously been identified in connection with Svalbard glaciers, either from glacial ice (*Methylotenera*, Thomas et al. 2020), cryoconites (*Arenimonas*, Segawa et al. 2014), meltwater (*Methylotenera* and *Sulfuricurvum*, Kohler et al. 2020; Thomas et al. 2020), or foreland soils (*Parablastomonas*, Ren et al. 2015). Glacier-associated organisms are likely carried downstream with meltwater, settling in sediments along the way. While often considered neutrophilic, iron oxidizing *Riverine* indicator taxa Gallionellaceae and *Sideroxyans* (Hedrich et al. 2011) have been identified in high abundances in acid mine drainage near Longyearbyen (García-Moyano et al. 2015) and in eastern Siberia (Kadnikov et al. 2019).

As melt sources and riverine biogeochemistry shift throughout the season (Nowak and Hodson 2015; Koziol et al. 2019; McGovern et al. 2020), I expected to find changes in riverine taxa as the melt season progressed. While clustering analysis showed distinctions between June and July-September riverine communities, overall, riverine communities were fairly stable seasonally. One main exception to this stability was Aquaspirillum (arcticum group), which was only found in relatively high abundances in June. This group can be very abundant in snow in the High Arctic (Harding et al. 2011), suggesting early snow melt in the catchment transports these cells to riverine communities.

Riverine taxa were found in all other communities, from the intertidal zone to the fjord system, suggesting downstream transport. They were most abundant in the *Melt-Influenced* cluster, sometimes comprising over 50% of the total reads, indicating a high degree of connectivity between the river and the *Melt-Influenced* communities in the tidal flats. Similarly, allochthonous riverine taxa have previously been found in Isfjorden surface waters and sediments

(Delpech et al. 2021) and in estuaries elsewhere in the Arctic (Hauptmann et al. 2016; Kellogg et al. 2019).

Transport of riverine taxa might confer new functional capacities in downstream communities, but only if the bacteria can realize these functions in their new environment. Riverine taxa possessed capabilities for a diverse range of biogeochemical processes, including degradation or incorporation of organic compounds (*Oryzihumus* Kageyama and Takahashi 2015), carbon fixation through the oxidation of sulfur or iron (*Thiobacillus,* Boden et al. 2019; Gallionellaceae, Hedrich et al. 2011), anoxygenic photosynthesis (*Rhodoferax*, Hiraishi et al. 1991; Madigan et al. 2000), and nitrate reduction (*Thiobacillus,* Boden et al. 2019; *Sulfuricurvum*, Kodama and Watanabe 2004; *Leeia*, Lim et al. 2007). While some cultured members of these groups tolerate wide ranges of salinity (Huber and Stetter 1989; Kageyama et al. 2005; Lim et al. 2014), others are known to have low salinity tolerances (Hiraishi et al. 1991; Kaden et al. 2014; Farh et al. 2017; Kim et al. 2017; Zhou et al. 2019). It is possible that some riverine taxa were unable to grow when deposited in the marine environments of the fjord and subtidal. In the fresh to brackish *Melt-Influenced* communities, however, these transported bacteria were likely more readily able to survive and grow. They may alter local biogeochemical gradients with implications for the fate of terrestrially derived carbon and nutrients at the river-fjord interface.

4.2 Combination of riverine inputs and local processes shape bacterial community structure and potential functions

Environmental variables, linked to both seasonality and spatial variability, were strongly associated with differences in community composition across this study. As it has been widely documented that microbial communities respond to environmental changes (Baas-Becking, 1934; Allison and Martiny, 2008; Gilbert et al., 2012; Shade et al., 2012; Logue et al. 2015;

Fierer 2017), this was expected. Porewater salinity was the most important factor for shaping community composition, as previously observed in temperate tidal flats (Lv et al. 2016; Zhang et al. 2017; Zhao et al. 2019; Li et al. 2021; Niu et al. 2022). However, while previous studies have found that nutrient concentrations can be important for shaping microbial communities in tidal flats (Yan et al. 2018; Li et al. 2021; Mohapatra et al. 2021; Niu et al. 2022), none of the measured inorganic nutrients in porewater were identified as significant in the model selection process. In addition to salinity, microbial communities were largely shaped by physical properties of the sediments (grain size and porosity) and by the availability and quality of OM (chl-*a* concentration, cDOM concentration, and cDOM molecular weight) as found in pelagic systems (Sipler et al. 2017; Kellogg et al. 2019). Some of the variation in these significant variables is directly linked to riverine influx (e.g. salinity), while others can be attributed to marine processes, like the concentration of chl-*a* following the spring bloom.

Melt-Influenced environment and communities

Flushing of tidal flat sediments, porewater, and microbial communities with high riverine discharge likely caused the dramatic shift in environmental conditions and bacterial communities and potential observed in intertidal sites from May into June (following spring freshet) and in subtidal sites from June into July (following high rates of riverine discharge). May intertidal and June subtidal bacterial communities grouped together in the *Pre-Melt* cluster, dominated by characteristic marine taxa — *Woesia*, Flavobacteriaceae, *Lutibacter*, Sva1033 (Desulfuromonadales), and *Yoonia-Loktanella* —which have all previously been found in Svalbard fjord sediments or waters (Zeng et al. 2017; Buongiorno et al. 2020; Du et al. 2020; Delpech et al. 2021; Vishnupriya et al. 2021; Zeng et al. 2021). With the onset of the melt season, freshwater discharge from the river flushed out the intertidal, and later subtidal, sediments, decreasing porewater salinity, cDOM absorbance at 254nm, and cDOM molecular weight. The

composition of *Melt-Influenced* bacterial communities responded to these seasonal environmental changes (Figure 13), becoming dominated by the river-associated genera *Rhodoferax*, *Thiobacillus*, and *Oryzihumus*, with the addition of marine and generalist taxa that are found in a range of habitats. This combination of freshwater and marine organisms in Arctic tidal flats has been observed in macrofaunal communities as well (Churchwell et al. 2016). Two strains of *Rhodoferax* were identified as indicator taxa for the *Melt-Influenced* cluster, suggesting that some freshwater taxa can adapt to the more dynamic tidal flat environment.

Correspondingly, potential community function from Tax4Fun showed strong similarities between *Riverine* and *Melt-Influenced* communities. Recent work has suggested that microbial community functional capacity can be correlated with the chemodiversity of available OM (Rivers et al. 2013; Berggren and Giorgio 2015; Ruiz-González et al. 2015; Orland et al. 2020; Sala et al. 2020). Arctic riverine systems often have a high proportion of complex Terr-OM (Behnke et al. 2021), and Svalbard glacial-fed rivers are no different (McGovern et al. 2020; Kellerman et al. 2021). *Riverine* and *Melt-Influenced* clusters had a high capacity for degradation of more complex organic molecules (including naphthalene, xylene, and polycyclic aromatic hydrocarbons), likely reflecting the available OM. This suggests that deposited Terr-OM might be remineralized or taken up by bacterial communities in these fresh to brackish environments.

Differences in environmental conditions between the *Melt-Influenced* and *Riverine* clusters were likely driven by local processes and, in turn, shaped community composition and potential function. Differences included higher porewater salinity, chl-*a* concentrations, and cDOM molecular weight and concentrations, with lower phaeopigments in the *Melt-Influenced* cluster compared with the *Riverine*. Local processes in the tidal flat might have, for example, made phytodetritus more available than in the river, which could be expected given the high importance of microphytobenthos in tidal flats globally (Paterson et al. 2003; Underwood et

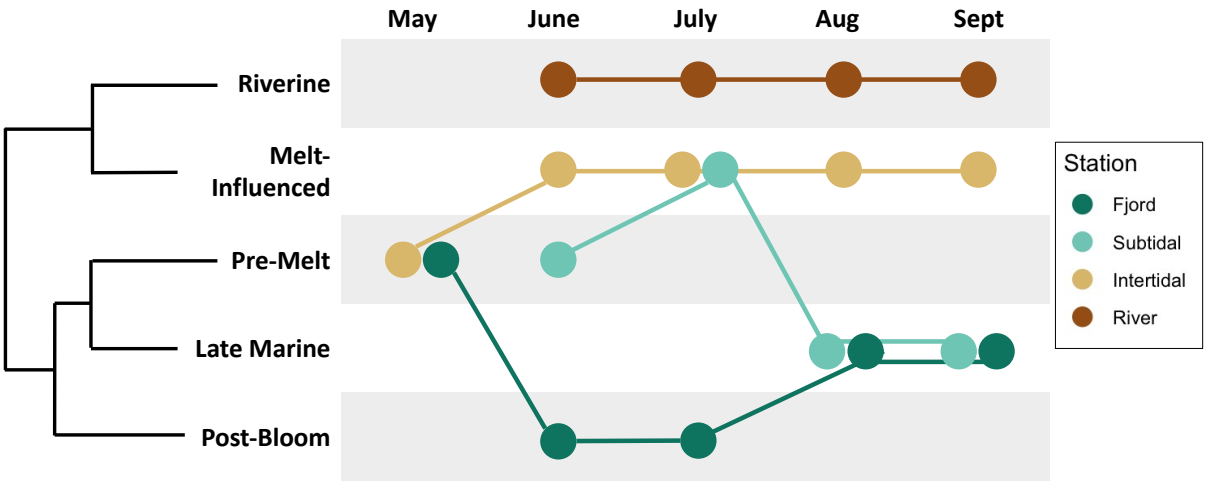

Figure 13. Conceptual diagram showing seasonal progression of microbial communities from each station through different clusters with differing levels of similarity, as determined by hierarchical clustering (Figure 7A). Each circle is representative of all replicates from each station each month.

al. 2005; Billerbeck, 2007) and locally in certain regions of the Adventfjorden tidal flat (Wiktor et al. 2016). Correspondingly, I found higher relative abundance of heterotrophic bacteria in these communities than in the river, which was more dominated by autotrophic taxa. Two heterotrophic genera, the marine and intertidal genus *Lutibacter* (Le Moine Bauer et al. 2016) and the ecologically diverse genus *Flavobacterium* (Bernardet and Bowman 2015), were among the most abundant in the *Melt-Influenced* cluster. Furthermore, all abundant indicator taxa other than *Rhodoferax* were members of heterotrophic genera (Uchino et al. 2002; Yoon et al. 2008; Cardman et al. 2014; Feng et al. 2020), largely from groups known to tolerate wide ranges of environmental conditions (Yoon et al. 2008; Chen et al. 2013; Kim et al. 2015). For example, *Luteolibacter*, an indicator taxon, has been associated with degradation of complex carbohydrates and aging phytoplankton in Svalbard fjords (Cardman et al. 2014, Wietz et al. 2021). The higher relative abundance and importance of heterotrophic taxa for distinguishing the *Melt-Influenced* communities could suggest an increased potential for degradation of OM in these communities as compared to riverine communities. With low rates of sedimentation in the intertidal flats (Weslawski et al. 1999) limiting the possibility of OM burial, during the melt season, the intertidal and occasionally subtidal flats could therefore be an important site for the

microbial loop, with heterotopic bacteria incorporating or remineralizing OM, potentially releasing carbon dioxide and inorganic nutrients to the water column (and atmosphere).

Post-Bloom environment and communities

While the subtidal and intertidal reflected the influence of freshwater inflow transitioning into June and July, the fjord communities followed a very different trajectory, likely shaped by the deposition of phytodetritus following the spring phytoplankton bloom. The *Post-Bloom* cluster (fjord sediments in June and July) was characterized by very high chl-*a* concentrations, perhaps sustained through July by a second bloom, suggested by a peak in chl-*a* in the inner fjord surface waters. All abundant indicator taxa for these communities were strongly positively correlated with chl-*a* concentrations in the sediments, and many of the abundant prokaryotic genera and indicator taxa (*Psychromonas*, *Marinifilum*, *Colwellia*, Arcobacteraceae, and *Polaribacter*) have previously been associated with additions of phytodetritus in experimental studies (Teeling et al. 2012; Xing et al. 2015; Müller et al. 2018a; Jain et al. 2020; Valdés-Castro et al. 2022). This was further reflected in the functional predictions, showing distinctly high potential for porphyrin and chlorophyll metabolism. Community shifts with addition of phytodetritus have been found across a range of benthic ecosystems, from the deep sea to coastal sediments (Franco et al. 2007; Gihring 2009; Tait et al. 2015; Hoffmann et al. 2017), and the distinct *Post-Bloom* communities are likely a result of this type of fertilization from fjord processes, rather than a downstream response to riverine influence. Many of the abundant genera and indicator taxa in *Post-Bloom* communities were from groups known to be either obligately or facultatively anaerobic (e.g. *Colwellia*, Deming and Junge 2015; *Psychromonas,* The Editorial Board 2015; *Desulfofrigus,* Galushko and Kuever 2019; *Desulfuromusa,* Liesak and Finster 2015), with anaerobic conditions likely forming within OM aggregates in the surface sediments (Reise 1985). These taxa and conditions contribute unique biogeochemical

functional potential, including sulfur and iron reduction and OM fermentation (Schutte et al. 2019).

Late-Marine environment and communities

Riverine inputs did alter fjord and subtidal environmental conditions through the deposition of sediments, though the impact this has on microbial communities remains uncertain. Previous studies have found high rates of sedimentation from riverine discharge in these regions (Weslawski et al. 1999; Zajączkowski and Włodarska-Kowalczuk 2007), and the seasonal decrease in sediment grain size, coupled with increasing porosity and organic content found in this study suggests that these samples were also impacted by sediment deposition from riverine inputs. Sediments deposited by Adventelva are on average very fine, less than 63 μm (Rodenburg 2019). The high correlation between fine grain size, porosity, and organic content follows similar patterns to those found in temperate tidal flats (Longbottom 1970; Dale 1974; Watling 1991; Alongi and Christoffersen 1992; Vigano et al. 2003). The abundant indicator taxa for the *Late-Marine* cluster were highly correlated with these sediment characteristics, suggesting the riverine deposits might play a role in shaping the community, as has previously been found in a temperate river delta (Alvisi et al. 2019; Fazi et al. 2020). One abundant genus from this cluster, *Fluviicola,* has previously been found in higher abundances in silty rather than sandy environments in coastal Svalbard (Miksch et al. 2021). However, with the strong seasonal covariance of many environmental variables, it is difficult to separate out the important drivers individually.

Overall, the bacterial communities in the *Late-Marine* cluster did not show a clear response to riverine inputs and seemed to be more influenced by local marine conditions. The *Late-Marine* cluster converged on communities similar to the *Pre-Melt* cluster (also dominated by *Lutibacter* and Sva1033) (Figure 13), though certain transported riverine taxa, as discussed

in more detail above, were abundant in the *Late-Marine* communities as well. Two of the abundant indicator taxa for the *Late-Marine* cluster, the globally distributed marine groups SAR11 Clade Ia and the OM60 clade (Yan et al. 2009; Haro-Moreno et al. 2020), have previously been identified as indicator taxa for August pelagic communities in Isfjorden (Delpech et al. 2021), suggesting a high degree of connectivity between the water column and the sediments in the late summer. Interestingly, two other abundant indicator taxa from *Late-Marine* communities, *Motiliproteus* and *Oleispira antarctica*, are associated with oil spills (Noirungsee et al. 2020; Hazen et al. 2010; Mason et al. 2012). While *Motiliproteus* members can utilize a wide range of organic compounds (Wang et al. 2014), *Oleispira* are hydrocarbonoclasts with a highly limited range of substrates they use for growth (Yakimov et al. 2003; Yakimov et al. 2007). High volumes of boat traffic in Adventfjorden (over 1800 port calls in 2019, Port of Longyearbyen 2022) might contribute to accumulation of hydrocarbons in the sediments — concentrations of polycyclic aromatic hydrocarbons in Adventfjorden sediments in August can be up to 16 times higher than expected background levels (Holte et al. 1996). Functional predictions for the *Late-Marine* communities showed a high capacity for degradation of more simple or bioavailable molecules, such as amino sugars, glucose, and fructose, which are often available in marine systems (Benner and Kaiser 2003; Davis and Benner 2005). The largely heterotrophic taxa in the *Late-Marine* cluster indicate high potential for degradation or incorporation of deposited OM, though with elevated functional potential for degradation of highly bioavailable sugars and amino sugars over more complex compounds, they might be more capable of utilizing fresh marine detritus, or for some hydrocarbons from the fjord, rather than Terr-OM.

4.3 Potential functional capacity may not be realized under local environmental conditions

Potential community functions, predicted from taxonomic assignments, may not be realized in *in-situ* conditions. While Tax4Fun showed distinctly different functional potential between clusters, splitting the freshwater and marine systems, these potential functions are based on DNA relative abundances, which may not reflect active communities. It is widely understood that only a fraction of bacterial cells in aquatic systems may be alive and active (Stevenson 1977; Rodriguez et al. 1992; Smith and Delgiorgio 2003). In coastal sediments especially, a very small proportion of the bacterial cells present may be active (Luna et al. 2002, First and Hollibaugh 2010), and the whole community may not be taxonomically representative for the active subset (Yan et al. 2018). The inactive or dead cells may still contain DNA, and thereby influence predictions of community functionality based on 16S rRNA gene amplicon data. This makes interpretation of predicted metabolic functions more challenging in these dynamic regions with high potential for passive transport of bacteria cells (Sun et al. 2020; Breitkruez et al. 2021).

To investigate active community functionality more directly, I used Biolog EcoPlates™ (Insam 1997). All communities exhibited high usage of most polymers and some carbohydrates, primarily glucose derivatives, as previously found in EcoPlates studies of pelagic polar bacteria (Sala et al. 2005; Sala et al. 2008; Sala et al. 2010). Many of these compounds are widely found in both marine and terrestrial systems, e.g., mannitol is synthesized by terrestrial plants, phytoplankton, and macroalgae (Yamaguchi et al. 1969; Schmitz and Srivastava 1975; Rumpho et al. 1983; Stoop et al. 1996; Obata et al. 2013). Seasonal variation in community composition had no apparent impact on functional capacity, with little seasonal change in substrate usage observed.

The water used for sediment suspensions influenced community level functional profiles more than sampling location did. This was unexpected based on the high degree of variability

in community composition between sampling locations, and it suggests that these variable communities can utilize a similar range of carbon sources when grown under the same environmental conditions. Previous work has established that the degree to which microbial community functionality is realized is shaped by environmental conditions (Strickland et al. 2009; Fierer et al. 2012), and this study confirms that this paradigm applies to Arctic tidal flat communities. I suspect that transported riverine bacteria played a large role in the fresh and brackish water intertidal and subtidal incubations, while they were made inactive with higher salinity. This would not be surprising given that many cultured members of riverine-associated genera exhibit low salt tolerances (Hiraishi et al. 1991; Kaden et al. 2014; Farh et al. 2017; Kim et al. 2017; Zhou et al. 2019). It does not seem that transported riverine taxa augment functional capacity in the marine system, as functional capacity in marine water suspensions did not increase with higher proportions of riverine-associated taxa. To my knowledge, this is the first study of tidal flat sediment community functional profiles to use a range of salinities for suspension water. My findings suggest that future work in tidal flats cannot ignore the high amount of variation in microbial functional capacity related to changes in salinity.

The most pronounced pattern in substrate utilization was the broader range of substrates used in fresh and brackish suspensions than in marine suspensions, regardless of where the sediments were collected. The eleven additional substrates utilized in fresh and brackish suspensions were quite stable both spatially and seasonally, and this discrepancy was even true for the subtidal communities that primarily lived in a high salinity environment. This pattern was unexpected, as previous work has found tradeoffs with salinity increases — utilization of some substrates decreased while others increased (Chen et al. 2017) — and lower functional diversity in Arctic freshwater than marine pelagic communities (Tam et al. 2003). Some of the substrates used more often by fresh or brackish suspensions aligned with functional predictions from Tax4Fun, e.g., predicted serine and arginine metabolisms were higher in freshwater

communities and both were utilized more frequently in fresh and brackish suspensions. Several of the carboxylic acid substrates were also more heavily utilized by fresh or brackish suspensions. They can be used to inhibit bacterial growth (Vázquez et al. 2011; Nguyen et al. 2019), but polar soil bacteria do utilize carboxylic acids in similar experiments (Lahav Lavian et al. 2001; Kenarova et al. 2013). Amino acids were also utilized more often by fresh or brackish suspensions, and pelagic bacteria in polar marine systems have shown low uptake of amino acids (Sala et al. 2005; Sala et al. 2008; Sala et al. 2010).

Bacterial carbon metabolic capabilities can reflect variations in available OM (Rivers et al. 2013; Berggren and Giorgio 2015; Ruiz-González et al. 2015; Orland et al. 2020; Sala et al. 2020). Heterotrophic bacteria in Svalbard freshwater environments must make do with what is available, which can be lower quality, less bioavailable compounds (Raymond et al. 2001; Sobczak et al. 2002; Brett et al. 2017), and bacterial communities from different freshwater environments can be adapted to degrade different types of Terr-OM (Fasching et al. 2014; Logue et al. 2016). Therefore, I suspect the wider range of substrate utilization capacity in fresh and brackish water suspensions reflects the high diversity (Kellerman et al. 2021), but low availability, of OM in the river system. Riverine Arctic bacteria seem to possess carbon metabolisms that are not often found in the Arctic marine system, but while freshwater taxa are transported to coastal environments, their unique functional capabilities seem not to be.

As DNA is generally easier to work with than RNA, both in terms of field sampling and laboratory analysis, molecular work on the impact of riverine inflow to Arctic microbial communities has largely focused on DNA based studies (e.g., Sipler et al. 2017; Kellogg et al. 2019; Delpech et al. 2021). However, there are clear drawbacks in our ability to investigate functional capacity with such data in highly dynamic deltaic systems. I suggest future work examine the metatranscriptome of riverine-influenced sediment communities to more directly assess the ways allochthonous riverine taxa might influence functional capacities under

changing environmental conditions. Similar studies in a wide range of systems have elucidated clear environmental controls on bacterial processes (e.g., de Menezes et al. 2012; De Filippis et al. 2016; Bei et al. 2019).

4.4 Implications and perspectives in a warming Arctic

My findings suggest that bacterial communities in Arctic riverine sediments are capable of degrading a wide range of complex Terr-OM. However, with fairly low rates of sediment and OM deposition in riverine sediments (Weslawski et al. 1999), carbon fixation through chemolithoautotrophy and anoxygenic photosynthesis more likely dominates processes in these systems. With high rates of sedimentation, Arctic fjord sediments are known to be important sites for carbon burial, accumulating Terr-OM (Koziorowska et al. 2016; Bianchi 2020; M. McGovern unpublished data), and I found little evidence to contradict this. While transported riverine taxa could potentially degrade deposited Terr-OM, their functionality seems likely inhibited by marine conditions and marine heterotrophs, which might be specialized for utilization of highly labile marine OM (Moran et al. 2016), dominate these systems. Estuarine tidal flats, however, exhibit a more complex story, influenced by both fresh and marine conditions and microbial communities. Under fresh or brackish conditions, tidal flat communities seem to have a high potential for degradation of complex organic molecules, likely conferred by deposited freshwater taxa, but they might lack this capacity under marine conditions as the activity of freshwater taxa can be inhibited with high salinities (Hiraishi et al. 1991; Kaden et al. 2014; Farh et al. 2017; Kim et al. 2017; Zhou et al. 2019). Arctic river deltas might therefore oscillate between acting as hotspots for processing of Terr-OM or sites of high Terr-OM burial with changes in the tidal cycle and freshwater discharge rates.

Precipitation and riverine discharge across the Arctic are expected to increase with climate change (Haine et al. 2015; Hanssen-Bauer et al. 2019; Meredith et al. 2019). As I found in July,

pulses of discharge can extend the area of tidal flats that is flushed by freshwater, shifting communities towards a more riverine composition and decreasing porewater salinity. With more frequent high discharge events, as predicted for Arctic regions (Hanssen-Bauer et al. 2019), there is the potential for an extension of the spatial and temporal extent of melt-influenced environments and communities in tidal flats. If the high deposition of sediments along the edge of tidal flats continues, this increased extent of melt-influenced sediments might allow for increased breakdown of terrestrial OM, as freshwater taxa are no longer inhibited by high salinity conditions. With the increase in Terr-OM expected to enter coastal systems in a changing climate (Parmentier et al. 2017), even if only a small proportion of the tidal flat microbial community is able to utilize this Terr-OM (and OM-associated nutrients), microbial processing could have reverberating implications up the marine food web (Müller 2018b).

The nature of allochthonous taxa entering Arctic river systems will likely shift as catchments undergo potentially dramatic shifts with climate change. The Arctic is warming at twice the rate of the global average, causing widespread impacts to Arctic landscapes and ecosystems (Meredith et al. 2019). The permafrost active layer will likely deepen (Hanssen-Bauer et al. 2019; Meredith et al. 2019) in a warmer climate, and the active layer often has higher microbial biomass with a community composition distinct from frozen permafrost (Xue et al. 2020; Gilichinsky et al. 2008). In this study, I already found taxa associated with the active layer in the river system, and I expect their abundance would increase with a larger biomass reservoir. Furthermore, with a longer growth season, vegetation throughout terrestrial Arctic systems will likely increase and plant communities will shift through greening and shrubification (Gauthier et al. 2013; Mekonnen et al. 2021). As microbial communities are often strongly influenced by vegetation (Hoch et al. 2019; Zhao et al. 2019; Cagle et al. 2020; Mohapatra et al. 2021), soil bacterial communities in the active layer are likely to change, impacting which organisms are transported with meltwater. Glacial taxa were also abundant in the river system, and as glaciers

melt at faster rates (Meredith et al. 2019), the transport of glacial biota into rivers and coasts will likely increase. However, if glaciers fully melt, as is expected within the next fifty years for some of the smaller glaciers in Adventdalen (Hanssen-Bauer et al. 2019), the sources for glacial-associated taxa would vanish, likely removing these organisms from Arctic rivers. Overall, I expect climate change will lead to higher transport of terrestrial microbial taxa into Arctic riverine systems, but the transported organisms will likely be somewhat different from the ones we find today as their environments of origin are themselves transformed.

5 Conclusion

In this study, I aimed to identify the ways terrestrial runoff influences microbial community structure and function in a High Arctic estuarine mudflat. I found clear evidence that freshwater discharge shapes environmental conditions, which in turn structure community composition. Porewater salinity was identified as a key factor for shaping bacterial communities, with physical sediment properties and organic matter availability and quality playing important roles as well. Meltwater inputs also directly shaped downstream communities through the deposition of transported taxa. I identified taxa commonly associated with glacier and permafrost systems in riverine communities and a high proportion of riverine taxa in all other sampling locations.

Communities differed in their potential functional capacity along a salinity gradient, with higher capacity for degradation of complex molecules in freshwater communities and higher capacity for breakdown of more simple compounds in marine communities. However, carbon-source substrate utilization experiments demonstrated that environmental conditions strongly impact realized functions, with communities exhibiting higher diversity of substrate use in fresh and brackish water than in marine water regardless of community composition.

Here, I studied a single system for the duration of one melt season, but the processes identified are likely relevant for other Arctic coastal systems, especially those impacted by glacially-fed rivers. Under current environmental conditions, microbial communities and their biogeochemical processes in Arctic estuarine tidal flats seem divided between the freshwater dominated intertidal and the marine dominated subtidal. While intertidal communities are more likely to be able to utilize deposited Terr-OM, they might be limited by its availability. Particulate deposition, including Terr-OM, is much higher in subtidal regions, but here, marine water limits the functional capacity of transported riverine taxa, reducing the likelihood of incorporation or degradation of deposited Terr-OM. Our understanding of these processes and the role of coastal Arctic systems as sinks for sedimented Terr-OM would benefit from targeted studies

of the current sediment metabolism in Arctic mudflats along with more detailed characterization of OM composition and mineralization rates in these systems.

In a changing Arctic, increased rates of riverine discharge carrying more labile Terr-OM might shift the balance in estuarine tidal flats. Permafrost thaw and glacier melt will likely increase the amount labile Terr-OM released from terrestrial systems and, as the freshwater zone could extend further across tidal flats with increased discharge, microbial communities might be able to exhibit greater utilization of deposited Terr-OM. Tidal flats, and the diverse microbial communities that inhabit them, need to be considered to fully understand the impacts of a changing climate on Arctic coastal ecosystems.

6 References

Allison, S. D., and J. B. H. Martiny. 2008. Resistance, resilience, and redundancy in microbial communities. Proceedings of the National Academy of Sciences **105**:11512-11519.

Alongi, D. M. 1998. Coastal ecosystem processes / Daniel M. Alongi. CRC Press, Boca Raton.

Alongi, D. M., and P. Christoffersen. 1992. Benthic infauna and organism-sediment relations in a shallow, tropical coastal area - Influence of outwelled mangrove detritus and physical disturbance. Marine Ecology Progress Series **81**:229-245.

Alvisi, F., T. Cibic, S. Fazi, L. Bongiorni, F. Relitti, and P. D. Negro. 2019. Role of depositional dynamics and riverine input in shaping microbial benthic community structure of Po prodelta system (NW Adriatic, Italy). Estuarine, Coastal and Shelf Science **227**:106305.

Andersen, S. D. J. in press. Turbid Fjord Waters — Arctic Hotspots for Primary Productivity. Master Thesis in Arctic and Marine Biology. UiT — The Arctic University of Norway, Tromsø.

Apprill, A., S. McNally, R. Parsons, and L. Weber. 2015. Minor revision to V4 region SSU rRNA 806R gene primer greatly increases detection of SAR11 bacterioplankton. Aquatic Microbial Ecology **75**:129-137.

Arashkevich, E. G., A. V. Drits, A. F. Pasternak, M. V. Flint, A. B. Demidov, A. B. Amelina, M. D. Kravchishina, I. N. Sukhanova, and S. A. Shchuka. 2018. Distribution and Feeding of Herbivorous Zooplankton in the Laptev Sea. Oceanology **58**:381-395.

Aßhauer, K. P., B. Wemheuer, R. Daniel, and P. Meinicke. 2015. Tax4Fun: predicting functional profiles from metagenomic 16S rRNA data. Bioinformatics **31**:2882-2884.

Baas Becking, L. G. M. 1934. Geobiologie of inleiding tot de milieukunde. W.P. Van Stockum & Zoon, Den Haag.

Bale, A., and A. Kenny. 2005. Sediment analysis and seabed characterization. Pages 43-86 *in* A. Eleftheriou and A. McIntyre, editors. Methods for the study of marine benthos. Blackwell Publishing, Oxford.

Bange, H. W., U. H. Bartell, S. Rapsomanikis, and M. O. Andreae. 1994. Methane in the Baltic and North Seas and a reassessment of the marine emissions of methane. Global Biogeochemical Cycles **8**:465-480.

Behnke, M. I., J. W. McClelland, S. E. Tank, A. M. Kellerman, R. M. Holmes, N. Haghipour, T. I. Eglinton, P. A. Raymond, A. Suslova, A. V. Zhulidov, T. Gurtovaya, N. Zimov, S. Zimov, E. A. Mutter, E. Amos, and R. G. M. Spencer. 2021. Pan-Arctic Riverine Dissolved Organic Matter: Synchronous Molecular Stability, Shifting Sources and Subsidies. Global Biogeochemical Cycles **35**:e2020GB006871.

Bei, Q., G. Moser, X. Wu, C. Müller, and W. Liesack. 2019. Metatranscriptomics reveals climate change effects on the rhizosphere microbiomes in European grassland. Soil Biology and Biochemistry **138**:107604.

Benjamini, Y., and Y. Hochberg. 1995. Controlling the False Discovery Rate: A Practical and Powerful Approach to Multiple Testing. Journal of the Royal Statistical Society. Series B (Methodological) **57**:289-300.

Benner, R., and K. Kaiser. 2003. Abundance of amino sugars and peptidoglycan in marine particulate and dissolved organic matter. Limnology and Oceanography **48**:118-128.

Berggren, M., and P. A. del Giorgio. 2015. Distinct patterns of microbial metabolism associated to riverine dissolved organic carbon of different source and quality. Journal of Geophysical Research: Biogeosciences **120**:989-999.

Bernardet, J.-F., and J. P. Bowman. 2015. Flavobacterium. Pages 1-75 *in* M. E. Trujillo, S. Dedysh, P. DeVos, B. Hedlund, P. Kämpfer, F. A. Rainey, and W. B. Whitman, editors. Bergey's Manual of Systematics of Archaea and Bacteria.

Bianchi, T. S., S. Arndt, W. E. N. Austin, D. I. Benn, S. Bertrand, X. Cui, J. C. Faust, K. Koziorowska-Makuch, C. M. Moy, C. Savage, C. Smeaton, R. W. Smith, and J. Syvitski. 2020. Fjords as Aquatic Critical Zones (ACZs). Earth-Science Reviews **203**:103145.

Billerbeck, M., H. Røy, K. Bosselmann, and M. Huettel. 2007. Benthic photosynthesis in submerged Wadden Sea intertidal flats. Estuarine, Coastal and Shelf Science **71**:704-716.

Blanchet, F. G., P. Legendre, and D. Borcard. 2008. Forward Selection of Explanatory Variables. Ecology **89**:2623-2632.

Blighe, K., and A. Lun. 2021. PCAtools: Everything Principal Components Analysis.

Boden, R., L. P. Hutt, and A. Rae. 2019. Thiobacillus. Pages 1-9 *in* M. E. Trujillo, S. Dedysh, P. DeVos, B. Hedlund, P. Kämpfer, F. A. Rainey, and W. B. Whitman, editors. Bergey's Manual of Systematics of Archaea and Bacteria.

Böer, S. I., S. I. C. Hedtkamp, J. E. E. van Beusekom, J. A. Fuhrman, A. Boetius, and A. Ramette. 2009. Time- and sediment depth-related variations in bacterial diversity and community structure in subtidal sands. The ISME Journal **3**:780-791.

Bogen, J., and T. E. Bønsnes. 2003. Erosion and sediment transport in High Arctic rivers, Svalbard. Polar Research **22**:175-189.

Borcard, D., P. Legendre, and P. Drapeau. 1992. Partialling out the Spatial Component of Ecological Variation. Ecology **73**:1045-1055.

Breitkreuz, C., A. Heintz-Buschart, F. Buscot, S. F. M. Wahdan, M. Tarkka, and T. Reitz. 2021. Can We Estimate Functionality of Soil Microbial Communities from Structure-Derived Predictions? A Reality Test in Agricultural Soils. Microbiol Spectr **9**:e0027821.

Brett, M. T., S. E. Bunn, S. Chandra, A. W. E. Galloway, F. Guo, M. J. Kainz, P. Kankaala, D. C. P. Lau, T. P. Moulton, M. E. Power, J. B. Rasmussen, S. J. Taipale, J. H. Thorp, and J. D. Wehr. 2017. How important are terrestrial organic carbon inputs for secondary production in freshwater ecosystems? Freshwater Biology **62**:833-853.

Brown, K. A., J. M. Holding, and E. C. Carmack. 2020. Understanding Regional and Seasonal Variability Is Key to Gaining a Pan-Arctic Perspective on Arctic Ocean Freshening. Frontiers in Marine Science **7**.

Brown, S., S. Kendall, R. Churchwell, A. Taylor, and A.-M. Benson. 2012. Relative Shorebird Densities at Coastal Sites in the Arctic National Widlife Refuge. **v. 35**.

Brown, T., E. Edinger, R. G. Hooper, and K. Belliveau. 2011. Benthic Marine Fauna and Flora of Two Nearshore Coastal Locations in the Western and Central Canadian Arctic. Arctic **64**:281-301.

Buongiorno, J., K. Sipes, K. Wasmund, A. Loy, and K. G. Lloyd. 2020. Woeseiales transcriptional response to shallow burial in Arctic fjord surface sediment. PLOS ONE **15**:e0234839.

Cabrita, M. T., and V. Brotas. 2000. Seasonal variation in denitrification and dissolved nitrogen fluxes in intertidal sediments of the Tagus estuary, Portugal. Marine Ecology Progress Series **202**:51-65.

Cagle, G., Q. Lin, S. A. Graham, I. Mendelssohn, J. W. Fleeger, D. Deis, D. S. Johnson, J. Zhou, and A. Hou. 2020. Planting Spartina alterniflora in a salt marsh denuded of vegetation by an oil spill induces a rapid response in the soil microbial community. Ecological Engineering **151**:105815.

Callahan, B. J., P. J. McMurdie, M. J. Rosen, A. W. Han, A. J. A. Johnson, and S. P. Holmes. 2016. DADA2: High-resolution sample inference from Illumina amplicon data. Nature Methods **13**:581-583.

Cardman, Z., C. Arnosti, A. Durbin, K. Ziervogel, C. Cox, A. D. Steen, A. Teske, and A. M. Spormann. 2014. Verrucomicrobia Are Candidates for Polysaccharide-Degrading Bacterioplankton in an Arctic Fjord of Svalbard. Applied and Environmental Microbiology **80**:3749-3756.

Carmack, E. C., M. Yamamoto-Kawai, T. W. N. Haine, S. Bacon, B. A. Bluhm, C. Lique, H. Melling, I. V. Polyakov, F. Straneo, M. L. Timmermans, and W. J. Williams. 2016. Freshwater and its role in the Arctic Marine System: Sources, disposition, storage, export, and physical and biogeochemical consequences in the Arctic and global oceans. Journal of Geophysical Research: Biogeosciences **121**:675-717.

Casper, A. F., M. Rautio, C. Martineau, and W. F. Vincent. 2015. Variation and Assimilation of Arctic Riverine Sestonin the Pelagic Food Web of the Mackenzie River Delta and Beaufort Sea Transition Zone. Estuaries and Coasts **38**:1656-1663.

Chao, A. 1984. Nonparametric Estimation of the Number of Classes in a Population. Scandinavian Journal of Statistics **11**:265-270.

Chao, A., and S.-M. Lee. 1992. Estimating the Number of Classes via Sample Coverage. Journal of the American Statistical Association **87**:210-217.

Chen, C.-X., X.-Y. Zhang, C. Liu, Y. Yu, A. Liu, G.-W. Li, H. Li, X.-L. Chen, B. Chen, B.-C. Zhou, and Y.-Z. Zhang. 2013. *Pseudorhodobacter antarcticus* sp. nov., isolated from Antarctic intertidal sandy sediment, and emended description of the genus *Pseudorhodobacter* Uchino et al. 2002 emend. Jung et al. 2012. International Journal of Systematic and Evolutionary Microbiology **63**:849-854.

Chen, H. 2021. VennDiagram: Generate High-Resolution Venn and Euler Plots.

Cheung, M. K., C. K. Wong, K. H. Chu, and H. S. Kwan. 2018. Community Structure, Dynamics and Interactions of Bacteria, Archaea and Fungi in Subtropical Coastal Wetland Sediments. Scientific Reports **8**:14397.

Christiansen, H. H., H. M. French, and O. Humlum. 2005. Permafrost in the Gruve-7 mine, Adventdalen, Svalbard. Norsk Geografisk Tidsskrift - Norwegian Journal of Geography **59**:109-115.

Chu, H., N. Fierer, C. L. Lauber, J. G. Caporaso, R. Knight, and P. Grogan. 2010. Soil bacterial diversity in the Arctic is not fundamentally different from that found in other biomes. Environmental Microbiology **12**:2998-3006.

Church, M., and J. M. Ryder. 1972. Paraglacial Sedimentation: A Consideration of Fluvial Processes Conditioned by Glaciation. GSA Bulletin **83**:3059-3072.

Churchwell, R. T., S. Kendall, S. C. Brown, A. L. Blanchard, T. E. Hollmen, and A. N. Powell. 2018. The First Hop: Use of Beaufort Sea Deltas by Hatch-Year Semipalmated Sandpipers. Estuaries and Coasts **41**:280-292.

Churchwell, R. T., S. J. Kendall, A. L. Blanchard, K. H. Dunton, and A. N. Powell. 2016. Natural Disturbance Shapes Benthic Intertidal Macroinvertebrate Communities of High Latitude River Deltas. Estuaries and Coasts **39**:798-814.

Colby, G. A., M. O. Ruuskanen, K. A. St.Pierre, V. L. St.Louis, A. J. Poulain, and S. Aris-Brosou. 2020. Warming Climate Is Reducing the Diversity of Dominant Microbes in the Largest High Arctic Lake. Frontiers in Microbiology **11**.

Cole, J. J., Y. T. Prairie, N. F. Caraco, W. H. McDowell, L. J. Tranvik, R. G. Striegl, C. M. Duarte, P. Kortelainen, J. A. Downing, J. J. Middelburg, and J. Melack. 2007. Plumbing the Global Carbon Cycle: Integrating Inland Waters into the Terrestrial Carbon Budget. Ecosystems **10**:172-185.

Comeau, A. M., G. M. Douglas, M. G. I. Langille, and J. Eisen. 2017. Microbiome Helper: a Custom and Streamlined Workflow for Microbiome Research. mSystems **2**:e00127-00116.

Cottrell, M. T., and D. L. Kirchman. 2000. Natural Assemblages of Marine Proteobacteria and Members of the *Cytophaga-Flavobacter* Cluster Consuming Low- and High-Molecular-Weight Dissolved Organic Matter. Applied and Environmental Microbiology **66**:1692-1697.

Dale, N. G. 1974. Bacteria in intertidal sediments: Factors related to their distribution1. Limnology and Oceanography **19**:509-518.

Davis, J., and R. Benner. 2005. Seasonal trends in the abundance, composition and bioavailability of particulate and dissolved organic matter in the Chukchi/Beaufort Seas and western Canada Basin. Deep Sea Research Part II: Topical Studies in Oceanography **52**:3396-3410.

Davis, N. M., D. M. Proctor, S. P. Holmes, D. A. Relman, and B. J. Callahan. 2018. Simple statistical identification and removal of contaminant sequences in marker-gene and metagenomics data. Microbiome **6**:226.

De Cáceres, M., and P. Legendre. 2009. Associations between species and groups of sites: indices and statistical inference. Ecology **90**:3566-3574.

De Filippis, F., A. Genovese, P. Ferranti, J. A. Gilbert, and D. Ercolini. 2016. Metatranscriptomics reveals temperature-driven functional changes in microbiome impacting cheese maturation rate. Scientific Reports **6**:21871.

De Haan, H., and T. De Boer. 1987. Applicability of light absorbance and fluorescence as measures of concentration and molecular size of dissolved organic carbon in humic Lake Tjeukemeer. Water Research **21**:731-734.

de Menezes, A., N. Clipson, and E. Doyle. 2012. Comparative metatranscriptomics reveals widespread community responses during phenanthrene degradation in soil. Environmental Microbiology **14**:2577-2588.

DeBruyn, J. M., L. T. Nixon, M. N. Fawaz, A. M. Johnson, and M. Radosevich. 2011. Global biogeography and quantitative seasonal dynamics of Gemmatimonadetes in soil. Applied and Environmental Microbiology **77**:6295-6300.

Delpech, L.-M., T. R. Vonnahme, M. McGovern, R. Gradinger, K. Præbel, and A. E. Poste. 2021. Terrestrial Inputs Shape Coastal Bacterial and Archaeal Communities in a High Arctic Fjord (Isfjorden, Svalbard). Frontiers in Microbiology **12**.

Deming, J. W., and K. Junge. 2015. Colwellia. Pages 1-12 *in* M. E. Trujillo, S. Dedysh, P. DeVos, B. Hedlund, P. Kämpfer, F. A. Rainey, and W. B. Whitman, editors. Bergey's Manual of Systematics of Archaea and Bacteria.

Du, Z.-Z., L.-Y. Zhou, T.-J. Wang, H.-R. Li, and Z.-J. Du. 2020. Lutibacter citreus sp. nov., isolated from Arctic surface sediment. International Journal of Systematic and Evolutionary Microbiology **70**:3154-3161.

Dunn, O. J. 1964. Multiple Comparisons Using Rank Sums. Technometrics **6**:241-252.

Epstein, S. S. 1997. Microbial Food Webs in Marine Sediments. II. Seasonal Changes in Trophic Interactions in a Sandy Tidal Flat Community. Microb Ecol **34**:199-209.

Farh, M. E.-A., Y.-J. Kim, P. Singh, S. Y. Jung, J.-P. Kang, and D.-C. Yang. 2017. Rhodoferax koreense sp. nov, an obligately aerobic bacterium within the family Comamonadaceae, and emended description of the genus Rhodoferax. Journal of Microbiology **55**:767-774.

Fasching, C., B. Behounek, G. A. Singer, and T. J. Battin. 2014. Microbial degradation of terrigenous dissolved organic matter and potential consequences for carbon cycling in brown-water streams. Scientific Reports **4**:4981.

Fazi, S., L. Baldassarre, D. Cassin, G. M. Quero, I. Pizzetti, T. Cibic, G. M. Luna, R. Zonta, and P. Del Negro. 2020. Prokaryotic community composition and distribution in coastal sediments following a Po river flood event (northern Adriatic Sea, Italy). Estuarine, Coastal and Shelf Science **233**:106547.

Feng, G.-D., X.-J. Zhang, S.-Z. Yang, A.-Z. Li, Q. Yao, and H. Zhu. 2020. Transfer of *Sphingorhabdus marina*, *Sphingorhabdus litoris*, *Sphingorhabdus flavimaris* and *Sphingorhabdus pacifica* corrig. into the novel genus *Parasphingorhabdus* gen. nov. and *Sphingopyxis baekryungensis* into the novel genus *Novosphingopyxis* gen. nov. within the family *Sphingomonadaceae*. International Journal of Systematic and Evolutionary Microbiology **70**:2147-2154.

Fierer, N. 2017. Embracing the unknown: disentangling the complexities of the soil microbiome. Nature Reviews Microbiology **15**:579-590.

Fierer, N., J. W. Leff, B. J. Adams, U. N. Nielsen, S. T. Bates, C. L. Lauber, S. Owens, J. A. Gilbert, D. H. Wall, and J. G. Caporaso. 2012. Cross-biome metagenomic analyses of soil microbial communities and their functional attributes. Proceedings of the National Academy of Sciences **109**:21390-21395.

First, M. R., and J. T. Hollibaugh. 2010. Environmental factors shaping microbial community structure in salt marsh sediments. Marine Ecology Progress Series **399**:15-26.

Franco, M. A., I. D. Mesel, M. D. Diallo, K. V. d. Gucht, D. V. Gansbeke, P. v. Rijswijk, M. J. Costa, M. Vincx, and J. Vanaverbeke. 2007. Effect of phytoplankton bloom deposition on benthic bacterial communities in two contrasting sediments in the southern North Sea. Aquatic Microbial Ecology **48**:241-254.

Frankignoulle, M., G. Abril, A. Borges, I. I. Bourge, C. Canon, B. Delille, E. Libert, and J. M. Theate. 1998. Carbon dioxide emission from european estuaries. Science **282**:434-436.

Galushko, A., and J. Kuever. 2019. Desulfofrigus. Pages 1-4 *in* M. E. Trujillo, S. Dedysh, P. DeVos, B. Hedlund, P. Kämpfer, F. A. Rainey, and W. B. Whitman, editors. Bergey's Manual of Systematics of Archaea and Bacteria.

García-Moyano, A., A. E. Austnes, A. Lanzén, E. González-Toril, Á. Aguilera, and L. Øvreås. 2015. Novel and Unexpected Microbial Diversity in Acid Mine Drainage in Svalbard (78° N), Revealed by Culture-Independent Approaches. Microorganisms **3**:667-694.

Garland, J. L. 1996. Analytical approaches to the characterization of samples of microbial communities using patterns of potential C source utilization. Soil Biology and Biochemistry **28**:213-221.

Garland, J. L., and A. L. Mills. 1991. Classification and characterization of heterotrophic microbial communities on the basis of patterns of community-level sole-carbon-source utilization. Applied and Environmental Microbiology **57**:2351-2359.

Gauthier, G., J. Bêty, M.-C. Cadieux, P. Legagneux, M. Doiron, C. Chevallier, S. Lai, A. Tarroux, and D. Berteaux. 2013. Long-term monitoring at multiple trophic levels suggests heterogeneity in responses to climate change in the Canadian Arctic tundra. Philosophical Transactions of the Royal Society B: Biological Sciences **368**:20120482.

Gihring, T. M., M. Humphrys, H. J. Mills, M. Huette, and J. E. Kostka. 2009. Identification of phytodetritus-degrading microbial communities in sublittoral Gulf of Mexico sands. Limnology and Oceanography **54**:1073-1083.

Gilbert, J. A., J. A. Steele, J. G. Caporaso, L. Steinbruck, J. Reeder, B. Temperton, S. Huse, A. C. McHardy, R. Knight, I. Joint, P. Somerfield, J. A. Fuhrman, and D. Field. 2012. Defining seasonal marine microbial community dynamics. ISME J **6**:298-308.

Gilichinsky, D., T. Vishnivetskaya, M. Petrova, E. Spirina, V. Mamykin, and E. Rivkina. 2008. Bacteria in Permafrost. Pages 83-102 *in* R. Margesin, F. Schinner, J.-C. Marx, and C. Gerday, editors. Psychrophiles: from Biodiversity to Biotechnology. Springer Berlin Heidelberg, Berlin, Heidelberg.

Gloor, G. B., J. M. Macklaim, V. Pawlowsky-Glahn, and J. J. Egozcue. 2017. Microbiome Datasets Are Compositional: And This Is Not Optional. Frontiers in Microbiology **8**.

Grabs, W. E., F. Portmann, and T. de Couet. 2000. Discharge Observation Networks in Arctic Regions: Computation of the River Runoff into the Arctic Ocean, Its Seasonality and Variability. Pages 249-267 *in* E. L. Lewis, E. P. Jones, P. Lemke, T. D. Prowse, and P. Wadhams, editors. The Freshwater Budget of the Arctic Ocean. Springer Netherlands, Dordrecht.

Guay, C. K., G. P. Klinkhammer, K. K. Falkner, R. Benner, P. G. Coble, T. E. Whitledge, B. Black, F. J. Bussell, and T. A. Wagner. 1999. High-resolution measurements of dissolved organic carbon in the Arctic Ocean by in situ fiber-optic spectrometry. Geophysical Research Letters **26**:1007-1010.

Guo, C., X. Zhang, S. Luan, H. Zhou, L. Liu, and Y. Qu. 2021. Diversity and structure of soil bacterial community in intertidal zone of Daliao River estuary, Northeast China. Marine Pollution Bulletin **163**:111965.

Guo, L., C.-L. Ping, and R. W. Macdonald. 2007. Mobilization pathways of organic carbon from permafrost to arctic rivers in a changing climate. Geophysical Research Letters **34**.

Hackett, C. A., and B. S. Griffiths. 1997. Statistical analysis of the time-course of Biolog substrate utilization. Journal of Microbiological Methods **30**:63-69.

Haine, T. W. N., B. Curry, R. Gerdes, E. Hansen, M. Karcher, C. Lee, B. Rudels, G. Spreen, L. de Steur, K. D. Stewart, and R. Woodgate. 2015. Arctic freshwater export: Status, mechanisms, and prospects. Global and Planetary Change **125**:13-35.

Han, D., H. K. Ha, C. Y. Hwang, B. Y. Lee, H.-G. Hur, and Y. K. Lee. 2015. Bacterial communities along stratified water columns at the Chukchi Borderland in the western Arctic Ocean. Deep Sea Research Part II: Topical Studies in Oceanography **120**:52-60.

Hansen, A. M., T. E. C. Kraus, B. A. Pellerin, J. A. Fleck, B. D. Downing, and B. A. Bergamaschi. 2016. Optical properties of dissolved organic matter (DOM): Effects of biological and photolytic degradation. Limnology and Oceanography **61**:1015-1032.

Hanssen-Bauer, I., E. J. Førland, H. Hisdal, S. Mayer, A. B. Sandø and A. Sorteberg (eds.). 2019. Climate in Svalbard 2100 - a knowledge base for climate adaptation. NCCS report 1/2019.

Harding, T., D. Jungblut Anne, C. Lovejoy, and F. Vincent Warwick. 2011. Microbes in High Arctic Snow and Implications for the Cold Biosphere. Applied and Environmental Microbiology **77**:3234-3243.

Haro-Moreno, J. M., F. Rodriguez-Valera, R. Rosselli, F. Martinez-Hernandez, J. J. Roda-Garcia, M. L. Gomez, O. Fornas, M. Martinez-Garcia, and M. López-Pérez. 2020. Ecogenomics of the SAR11 clade. Environmental Microbiology **22**:1748-1763.

Harrell Jr, F. E. 2021. Hmisc: Harrell Miscellaneous.

Hauptmann, A. L., T. N. Markussen, M. Stibal, N. S. Olsen, B. Elberling, J. Baelum, T. Sicheritz-Ponten, and C. S. Jacobsen. 2016. Upstream Freshwater and Terrestrial Sources Are Differentially Reflected in the Bacterial Community Structure along a Small Arctic River and Its Estuary. Front Microbiol **7**:1474.

Hazen, T. C., E. A. Dubinsky, T. Z. DeSantis, G. L. Andersen, Y. M. Piceno, N. Singh, J. K. Jansson, A. Probst, S. E. Borglin, J. L. Fortney, W. T. Stringfellow, M. Bill, M. E. Conrad, L. M. Tom, K. L. Chavarria, T. R. Alusi, R. Lamendella, D. C. Joyner, C. Spier, J. Baelum, M. Auer, M. L. Zemla, R. Chakraborty, E. L. Sonnenthal, P. D'haeseleer, H.-Y. N. Holman, S. Osman, Z. Lu, J. D. V. Nostrand, Y. Deng, J. Zhou, and O. U. Mason. 2010. Deep-Sea Oil Plume Enriches Indigenous Oil-Degrading Bacteria. Science **330**:204-208.

Hedrich, S., M. Schlömann, and D. B. Johnson. 2011. The iron-oxidizing proteobacteria. Microbiology **157**:1551-1564.

Heip, C., N. Goosen, P. Herman, J. Kromkamp, J. Middelburg, and K. Soetaert. 1995. Production and consumption of biological particles in temperate tidal estuaries. Oceanography and Marine Biology: an annual review.

Hiraishi, A., Y. Hoshino, and T. Satoh. 1991. Rhodoferax fermentans gen. nov., sp. nov., a phototrophic purple nonsulfur bacterium previously referred to as the "Rhodocyclus gelatinosus-like" group. Archives of Microbiology **155**:330-336.

Hoch, J. M. K., M. E. Rhodes, K. L. Shek, D. Dinwiddie, T. C. Hiebert, A. S. Gill, A. E. Salazar Estrada, K. L. Griffin, M. I. Palmer, and K. L. McGuire. 2019. Soil Microbial Assemblages Are Linked to Plant Community Composition and Contribute to Ecosystem Services on Urban Green Roofs. Frontiers in Ecology and Evolution **7**.

Hoffmann, K., C. Hassenrück, V. Salman-Carvalho, M. Holtappels, and C. Bienhold. 2017. Response of Bacterial Communities to Different Detritus Compositions in Arctic Deep-Sea Sediments. Frontiers in Microbiology **8**.

Holmer, M. 1999. The Effect of Oxygen Depletion on Anaerobic Organic Matter Degradation in Marine Sediments. Estuarine, Coastal and Shelf Science **48**:383-390.

Holte, B., S. Dahle, B. Gulliksen, and K. Naes. 1996. Some macrofaunal effects of local pollution and glacier-induced sedimentation, with indicative chemical analyses, in the sediments of two Arctic fjords. Polar Biology **16**:549-557.

Hood, E., J. Fellman, R. G. M. Spencer, P. J. Hernes, R. Edwards, D. D'Amore, and D. Scott. 2009. Glaciers as a source of ancient and labile organic matter to the marine environment. Nature **462**:1044-1047.

Huber, H., and K. O. Stetter. 1989. Thiobacillus prosperus sp. nov., represents a new group of halotolerant metal-mobilizing bacteria isolated from a marine geothermal field. Archives of Microbiology **151**:479-485.

Humlum, O., A. Instanes, and J. Sollid. 2003. Permafrost in Svalbard: A review of research history, climatic background and engineering challenges. Polar Research - POLAR RES **22**:191-215.

Insam, H. 1997. A New Set of Substrates Proposed for Community Characterization in Environmental Samples. Pages 259-260. Springer Berlin Heidelberg, Berlin, Heidelberg.

Jain, A., K. P. Krishnan, N. Begum, A. Singh, F. A. Thomas, and A. Gopinath. 2020. Response of bacterial communities from Kongsfjorden (Svalbard, Arctic Ocean) to macroalgal polysaccharide amendments. Mar Environ Res **155**:104874.

Jałowiecki, Ł., J. M. Chojniak, E. Dorgeloh, B. Hegedusova, H. Ejhed, J. Magnér, and G. A. Płaza. 2016. Microbial Community Profiles in Wastewaters from Onsite Wastewater Treatment Systems Technology. PLOS ONE **11**:e0147725.

Jassby, A. D., J. E. Cloern, and B. E. Cole. 2002. Annual primary production: Patterns and mechanisms of change in a nutrient-rich tidal ecosystem. Limnology and Oceanography **47**:698-712.

Jong, D., L. Bröder, G. Tanski, M. Fritz, H. Lantuit, T. Tesi, N. Haghipour, T. I. Eglinton, and J. E. Vonk. 2020. Nearshore Zone Dynamics Determine Pathway of Organic Carbon From Eroding Permafrost Coasts. Geophysical Research Letters **47**:e2020GL088561.

Jørgensen, L., C. A. Stedmon, H. Kaartokallio, M. Middelboe, and D. N. Thomas. 2015. Changes in the composition and bioavailability of dissolved organic matter during sea ice formation. Limnology and Oceanography **60**:817-830.

Kaden, R., C. Spröer, D. Beyer, and P. Krolla-Sidenstein. 2014. Rhodoferax saidenbachensis sp. nov., a psychrotolerant, very slowly growing bacterium within the family Comamonadaceae, proposal of appropriate taxonomic position of Albidiferax ferrireducens strain T118T in the genus Rhodoferax and emended description of the genus Rhodoferax. Int J Syst Evol Microbiol **64**:1186-1193.

Kadnikov, V. V., E. V. Gruzdev, D. A. Ivasenko, A. V. Beletsky, A. V. Mardanov, E. V. Danilova, O. V. Karnachuk, and N. V. Ravin. 2019. Selection of a Microbial Community in the Course of Formation of Acid Mine Drainage. Microbiology **88**:292-299.

Kageyama, A., and Y. Takahashi. 2015. Oryzihumus. Pages 1-4 *in* M. E. Trujillo, S. Dedysh, P. DeVos, B. Hedlund, P. Kämpfer, F. A. Rainey, and W. B. Whitman, editors. Bergey's Manual of Systematics of Archaea and Bacteria.

Kageyama, A., Y. Takahashi, T. Seki, H. Tomoda, and S. Ōmura. 2005. Oryzihumus leptocrescens gen. nov., sp. nov. International Journal of Systematic and Evolutionary Microbiology **55**:2555-2559.

Kaiser, K., M. Canedo-Oropeza, R. McMahon, and R. M. W. Amon. 2017. Origins and transformations of dissolved organic matter in large Arctic rivers. Scientific Reports **7**:13064.

Kaste, Ø., C. B. Gundersen, A. Poste, J. Sample, and D. Ø. Hjermann. 2022. The Norwegian river monitoring programme 2020

– water quality status and trends.

Kattner, G., J. M. Lobbes, H. P. Fitznar, R. Engbrodt, E. M. Nöthig, and R. J. Lara. 1999. Tracing dissolved organic substances and nutrients from the Lena River through Laptev Sea (Arctic). Marine Chemistry **65**:25-39.

Kellerman, A. M., J. Vonk, S. McColaugh, D. C. Podgorski, E. van Winden, J. R. Hawkings, S. E. Johnston, M. Humayun, and R. G. M. Spencer. 2021. Molecular Signatures of Glacial Dissolved Organic Matter From Svalbard and Greenland. Global Biogeochemical Cycles **35**:e2020GB006709.

Kellogg, C. T. E., J. W. McClelland, K. H. Dunton, and B. C. Crump. 2019. Strong Seasonality in Arctic Estuarine Microbial Food Webs. Frontiers in Microbiology **10**.

Kenarova, A., M. Encheva, V. Chipeva, N. Chipev, P. Hristova, and P. Moncheva. 2013. Physiological diversity of bacterial communities from different soil locations on Livingston Island, South Shetland archipelago, Antarctica. Polar Biology **36**:223-233.

Kenarova, A., G. Radeva, I. Traykov, and S. Boteva. 2014. Community level physiological profiles of bacterial communities inhabiting uranium mining impacted sites. Ecotoxicology and Environmental Safety **100**:226-232.

Kim, D.-U., S.-G. Kim, H. Lee, A.-Y. Park, and J.-O. Ka. 2017. Oryzihumus soli sp. nov., isolated from soil and emended description of the genus Oryzihumus. International Journal of Systematic and Evolutionary Microbiology **67**:3960-3964.

Kim, H. M., J. Y. Jung, E. Yergeau, C. Y. Hwang, L. Hinzman, S. Nam, S. G. Hong, O.-S. Kim, J. Chun, and Y. K. Lee. 2014. Bacterial community structure and soil properties of a subarctic tundra soil in Council, Alaska. FEMS Microbiology Ecology **89**:465-475.

Kim, J., A. H. Lee, and W. Chang. 2018. Enhanced bioremediation of nutrient-amended, petroleum hydrocarbon-contaminated soils over a cold-climate winter: The rate and extent of hydrocarbon biodegradation and microbial response in a pilot-scale biopile subjected to natural seasonal freeze-thaw temperatures. Science of The Total Environment **612**:903-913.

Kim, M., S. Pak, S. Rim, L. Ren, F. Jiang, X. Chang, P. Liu, Y. Zhang, C. Fang, C. Zheng, and F. Peng. 2015. Luteolibacter arcticus sp. nov., isolated from high Arctic tundra soil, and emended description of the genus Luteolibacter. International Journal of Systematic and Evolutionary Microbiology **65**:1922-1928.

Kipp, L. E., P. B. Henderson, Z. A. Wang, and M. A. Charette. 2020. Deltaic and Estuarine Controls on Mackenzie River Solute Fluxes to the Arctic Ocean. Estuaries and Coasts **43**:1992-2014.

Klein, G. d. 1985. Intertidal Flats and Intertidal Sand Bodies. Pages 187-224 *in* R. A. Davis, editor. Coastal Sedimentary Environments. Springer New York, New York, NY.

Klein, K. P., H. Lantuit, B. Heim, D. Doxaran, B. Juhls, I. Nitze, D. Walch, A. Poste, and J. E. Søreide. 2021. The Arctic Nearshore Turbidity Algorithm (ANTA) - A multi sensor turbidity algorithm for Arctic nearshore environments. Science of Remote Sensing **4**:100036.

Kleine Bardenhorst, S., M. Vital, A. Karch, and N. Rübsamen. 2022. Richness estimation in microbiome data obtained from denoising pipelines. Computational and Structural Biotechnology Journal **20**:508-520.

Klindworth, A., E. Pruesse, T. Schweer, J. Peplies, C. Quast, M. Horn, and F. O. Glöckner. 2012. Evaluation of general 16S ribosomal RNA gene PCR primers for classical and next-generation sequencing-based diversity studies. Nucleic Acids Research **41**:e1-e1.

Kodama, Y., and K. Watanabe. 2004. Sulfuricurvum kujiense gen. nov., sp. nov., a facultatively anaerobic, chemolithoautotrophic, sulfur-oxidizing bacterium isolated from an underground crude-oil storage cavity. Int J Syst Evol Microbiol **54**:2297-2300.

Köhler, H., B. Meon, V. V. Gordeev, A. Spitzy, and R. M. W. Amon. 2003. Dissolved organic matter (DOM) in the estuaries of Ob and Yenisei and the adjacent Kara Sea, Russia. Pages 281–308 *in* R. Stein, K. Fahl, D. K. Fütterer, E. M. Galimov, and O. V. Stepanets, editors. Siberian River Runoff in the Kara Sea, New York.

Kohler, T. J., P. Vinšová, L. Falteisek, J. D. Žárský, J. C. Yde, J. E. Hatton, J. R. Hawkings, G. Lamarche-Gagnon, E. Hood, K. A. Cameron, and M. Stibal. 2020. Patterns in Microbial Assemblages Exported From the Meltwater of Arctic and Sub-Arctic Glaciers. Frontiers in Microbiology **11**.

Köpke, B., R. Wilms, B. Engelen, H. Cypionka, and H. Sass. 2005. Microbial Diversity in Coastal Subsurface Sediments: a Cultivation Approach Using Various Electron Acceptors and Substrate Gradients. Applied and Environmental Microbiology **71**:7819-7830.

Kosek, K., A. Luczkiewicz, K. Kozioł, K. Jankowska, M. Ruman, and Ż. Polkowska. 2019. Environmental characteristics of a tundra river system in Svalbard. Part 1: Bacterial abundance, community structure and nutrient levels. Science of The Total Environment **653**:1571-1584.

Koziol, K. A., H. L. Moggridge, J. M. Cook, and A. J. Hodson. 2019. Organic carbon fluxes of a glacier surface: A case study of Foxfonna, a small Arctic glacier. Earth Surface Processes and Landforms **44**:405-416.

Koziorowska, K., K. Kuliński, and J. Pempkowiak. 2016. Sedimentary organic matter in two Spitsbergen fjords: Terrestrial and marine contributions based on carbon and nitrogen contents and stable isotopes composition. Continental Shelf Research **113**:38-46.

Kristensen, E., S. I. Ahmed, and A. H. Devol. 1995. Aerobic and anaerobic decomposition of organic matter in marine sediment: Which is fastest? Limnology and Oceanography **40**:1430-1437.

Kruskal, W. H., and W. A. Wallis. 1952. Use of Ranks in One-Criterion Variance Analysis. Journal of the American Statistical Association **47**:583-621.

Kuipers, B., P. de Wilde, and F. Creutzberg. 1981. Energy Flow in a Tidal Flat Ecosystem. Marine Ecology Progress Series **5**:215-221.

Lahav Lavian, I., S. Vishnevetsky, G. Barness, and Y. Steinberger. 2001. Soil microbial community and bacterial functional diversity at Machu Picchu, King George Island, Antarctica. Polar Biology **24**:411-416.

Lahti, L., S. Shetty, and et al. 2017-2020. microbiome: Tools for microbiome analysis in R. Bioconductor.

Lasareva, E. V., A. M. Parfenova, E. A. Romankevich, N. V. Lobus, and A. N. Drozdova. 2019. Organic Matter and Mineral Interactions Modulate Flocculation Across Arctic River Mixing Zones. Journal of Geophysical Research: Biogeosciences **124**:1651-1664.

Le Moine Bauer, S., I. Roalkvam, I. H. Steen, and H. Dahle. 2016. Lutibacter profundi sp. nov., isolated from a deep-sea hydrothermal system on the Arctic Mid-Ocean Ridge and emended description of the genus Lutibacter. International Journal of Systematic and Evolutionary Microbiology **66**:2671-2677.

Li, W., X. Lv, J. Ruan, M. Yu, Y.-B. Song, J. Yu, and M. Dong. 2019. Variations in Soil Bacterial Composition and Diversity in Newly Formed Coastal Wetlands. Frontiers in Microbiology **9**.

Li, Y., E. Kang, B. Song, J. Wang, X. Zhang, J. Wang, M. Li, L. Yan, Z. Yan, K. Zhang, H. Wu, and X. Kang. 2021. Soil salinity and nutrients availability drive patterns in bacterial community and diversity along succession gradient in the Yellow River Delta. Estuarine, Coastal and Shelf Science **262**:107621.

Liesack, W., and K. Finster. 2015. Desulfuromusa. Pages 1-6 *in* M. E. Trujillo, S. Dedysh, P. DeVos, B. Hedlund, P. Kämpfer, F. A. Rainey, and W. B. Whitman, editors. Bergey's Manual of Systematics of Archaea and Bacteria.

Lim, J.-M., C. O. Jeon, G. S. Lee, D.-J. Park, U.-G. Kang, C.-Y. Park, and C.-J. Kim. 2007. Leeia oryzae gen. nov., sp. nov., isolated from a rice field in Korea. International Journal of Systematic and Evolutionary Microbiology **57**:1204-1208.

Lim, J.-M., S.-J. Kim, M. Hamada, J.-H. Ahn, H.-Y. Weon, K.-i. Suzuki, T.-Y. Ahn, and S.-W. Kwon. 2014. Oryzihumus terrae sp. nov., isolated from soil and emended description of the genus Oryzihumus. International Journal of Systematic and Evolutionary Microbiology **64**:2395-2399.

Lisitzin, A. P. 1999. The Continental-Ocean Boundary as a Marginal Filter in the World Oceans. Pages 69-103 *in* J. S. Gray, W. Ambrose, and A. Szaniawska, editors. Biogeochemical Cycling and Sediment Ecology. Springer Netherlands, Dordrecht.

Loganathachetti, D. S., S. Venkatachalam, T. Jabir, P. V. Vipindas, and K. P. Krishnan. 2022. Total nitrogen influence bacterial community structure of active layer permafrost across summer and winter seasons in Ny-Ålesund, Svalbard. World Journal of Microbiology and Biotechnology **38**:28.

Logue, J. B., S. E. G. Findlay, and J. Comte. 2015. Editorial: Microbial Responses to Environmental Changes. Frontiers in Microbiology **6**.

Logue, J. B., C. A. Stedmon, A. M. Kellerman, N. J. Nielsen, A. F. Andersson, H. Laudon, E. S. Lindström, and E. S. Kritzberg. 2016. Experimental insights into the importance of aquatic bacterial community composition to the degradation of dissolved organic matter. The ISME Journal **10**:533-545.

Longbottom, M. R. 1970. The distribution of Arenicola marina (L.) with particular reference to the effects of particle size and organic matter of the sediments. Journal of Experimental Marine Biology and Ecology **5**:138-157.

Luna, G. M., E. Manini, and R. Danovaro. 2002. Large Fraction of Dead and Inactive Bacteria in Coastal Marine Sediments: Comparison of Protocols for Determination and Ecological Significance. Applied and Environmental Microbiology **68**:3509-3513.

Lv, X., B. Ma, J. Yu, S. X. Chang, J. Xu, Y. Li, G. Wang, G. Han, G. Bo, and X. Chu. 2016. Bacterial community structure and function shift along a successional series of tidal flats in the Yellow River Delta. Scientific Reports **6**:36550.

Macdonald, R. W., S. M. Solomon, R. E. Cranston, H. E. Welch, M. B. Yunker, and C. Gobeil. 1998. A sediment and organic carbon budget for the Canadian Beaufort Shelf. Marine Geology **144**:255-273.

Macdonald, R. W., and Y. Yu. 2006. The Mackenzie Estuary of the Arctic Ocean. Pages 91-120 *in* P. J. Wangersky, editor. Estuaries. Springer Berlin Heidelberg, Berlin, Heidelberg.

Madigan, M. T., D. O. Jung, C. R. Woese, and L. A. Achenbach. 2000. Rhodoferax antarcticus sp. nov., a moderately psychrophilic purple nonsulfur bacterium isolated from an Antarctic microbial mat. Arch Microbiol **173**:269-277.

Mann, P. J., T. I. Eglinton, C. P. McIntyre, N. Zimov, A. Davydova, J. E. Vonk, R. M. Holmes, and R. G. M. Spencer. 2015. Utilization of ancient permafrost carbon in headwaters of Arctic fluvial networks. Nature Communications **6**:7856.

Mann, P. J., R. G. M. Spencer, P. J. Hernes, J. Six, G. R. Aiken, S. E. Tank, J. W. McClelland, K. D. Butler, R. Y. Dyda, and R. M. Holmes. 2016. Pan-Arctic Trends in Terrestrial Dissolved Organic Matter from Optical Measurements. Frontiers in Earth Science **4**.

Männistö, M. K., E. Kurhela, M. Tiirola, and M. M. Häggblom. 2013. Acidobacteria dominate the active bacterial communities of Arctic tundra with widely divergent winter-time snow accumulation and soil temperatures. FEMS Microbiology Ecology **84**:47-59.

Marquardt, M., A. Vader, E. I. Stubner, M. Reigstad, and T. M. Gabrielsen. 2016. Strong Seasonality of Marine Microbial Eukaryotes in a High-Arctic Fjord (Isfjorden, in West Spitsbergen, Norway). Appl Environ Microbiol **82**:1868-1880.

Martin, M. 2011. Cutadapt removes adapter sequences from high-throughput sequencing reads. 2011 **17**:3.

Martini, I. P., R. I. G. Morrison, K. F. Abraham, L. A. Sergienko, and R. L. Jefferies. 2019. Chapter 4 - Northern Polar Coastal Wetlands: Development, Structure, and Land Use. Pages 153-186 *in* G. M. E. Perillo, E. Wolanski, D. R. Cahoon, and C. S. Hopkinson, editors. Coastal Wetlands (Second Edition). Elsevier.

Mason, O. U., T. C. Hazen, S. Borglin, P. S. G. Chain, E. A. Dubinsky, J. L. Fortney, J. Han, H.-Y. N. Holman, J. Hultman, R. Lamendella, R. Mackelprang, S. Malfatti, L. M. Tom, S. G. Tringe, T. Woyke, J. Zhou, E. M. Rubin, and J. K. Jansson. 2012. Metagenome, metatranscriptome and single-cell sequencing reveal microbial response to Deepwater Horizon oil spill. The ISME Journal **6**:1715-1727.

Mayor, D. J., B. Thornton, H. Jenkins, and S. L. Felgate. 2018. Microbiota: The Living Foundation. Pages 43-61 *in* P. G. Beninger, editor. Mudflat Ecology. Springer International Publishing, Cham.

McClelland, J. W., S. J. Déry, B. J. Peterson, R. M. Holmes, and E. F. Wood. 2006. A pan-arctic evaluation of changes in river discharge during the latter half of the 20th century. Geophysical Research Letters **33**.

McCrystall, M. R., J. Stroeve, M. Serreze, B. C. Forbes, and J. A. Screen. 2021. New climate models reveal faster and larger increases in Arctic precipitation than previously projected. Nature Communications **12**:6765.

McGovern, M., A. K. Pavlov, A. Deininger, M. A. Granskog, E. Leu, J. E. Søreide, and A. E. Poste. 2020. Terrestrial Inputs Drive Seasonality in Organic Matter and Nutrient Biogeochemistry in a High Arctic Fjord System (Isfjorden, Svalbard). Frontiers in Marine Science **7**.

McMurdie, P. J., and S. Holmes. 2013. phyloseq: An R Package for Reproducible Interactive Analysis and Graphics of Microbiome Census Data. PLOS ONE **8**:e61217.

Mekonnen, Z. A., W. J. Riley, L. T. Berner, N. J. Bouskill, M. S. Torn, G. Iwahana, A. L. Breen, I. H. Myers-Smith, M. G. Criado, Y. Liu, E. S. Euskirchen, S. J. Goetz, M. C. Mack, and R. F. Grant. 2021. Arctic tundra shrubification: a review of mechanisms and impacts on ecosystem carbon balance. Environmental Research Letters **16**:053001.

Meredith, M., M. Sommerkorn, S. Cassotta, C. Derksen, A. Ekaykin, A. Hollowed, G. Kofinas, A. Mackintosh, J. Melbourne-Thomas, M. Muelbert, G. Ottersen, H. Pritchard, and S. A.G. 2019. Chapter 3: Polar Regions.*in* H.-O. Pörtner, D. C. Roberts, V. Masson-Delmotte, P. Zhai, M. Tignor, E. Poloczanska, K. Mintenbeck, A. Alegría, M. Nicolai, A. Okem, J. Petzold, B. Rama, and N. M. Weyer, editors. IPCC Special Report on the Ocean and Cryosphere in a Changing Climate.

Meslard, F., F. Bourrin, G. Many, and P. Kerhervé. 2018. Suspended particle dynamics and fluxes in an Arctic fjord (Kongsfjorden, Svalbard). Estuarine, Coastal and Shelf Science **204**:212-224.

Miksch, S., M. Meiners, A. Meyerdierks, D. Probandt, G. Wegener, J. Titschack, M. A. Jensen, A. Ellrott, R. Amann, and K. Knittel. 2021. Bacterial communities in temperate and polar coastal sands are seasonally stable. ISME Communications **1**:29.

Mohapatra, M., R. Yadav, V. Rajput, M. S. Dharne, and G. Rastogi. 2021. Metagenomic analysis reveals genetic insights on biogeochemical cycling, xenobiotic degradation, and stress resistance in mudflat microbiome. Journal of Environmental Management **292**:112738.

Moran, M. A., E. B. Kujawinski, A. Stubbins, R. Fatland, L. I. Aluwihare, A. Buchan, B. C. Crump, P. C. Dorrestein, S. T. Dyhrman, N. J. Hess, B. Howe, K. Longnecker, P. M. Medeiros, J. Niggemann, I. Obernosterer, D. J. Repeta, and J. R. Waldbauer. 2016. Deciphering ocean carbon in a changing world. Proceedings of the National Academy of Sciences **113**:3143-3151.

Morata, N., E. Michaud, M.-A. Poullaouec, J. Devesa, M. Le Goff, R. Corvaisier, and P. E. Renaud. 2020. Climate change and diminishing seasonality in Arctic benthic processes. Philosophical Transactions of the Royal Society A: Mathematical, Physical and Engineering Sciences **378**:20190369.

Morency, C., L. Jacquemot, M. Potvin, and C. Lovejoy. 2022. A microbial perspective on the local influence of Arctic rivers and estuaries on Hudson Bay (Canada). Elementa: Science of the Anthropocene **10**.

Mosier, A., C. Kroeze, C. Nevison, O. Oenema, S. Seitzinger, and O. van Cleemput. 1998. Closing the global N2O budget: nitrous oxide emissions through the agricultural nitrogen cycle. Nutrient Cycling in Agroecosystems **52**:225-248.

Mougi, A. 2020. Coupling of green and brown food webs and ecosystem stability. Ecology and evolution **10**:9192-9199.

Mulholland, P. J. 1981. Formation of particulate organic carbon in water from a southeastern swamp-stream1. Limnology and Oceanography **26**:790-795.

Müller, A. L., C. Pelikan, J. R. de Rezende, K. Wasmund, M. Putz, C. Glombitza, K. U. Kjeldsen, B. B. Jørgensen, and A. Loy. 2018. Bacterial interactions during sequential degradation of cyanobacterial necromass in a sulfidic arctic marine sediment. Environmental Microbiology **20**:2927-2940.

Müller, O. 2018. Implications of a changing Arctic on microbial communities: Following the effects of thawing permafrost from land to sea. Thesis for the Degree of Philosophiae Doctor (PhD). University of Bergen, Norway.

Müller, O., L. Seuthe, G. Bratbak, and M. L. Paulsen. 2018. Bacterial Response to Permafrost Derived Organic Matter Input in an Arctic Fjord. Frontiers in Marine Science **5**.

Murray, N. J., S. R. Phinn, M. DeWitt, R. Ferrari, R. Johnston, M. B. Lyons, N. Clinton, D. Thau, and R. A. Fuller. 2019. The global distribution and trajectory of tidal flats. Nature **565**:222-225.

Nguyen, T. V., A. C. Alfaro, T. Young, S. Green, E. Zarate, and F. Merien. 2019. Itaconic acid inhibits growth of a pathogenic marine Vibrio strain: A metabolomics approach. Scientific Reports **9**:5937.

Niu, L., X. Xie, Y. Li, Q. Hu, C. Wang, W. Zhang, H. Zhang, and L. Wang. 2022. Effects of nitrogen on the longitudinal and vertical patterns of the composition and potential function of bacterial and archaeal communities in the tidal mudflats. Science of The Total Environment **806**:151210.

Noirungsee, N., S. Hackbusch, J. Viamonte, P. Bubenheim, A. Liese, and R. Müller. 2020. Influence of oil, dispersant, and pressure on microbial communities from the Gulf of Mexico. Scientific Reports **10**:7079.

Nowak, A., R. Hodgkins, A. Nikulina, M. Osuch, T. Wawrzyniak, J. Kavan, E. Łepkowska, M. Majerska, K. Romashova, I. Vasilevich, I. Sobota, and G. Rachlewicz. 2021. From land to fjords: The review of Svalbard hydrology from 1970 to 2019 (SvalHydro). Pages 176-201 SESS report 2020 - The State of Environmental Science in Svalbard - an annual report. Svalbard Integrated Arctic Earth Observing System.

Nowak, A., and A. Hodson. 2015. On the biogeochemical response of a glacierized High Arctic watershed to climate change: revealing patterns, processes and heterogeneity among micro-catchments. Hydrological Processes **29**:1588-1603.

O'Donnell, J. A., G. R. Aiken, D. K. Swanson, S. Panda, K. D. Butler, and A. P. Baltensperger. 2016. Dissolved organic matter composition of Arctic rivers: Linking permafrost and parent material to riverine carbon. Global Biogeochemical Cycles **30**:1811-1826.

Obata, T., S. Schoenefeld, I. Krahnert, S. Bergmann, A. Scheffel, and A. R. Fernie. 2013. Gas-Chromatography Mass-Spectrometry (GC-MS) Based Metabolite Profiling Reveals Mannitol as a Major Storage Carbohydrate in the Coccolithophorid Alga Emiliania huxleyi. Metabolites **3**.

Ogilvie, B., D. B. Nedwell, R. M. Harrison, A. Robinson, and A. Sage. 1997. High nitrate, muddy estuaries as nitrogen sinks: the nitrogen budget of the River Colne estuary (United Kingdom). Marine Ecology Progress Series **150**:217-228.

Oksanen, J., F. G. Blanchet, M. Friendly, R. Kindt, P. Legendre, D. McGlinn, P. R. Minchin, R. B. O'Hara, G. L. Simpson, P. Solymos, M. H. H. Stevens, E. Szoecs, and H. Wagner. 2020. vegan: Community Ecology Package.

Orland, C., K. M. Yakimovich, N. C. S. Mykytczuk, N. Basiliko, and A. J. Tanentzap. 2020. Think global, act local: The small-scale environment mainly influences microbial community development and function in lake sediment. Limnology and Oceanography **65**:S88-S100.

Overeem, I., B. Hudson, J. Syvitski, A. Mikkelsen, B. Hasholt, M. Van den Broeke, B. Noël, and M. Morlighem. 2017. Substantial export of suspended sediment to the global oceans from glacial erosion in Greenland. Nature Geoscience **10**.

Parada, A. E., D. M. Needham, and J. A. Fuhrman. 2016. Every base matters: assessing small subunit rRNA primers for marine microbiomes with mock communities, time series and global field samples. Environmental Microbiology **18**:1403-1414.

Parmentier, F.-J. W., T. R. Christensen, S. Rysgaard, J. Bendtsen, R. N. Glud, B. Else, J. van Huissteden, T. Sachs, J. E. Vonk, and M. K. Sejr. 2017. A synthesis of the arctic terrestrial and marine carbon cycles under pressure from a dwindling cryosphere. Ambio **46**:53-69.

Parsons, T. R., Y. Maita, and C. M. Lalli. 1984. A Manual of Chemical and Biological Methods for Seawater Analysis. Elsevier Science & Technology Books.

Pasternak, A., A. Drits, E. Arashkevich, and M. Flint. 2022. Differential Impact of the Khatanga and Lena (Laptev Sea) Runoff on the Distribution and Grazing of Zooplankton. Frontiers in Marine Science **9**.

Pastor, A., A. Freixa, L. J. Skovsholt, N. Wu, A. M. Romani, and T. Riis. 2019. Microbial Organic Matter Utilization in High-Arctic Streams: Key Enzymatic Controls. Microb Ecol **78**:539-554.

Paterson, D., R. Perkins, M. Consalvey, and G. Underwood. 2003. Ecosystem Function, Cell Micro-Cycling and the Structure of Transient Biofilms. Pages 47-63 *in* W. E. Krumbein, D. M. Paterson, and G. A. Zavarzin, editors. Fossil and Recent Biofilms: A Natural History of Life on Earth. Kluwer, London.

Paulsen, M. L., S. E. B. Nielsen, O. Müller, E. F. Møller, C. A. Stedmon, T. Juul-Pedersen, S. Markager, M. K. Sejr, A. Delgado Huertas, A. Larsen, and M. Middelboe. 2017. Carbon Bioavailability in a High Arctic Fjord Influenced by Glacial Meltwater, NE Greenland. Frontiers in Marine Science **4**.

Pavlov, A. K., E. Leu, D. Hanelt, I. Bartsch, U. Karsten, S. R. Hudson, J.-C. Gallet, F. Cottier, J. H. Cohen, J. Berge, G. Johnsen, M. Maturilli, P. Kowalczuk, S. Sagan, J. Meler, and M. A. Granskog. 2019. The Underwater Light Climate in Kongsfjorden and Its Ecological Implications. Pages 137-170 *in* H. Hop and C. Wiencke, editors. The Ecosystem of Kongsfjorden, Svalbard. Springer International Publishing, Cham.

Pearman, J. K., G. Thomson-Laing, J. D. Howarth, M. J. Vandergoes, L. Thompson, A. Rees, and S. A. Wood. 2021. Investigating variability in microbial community composition in replicate environmental DNA samples down lake sediment cores. PLOS ONE **16**:e0250783.

Peterson, B. J., R. M. Holmes, J. W. McClelland, C. J. Vörösmarty, R. B. Lammers, A. I. Shiklomanov, I. A. Shiklomanov, and S. Rahmstorf. 2002. Increasing river discharge to the Arctic Ocean. Science **298**:2171-2173.

Port of Longyearbyen. 2022. Statistics Port of Longyearbyen 2007 and 2015-2021.

Preston-Mafham, J., L. Boddy, and P. F. Randerson. 2002. Analysis of microbial community functional diversity using sole-carbon-source utilisation profiles – a critique. FEMS Microbiology Ecology **42**:1-14.

Quast, C., E. Pruesse, P. Yilmaz, J. Gerken, T. Schweer, P. Yarza, J. Peplies, and F. O. Glöckner. 2013. The SILVA ribosomal RNA gene database project: improved data processing and web-based tools. Nucleic Acids Res **41**:D590-596.

R Core Team. 2021. R: A Language and Environment for Statistical Computing. R Foundation for Statistical Computing, Vienna, Austria.

Raymond, P. A., and J. E. Bauer. 2001. Riverine export of aged terrestrial organic matter to the North Atlantic Ocean. Nature **409**:497-500.

Reineck, H. E., and I. B. Singh. 1973. Depositional Sedimentary Environments: With Reference to Terrigenous Clastics. Springer Berlin Heidelberg.

Reise, K. 1985. Biogeochemistry of Tidal Sediments. Pages 17-24 Tidal Flat Ecology: An Experimental Approach to Species Interactions. Springer Berlin Heidelberg, Berlin, Heidelberg.

Ren, L., X. Chang, F. Jiang, W. Kan, Z. Qu, X. Qiu, C. Fang, and F. Peng. 2015. Parablastomonas arctica gen. nov., sp. nov., isolated from high Arctic glacial till. International Journal of Systematic and Evolutionary Microbiology **65**:260-266.

Rivers, A. R., S. Sharma, S. G. Tringe, J. Martin, S. B. Joye, and M. A. Moran. 2013. Transcriptional response of bathypelagic marine bacterioplankton to the Deepwater Horizon oil spill. The ISME Journal **7**:2315-2329.

Rodenburg, M. A. J. 2019. The Advent River system, Central Svalbard: A high temporal resolution analysis of sediment flux from a dynamic arctic river-mouth. Master Thesis. Vrije Universiteit.

Rodriguez, G. G., D. Phipps, K. Ishiguro, and H. F. Ridgway. 1992. Use of a fluorescent redox probe for direct visualization of actively respiring bacteria. Applied and Environmental Microbiology **58**:1801-1808.

RStudio Team. 2021. RStudio: Integrated Development Environment for R. RStudio, PBC, Boston, MA.

Ruiz-González, C., J. P. Niño-García, J.-F. Lapierre, and P. A. del Giorgio. 2015. The quality of organic matter shapes the functional biogeography of bacterioplankton across boreal freshwater ecosystems. Global Ecology and Biogeography **24**:1487-1498.

Rumpho, M. E., G. E. Edwards, and W. H. Loescher. 1983. A Pathway for Photosynthetic Carbon Flow to Mannitol in Celery Leaves 1: Activity and Localization of Key Enzymes. Plant Physiology **73**:869-873.

Sala, M. M., L. Arin, V. Balagué, J. Felipe, Ò. Guadayol, and D. Vaqué. 2005. Functional diversity of bacterioplankton assemblages in western Antarctic seawaters during late spring. Marine Ecology Progress Series **292**:13-21.

Sala, M. M., J. M. Arrieta, J. A. Boras, C. M. Duarte, and D. Vaqué. 2010. The impact of ice melting on bacterioplankton in the Arctic Ocean. Polar Biology **33**:1683-1694.

Sala, M. M., C. Ruiz-González, E. Borrull, I. Azúa, Z. Baña, B. Ayo, X. A. Álvarez-Salgado, J. M. Gasol, and C. M. Duarte. 2020. Prokaryotic Capability to Use Organic Substrates Across the Global Tropical and Subtropical Ocean. Frontiers in Microbiology **11**.

Sala, M. M., R. Terrado, C. Lovejoy, F. Unrein, and C. Pedrós-Alió. 2008. Metabolic diversity of heterotrophic bacterioplankton over winter and spring in the coastal Arctic Ocean. Environmental Microbiology **10**:942-949.

Schmitz, K., and L. M. Srivastava. 1975. On the fine structure of sieve tubes and the physiology of assimilate transport in Alaria marginata. Canadian Journal of Botany **53**:861-876.

Schostag, M., M. Stibal, C. S. Jacobsen, J. Bælum, N. Taş, B. Elberling, J. K. Jansson, P. Semenchuk, and A. Priemé. 2015. Distinct summer and winter bacterial communities in the active layer of Svalbard permafrost revealed by DNA- and RNA-based analyses. Frontiers in Microbiology **6**.

Schreiner, K. M., T. S. Bianchi, and B. E. Rosenheim. 2014. Evidence for permafrost thaw and transport from an Alaskan North Slope watershed. Geophysical Research Letters **41**:3117-3126.

Schröder, H. G. J., and F. B. Van Es. 1980. Distribution of bacteria in intertidal sediments of the EMS-Dollard estuary. Netherlands Journal of Sea Research **14**:268-287.

Schutte, C. A., S. Ahmerkamp, C. S. Wu, M. Seidel, D. de Beer, P. L. M. Cook, and S. B. Joye. 2019. Chapter 12 - Biogeochemical Dynamics of Coastal Tidal Flats. Pages 407-440 *in* G. M. E. Perillo, E. Wolanski, D. R. Cahoon, and C. S. Hopkinson, editors. Coastal Wetlands (Second Edition). Elsevier.

Segawa, T., S. Ishii, N. Ohte, A. Akiyoshi, A. Yamada, F. Maruyama, Z. Li, Y. Hongoh, and N. Takeuchi. 2014. The nitrogen cycle in cryoconites: naturally occurring nitrification-denitrification granules on a glacier. Environmental Microbiology **16**:3250-3262.

Semenova, E. M., T. L. Babich, D. S. Sokolova, A. S. Dobriansky, A. V. Korzun, and D. R. Kryukov. 2021. Microbial Diversity of Hydrocarbon-Contaminated Soils of the Franz Josef Land Archipelago. Microbiology **90**:721-730.

Shade, A., H. Peter, S. Allison, D. Baho, M. Berga, H. Buergmann, D. Huber, S. Langenheder, J. Lennon, J. Martiny, K. Matulich, T. Schmidt, and J. Handelsman. 2012. Fundamentals of Microbial Community Resistance and Resilience. Frontiers in Microbiology **3**.

Sholkovitz, E. R. 1976. Flocculation of dissolved organic and inorganic matter during the mixing of river water and seawater. Geochimica et Cosmochimica Acta **40**:831-845.

Sipler, R. E., C. T. E. Kellogg, T. L. Connelly, Q. N. Roberts, P. L. Yager, and D. A. Bronk. 2017. Microbial Community Response to Terrestrially Derived Dissolved Organic Matter in the Coastal Arctic. Front Microbiol **8**:1018.

Skogsberg, E., M. McGovern, A. Poste, S. Jonsson, M. T. Arts, Ø. Varpe, and K. Borgå. 2022. Seasonal pollutant levels in littoral high-Arctic amphipods in relation to food sources and terrestrial run-off. Environmental Pollution:119361.

Smith, E., and P. Delgiorgio. 2003. Low fractions of active bacteria in natural aquatic communities? Aquatic Microbial Ecology **31**:203-208.

Smith, K. G., and P. G. Connors. 1993. Postbreeding habitat selection by shorebirds, water birds, and land birds at Barrow, Alaska: a multivariate analysis. Canadian Journal of Zoology **71**:1629-1638.

Sobczak, W. V., J. E. Cloern, A. D. Jassby, and A. B. Müller-Solger. 2002. Bioavailability of organic matter in a highly disturbed estuary: The role of detrital and algal resources. Proceedings of the National Academy of Sciences **99**:8101-8105.

Sofo, A., and P. Ricciuti. 2019. A Standardized Method for Estimating the Functional Diversity of Soil Bacterial Community by Biolog® EcoPlatesTM Assay—The Case Study of a Sustainable Olive Orchard. Applied Sciences **9**:4035.

Solomon, A., C. Heuzé, B. Rabe, S. Bacon, L. Bertino, P. Heimbach, J. Inoue, D. Iovino, R. Mottram, X. Zhang, Y. Aksenov, R. McAdam, A. Nguyen, R. P. Raj, and H. Tang. 2021. Freshwater in the Arctic Ocean 2010–2019. Ocean Sci. **17**:1081-1102.

Stevenson, L. H. 1977. A case for bacterial dormancy in aquatic systems. Microbial Ecology **4**:127-133.

Stoop, J. M. H., J. D. Williamson, and D. Mason Pharr. 1996. Mannitol metabolism in plants: a method for coping with stress. Trends in Plant Science **1**:139-144.

Strickland, M. S., C. Lauber, N. Fierer, and M. A. Bradford. 2009. Testing the functional significance of microbial community composition. Ecology **90**:441-451.

Sun, S., R. B. Jones, and A. A. Fodor. 2020. Inference-based accuracy of metagenome prediction tools varies across sample types and functional categories. Microbiome **8**:46.

Sutherland, R. A. 1998. Loss-on-ignition estimates of organic matter and relationships to organic carbon in fluvial bed sediments. Hydrobiologia **389**:153-167.

Tait, K., R. L. Airs, C. E. Widdicombe, G. A. Tarran, M. R. Jones, and S. Widdicombe. 2015. Dynamic responses of the benthic bacterial community at the Western English Channel observatory site L4 are driven by deposition of fresh phytodetritus. Progress in Oceanography **137**:546-558.

Tam, L., P. Kevan, and J. Trevors. 2003. Viable bacterial biomass and functional diversity in fresh and marine waters in the Canadian Arctic. Polar Biology **26**:287-294.

Taylor, A. R., R. B. Lanctot, A. N. Powell, F. Huettmann, D. A. Nigro, and S. J. Kendall. 2010. Distribution and community characteristics of staging shorebirds on the northern coast of Alaska. Arctic **63**:451-467.

Tebbe, D. A., S. Geihser, B. Wemheuer, R. Daniel, H. Schäfer, and B. Engelen. 2022. Seasonal and Zonal Succession of Bacterial Communities in North Sea Salt Marsh Sediments. Microorganisms **10**:859.

Teeling, H., M. Fuchs Bernhard, D. Becher, C. Klockow, A. Gardebrecht, M. Bennke Christin, M. Kassabgy, S. Huang, J. Mann Alexander, J. Waldmann, M. Weber, A. Klindworth, A. Otto, J. Lange, J. Bernhardt, C. Reinsch, M. Hecker, J. Peplies, D. Bockelmann Frank, U. Callies, G. Gerdts, A. Wichels, H. Wiltshire Karen, O. Glöckner Frank, T. Schweder, and R. Amann. 2012. Substrate-Controlled Succession of Marine Bacterioplankton Populations Induced by a Phytoplankton Bloom. Science **336**:608-611.

Terhaar, J., R. Lauerwald, P. Regnier, N. Gruber, and L. Bopp. 2021. Around one third of current Arctic Ocean primary production sustained by rivers and coastal erosion. Nature Communications **12**:169.

The Editorial Board. 2015. Psychromonas. Pages 1-4 *in* M. E. Trujillo, S. Dedysh, P. DeVos, B. Hedlund, P. Kämpfer, F. A. Rainey, and W. B. Whitman, editors. Bergey's Manual of Systematics of Archaea and Bacteria.

Thomas, F. A., R. K. Sinha, and K. P. Krishnan. 2020. Bacterial community structure of a glacio-marine system in the Arctic (Ny-Ålesund, Svalbard). Science of The Total Environment **718**:135264.

Torsvik, T., J. Albretsen, A. Sundfjord, J. Kohler, A. D. Sandvik, J. Skarðhamar, K. Lindbäck, and A. Everett. 2019. Impact of tidewater glacier retreat on the fjord system: Modeling present and future circulation in Kongsfjorden, Svalbard. Estuarine, Coastal and Shelf Science **220**:152-165.

Trimmer, M., D. B. Nedwell, D. B. Sivyer, and S. J. Malcolm. 1998. Nitrogen fluxes through the lower estuary of the river Great Ouse, England: The role of the bottom sediments. Marine Ecology Progress Series **163**:109-124.

Uchino, Y., T. Hamada, and A. Yokota. 2002. Proposal of Pseudorhodobacter ferrugineus gen nov, comb nov, for a non-photosynthetic marine bacterium, Agrobacterium ferrugineum, related to the genus Rhodobacter. J Gen Appl Microbiol **48**:309-319.

Uchino, Y., T. Hamada, and A. Yokota. 2002. Proposal of *Pseudorhodobacter ferrugineus* gen. nov., comb. nov.,for a non-photosynthetic marine bacterium, *Agrobacterium ferrugineum*, related to the genus *Rhodobacter*. The Journal of General and Applied Microbiology **48**:309-319.

Underwood, G. J. C., and J. C. Kromkamp. 1999. Primary Production by Phytoplankton and Microphytobenthos in Estuaries. Advances in Ecological Research **29**:93-153.

Underwood, G. J. C., C. Michel, G. Meisterhans, A. Niemi, C. Belzile, M. Witt, A. J. Dumbrell, and B. P. Koch. 2019. Organic matter from Arctic sea-ice loss alters bacterial community structure and function. Nature Climate Change **9**:170-176.

Underwood, G. J. C., R. G. Perkins, M. C. Consalvey, A. R. M. Hanlon, K. Oxborough, N. R. Baker, and D. M. Paterson. 2005. Patterns in microphytobenthic primary productivity: Species-specific variation in migratory rhythms and photosynthetic efficiency in mixed-species biofilms. Limnology and Oceanography **50**:755-767.

UNESCO. 1981. Tenth report of the joint panel on oceanographic tables and standards. Paris.

Valdés-Castro, V., H. E. González, R. Giesecke, C. Fernández, and V. Molina. 2022. Assessment of Microbial Community Composition Changes in the Presence of Phytoplankton-Derived Exudates in Two Contrasting Areas from Chilean Patagonia. Diversity **14**.

Varpe, Ø., and B.-J. Bårdsen. 2014. Adventdalsdeltaet og fjæreplyttens sesongmessige bruk av det marine habitat.

Vázquez, J. A., A. Durán, I. Rodríguez-Amado, M. A. Prieto, D. Rial, and M. A. Murado. 2011. Evaluation of toxic effects of several carboxylic acids on bacterial growth by toxicodynamic modelling. Microbial Cell Factories **10**:100.

Viganò, L., A. Arillo, A. Buffagni, M. Camusso, R. Ciannarella, G. Crosa, C. Falugi, S. Galassi, L. Guzzella, A. Lopez, M. Mingazzini, R. Pagnotta, L. Patrolecco, G. Tartari, and S. Valsecchi. 2003. Quality assessment of bed sediments of the Po River (Italy). Water Res **37**:501-518.

Vihtakari, M. 2020. PlotSvalbard - Plot research data from Svalbard on maps.

Vishnupriya, S., T. Jabir, K. P. Krishnan, and A. A. Mohamed Hatha. 2021. Bacterial community structure and functional profiling of high Arctic fjord sediments. World Journal of Microbiology and Biotechnology **37**:133.

Volkman, J. K., D. Rohjans, J. Rullkötter, B. M. Scholz-Böttcher, and G. Liebezeit. 2000. Sources and diagenesis of organic matter in tidal flat sediments from the German Wadden Sea. Continental Shelf Research **20**:1139-1158.

Vonk, J. E., P. J. Mann, S. Davydov, A. Davydova, R. G. M. Spencer, J. Schade, W. V. Sobczak, N. Zimov, S. Zimov, E. Bulygina, T. I. Eglinton, and R. M. Holmes. 2013. High biolability of ancient permafrost carbon upon thaw. Geophysical Research Letters **40**:2689-2693.

Walch, D. 2021. Spatio-temporal variability in suspended particulate matter

in a high Arctic estuary (Adventfjorden, Svalbard): A combined Field- and Remote Sensing approach. Master Thesis. Potsdam University.

Wang, J., L. Wang, W. Hu, Z. Pan, P. Zhang, C. Wang, J. Wang, S. Wu, and Y.-z. Li. 2021. Assembly processes and source tracking of planktonic and benthic bacterial communities in the Yellow River estuary. Environmental Microbiology **23**:2578-2591.

Wang, N. F., T. Zhang, X. Yang, S. Wang, Y. Yu, L. L. Dong, Y. D. Guo, Y. X. Ma, and J. Y. Zang. 2016. Diversity and Composition of Bacterial Community in Soils and Lake Sediments from an Arctic Lake Area. Frontiers in Microbiology **7**.

Wang, Q., G. M. Garrity, J. M. Tiedje, and J. R. Cole. 2007. Naïve Bayesian Classifier for Rapid Assignment of rRNA Sequences into the New Bacterial Taxonomy. Applied and Environmental Microbiology **73**:5261-5267.

Wang, Q., Y. Li, and Y. Wang. 2011. Optimizing the weight loss-on-ignition methodology to quantify organic and carbonate carbon of sediments from diverse sources. Environ Monit Assess **174**:241-257.

Wang, Y., T. Healy, P. Augustinus, M. Baba, C. Bao, B. Flemming, M. Fortes, M. Han, E. Marone, A. Mehta, X. Ke, R. Kirby, B. Kjerfve, Y. Schaeffer-Novelli, and E. Wolanski. 2002. Definition, properties, and classification of muddy coasts. Pages 9-18 *in* T. Healy, Y. Wang, and J.-A. Healy, editors. Muddy Coasts of the World: Processes, Deposits and Function. Elsevier.

Wang, Z. J., Z. H. Xie, C. Wang, Z. J. Du, and G. J. Chen. 2014. Motiliproteus sediminis gen. nov., sp. nov., isolated from coastal sediment. Antonie Van Leeuwenhoek **106**:615-621.

Ward, J. H. 1963. Hierarchical Grouping to Optimize an Objective Function. Journal of the American Statistical Association **58**:236-244.

Warwick, R. M., I. R. Joint, and P. J. Radford. 1979. Secondary production of the benthos in an estuarine environment. Pages 429-450 *in* R. L. Jefferies and A. J. Davy, editors. Ecological processes in coastal environments. Blackwell Scientific, Oxford, U.K.

Watling, L. 1991. The Sedimentary Milieu and Its Consequences for Resident Organisms. American Zoologist **31**:789-796.

Weslawski, J., M. Gluchowska, L. Kotwicki, W. Szczuciński, A. Tatarek, J. Wiktor, M. Wlodarska-Kowalczuk, and M. Zajączkowski. 2011. Adventfjorden: Arctic sea in the backyard. Institute of Oceanology PAS, Sopot.

Weslawski, J. M., M. Szymelfenig, M. Zajaczkowski, and A. Keck. 1999. Influence of salinity and suspended matter on benthos of an Arctic tidal flat. ICES Journal of Marine Science **56**:194-202.

Wickham, H. 2016. ggplot2: Elegant Graphics for Data Analysis. Springer-Verlag New York.

Wickham, H., M. Averick, J. Bryan, W. Chang, L. D. A. McGowan, R. François, G. Grolemund, A. Hayes, L. Henry, and J. Hester. 2019. Welcome to the Tidyverse. Journal of open source software **4**:1686.

Wietz, M., C. Bienhold, K. Metfies, S. Torres-Valdés, W.-J. von Appen, I. Salter, and A. Boetius. 2021. The polar night shift: seasonal dynamics and drivers of Arctic Ocean microbiomes revealed by autonomous sampling. ISME Communications **1**:76.

Wiktor, J., A. Tatarek, J. M. Węsławski, L. Kotwicki, and M. Poulin. 2016. Colonies of Gyrosigma eximium: a new phenomenon in Arctic tidal flats. Oceanologia **58**:336-340.

Wild, B., A. Andersson, L. Bröder, J. Vonk, G. Hugelius, W. McClelland James, W. Song, A. Raymond Peter, and Ö. Gustafsson. 2019. Rivers across the Siberian Arctic unearth the patterns of carbon release from thawing permafrost. Proceedings of the National Academy of Sciences **116**:10280-10285.

Wilms, R., H. Sass, B. Köpke, J. Köster, H. Cypionka, and B. Engelen. 2006. Specific Bacterial, Archaeal, and Eukaryotic Communities in Tidal-Flat Sediments along a Vertical Profile of Several Meters. Applied and Environmental Microbiology **72**:2756-2764.

Xing, P., R. L. Hahnke, F. Unfried, S. Markert, S. Huang, T. Barbeyron, J. Harder, D. Becher, T. Schweder, F. O. Glöckner, R. I. Amann, and H. Teeling. 2015. Niches of two polysaccharide-degrading Polaribacter isolates from the North Sea during a spring diatom bloom. The ISME Journal **9**:1410-1422.

Xu, S., and G. Yu. 2021. MicrobiotaProcess: an R package for analysis, visualization and biomarker discovery of microbiome.

Xue, Y., I. Jonassen, L. Øvreås, and N. Taş. 2020. Metagenome-assembled genome distribution and key functionality highlight importance of aerobic metabolism in Svalbard permafrost. FEMS Microbiology Ecology **96**:fiaa057.

Yakimov, M. M., L. Giuliano, G. Gentile, E. Crisafi, T. N. Chernikova, W. R. Abraham, H. Lünsdorf, K. N. Timmis, and P. N. Golyshin. 2003. Oleispira antarctica gen. nov., sp. nov., a novel hydrocarbonoclastic marine bacterium isolated from Antarctic coastal sea water. Int J Syst Evol Microbiol **53**:779-785.

Yakimov, M. M., K. N. Timmis, and P. N. Golyshin. 2007. Obligate oil-degrading marine bacteria. Current Opinion in Biotechnology **18**:257-266.

Yamaguchi, T., T. Ikawa, and K. Nisizawa. 1969. Pathway of mannitol formation during photosynthesis in brown algae1. Plant and Cell Physiology **10**:425-440.

Yan, S., B. M. Fuchs, S. Lenk, J. Harder, J. Wulf, N. Z. Jiao, and R. Amann. 2009. Biogeography and phylogeny of the NOR5/OM60 clade of Gammaproteobacteria. Syst Appl Microbiol **32**:124-139.

Yan, Y.-W., Q.-Y. Jiang, J.-G. Wang, T. Zhu, B. Zou, Q.-F. Qiu, and Z.-X. Quan. 2018. Microbial Communities and Diversities in Mudflat Sediments Analyzed Using a Modified Metatranscriptomic Method. Frontiers in Microbiology **9**.

Yoon, J., Y. Matsuo, K. Adachi, M. Nozawa, S. Matsuda, H. Kasai, and A. Yokota. 2008. Description of Persicirhabdus sediminis gen. nov., sp. nov., Roseibacillus ishigakijimensis gen. nov., sp. nov., Roseibacillus ponti sp. nov., Roseibacillus persicicus sp. nov., Luteolibacter pohnpeiensis gen. nov., sp. nov. and Luteolibacter algae sp. nov., six marine members of the phylum 'Verrucomicrobia', and emended descriptions of the class Verrucomicrobiae, the order Verrucomicrobiales and the family Verrucomicrobiaceae. International Journal of Systematic and Evolutionary Microbiology **58**:998-1007.

Zaborska, A., J. Carroll, C. Papucci, L. Torricelli, M. L. Carroll, J. Walkusz-Miotk, and J. Pempkowiak. 2008. Recent sediment accumulation rates for the Western margin of the Barents Sea. Deep Sea Research Part II: Topical Studies in Oceanography **55**:2352-2360.

Zajączkowski, M., H. Nygård, E. N. Hegseth, and J. Berge. 2010. Vertical flux of particulate matter in an Arctic fjord: the case of lack of the sea-ice cover in Adventfjorden 2006–2007. Polar Biology **33**:223-239.

Zajączkowski, M., and M. Włodarska-Kowalczuk. 2007. Dynamic sedimentary environments of an Arctic glacier-fed river estuary (Adventfjorden, Svalbard). I. Flux, deposition, and sediment dynamics. Estuarine, Coastal and Shelf Science **74**:285-296.

Zak, J. C., M. R. Willig, D. L. Moorhead, and H. G. Wildman. 1994. Functional diversity of microbial communities: A quantitative approach. Soil Biology and Biochemistry **26**:1101-1108.

Zeng, Y.-X., Y. Yu, H.-R. Li, and W. Luo. 2017. Prokaryotic Community Composition in Arctic Kongsfjorden and Sub-Arctic Northern Bering Sea Sediments As Revealed by 454 Pyrosequencing. Frontiers in Microbiology **8**.

Zeng, Y. X., W. Luo, H. R. Li, and Y. Yu. 2021. High diversity of planktonic prokaryotes in Arctic Kongsfjorden seawaters in summer 2015. Polar Biology **44**:195-208.

Zhang, H., S. Zheng, J. Ding, O. Wang, and F. Liu. 2017. Spatial variation in bacterial community in natural wetland-river-sea ecosystems. Journal of Basic Microbiology **57**:536-546.

Zhang, T., J. Li, N. Wang, H. Wang, and L. Yu. 2022. Metagenomic analysis reveals microbiome and resistome in the seawater and sediments of Kongsfjorden (Svalbard, High Arctic). Science of The Total Environment **809**:151937.

Zhao, M., C. Yin, Y. Tao, C. Li, and S. Fang. 2019. Diversity of soil microbial community identified by Biolog method and the associated soil characteristics on reclaimed Scirpus mariqueter wetlands. SN Applied Sciences **1**:1408.

Zhou, D., X. Tan, W. Zhang, H.-Y. Chen, Q.-M. Fan, X.-L. He, and J. Lv. 2019. Rhodoferax bucti sp. nov., isolated from fresh water. International Journal of Systematic and Evolutionary Microbiology **69**:3903-3909.

Ziaja, W. 2005. Response of the Nordenskiöld Land (Spitsbergen) glaciers Grumantbreen, Håbergbreen and Dryadbreen to the climate warming after the Little Ice Age. Annals of Glaciology **42**:189-194.

Zou, K., E. Thébault, G. Lacroix, and S. Barot. 2016. Interactions between the green and brown food web determine ecosystem functioning. Functional Ecology **30**:1454-1465.

7 Appendix

Table A1. Sediment sampling dates, precise locations, times when sampling began, and tidal information.

Station	*Site*	*Date*	*Latitude*	*Longitude*	*Time*	*Tidal Height (cm)*	*Rising or falling?*
Intertidal	x	07/05/2021	78º13.448'N	15º41.182'E	17:28	28	Low
Intertidal	y	07/05/2021	78º13.430'N	15º41.118'E	18:20	28	Low
Intertidal	z	07/05/2021	78º13.410'N	15º40.998'E	18:35	28	Low
Fjord	x	11/05/2021	78º14.273'N	15º41.172'E	14:05	157	High
Fjord	y	11/05/2021	78º14.050'N	15º40.686'E	13:30	152	Rising
Fjord	z	12/05/2021	78º13.953'N	15º40.572'E	14:11	141	High
Intertidal	x	11/06/2021	78º13.407'N	15º42.026'E	12:30	116	Rising
Intertidal	y	11/06/2021	78º13.397'N	15º41.819'E	12:00	103	Rising
Intertidal	z	11/06/2021	78º13.419'N	15º41.678'E	11:37	94	Rising
River	x	11/06/2021	78º12.280'N	15º49.491'E	15:00	157	High
River	y	11/06/2021	78.12.269'N	15º49.448'E	14:41	157	High
River	z	11/06/2021	78º12.262'N	15º49.526'E	14:15	154	High
Fjord	x	14/06/2021	78º14.138'N	15º41.010'E	11:40	59	Rising
Fjord	y	14/06/2021	78º14.030'N	15º40.649'E	12:21	69	Rising
Fjord	z	14/06/2021	78º13.947'N	15º40.469'E	12:38	76	Rising
Subtidal	x	15/06/2021	78º13.957'N	15º41.556'E	14:05	90	Rising
Subtidal	y	15/06/2021	78º13.909'N	15º41.405'E	13:46	84	Rising
Subtidal	z	15/06/2021	78º13.854'N	15º41.243'E	13:17	77	Rising
Intertidal	x	10/07/2021	78º13.463'N	15º42.161'E	11:00	83	Rising
Intertidal	y	10/07/2021	78º13.443'N	15º42.108'E	11:22	91	Rising
Intertidal	z	10/07/2021	78º13.427'N	15º42.115'E	11:50	104	Rising
River	x	10/07/2021	78º12.287'N	15º49.452'E	14:40	150	High
River	y	10/07/2021	78º12.266'N	15º49.415'E	14:20	151	High
River	z	10/07/2021	78º12.265'N	15º49.494'E	14:01	149	High
Fjord	x	14/07/2021	78º14.188'N	15º40.896'E	14:44	112	Rising
Fjord	y	14/07/2021	78º14.072'N	15º40.630'E	15:04	122	Rising
Fjord	z	14/07/2021	78º13.957'N	15º40.564'E	15:08	125	Rising
Subtidal	x	15/07/2021	78º13.955'N	15º41.595'E	13:55	73	Rising
Subtidal	y	15/07/2021	78º13.898'N	15º41.465'E	13:35	67	Rising
Subtidal	z	15/07/2021	78º13.849'N	15º41.319'E	13:20	63	Rising
Intertidal	x	12/08/2021	78º13.410'N	15º42.042'E	13:59	100	Rising
Intertidal	y	12/08/2021	78º13.393'N	15º41.957'E	13:39	90	Rising
Intertidal	z	12/08/2021	78º13.366'N	15º41.997'E	14:30	118	Rising
River	x	12/08/2021	78º12.287'N	15º49.440'E	10:10	30	Falling
River	y	12/08/2021	78º12.274'N	15º49.467'E	10:00	33	Falling
River	z	12/08/2021	78º12.258'N	15º49.560'E	09:45	37	Falling
Fjord	x	16/08/2021	78º13.154'N	15º40.953'E	11:45	78	Falling
Fjord	y	16/08/2021	78º14.154'N	15º40.953'E	12:10	69	Falling
Fjord	z	16/08/2021	78º13.854'N	15º40.572'E	12:25	64	Falling
Subtidal	x	17/08/2021	78º13.957'N	15º41.553'E	13:55	58	Falling
Subtidal	y	17/08/2021	78º13.902'N	15º41.406'E	14:18	53	Falling
Subtidal	z	17/08/2021	78º13.855'N	15º41.240'E	14:38	52	Falling
Intertidal	x	10/09/2021	78º13.426'N	15º42.036'E	10:35	9	Rising
Intertidal	y	10/09/2021	78º13.411'N	15º42.056'E	10:15	7	Low
Intertidal	z	10/09/2021	78º13.393'N	15º41.936'E	11:00	16	Rising
River	x	10/09/2021	78º12.290'N	15º49.429'E	13:30	90	Rising
River	y	10/09/2021	78º12.269'N	15º49.444'E	13:08	78	Rising
River	z	10/09/2021	78º12.261'N	15º49.531'E	12:50	66	Rising
Fjord	x	13/09/2021	78º14.147'N	15º40.990'E	12:11	37	Low
Fjord	y	13/09/2021	78º14.044'N	15º40.692'E	12:30	37	Low
Fjord	z	13/09/2021	78º13.952'N	15º40.565'E	12:47	39	Rising
Subtidal	x	14/09/2021	78º13.954'N	15º41.527'E	13:23	45	Rising
Subtidal	y	14/09/2021	78º13.898'N	15º41.408'E	13:43	47	Rising
Subtidal	Z	14/09/2021	78º13.861'N	15º41.278'E	14:05	51	Rising

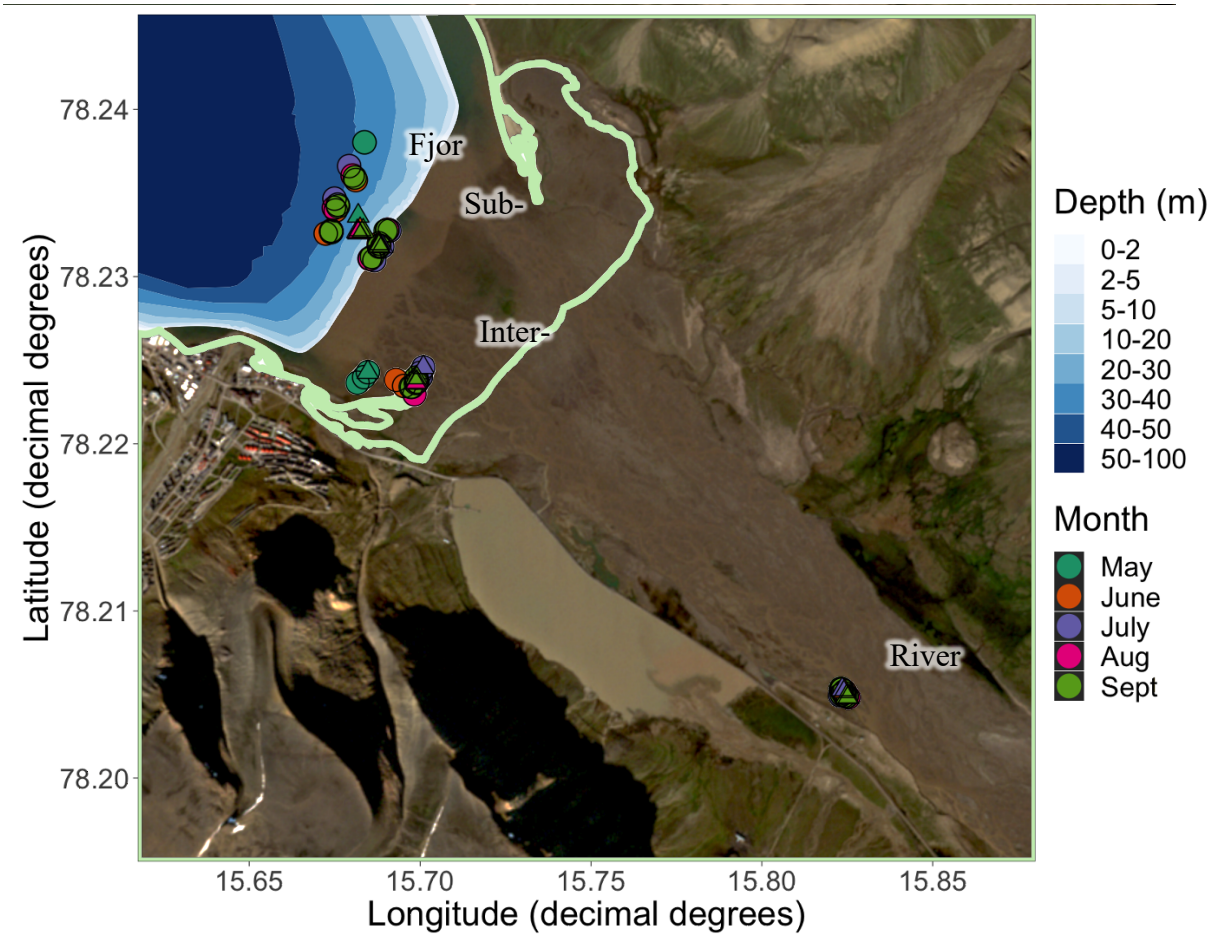

Figure A1. Map of all sampling sites, colored by month. Circles represent sediment samples while triangles represent adjacent water samples (one collected from each station, each month). Green line demarcates medium high tide level (Norwegian Mapping Authority). Satellite image from August 14, 2021 retrieved from Sentinel EO Browser.

Table A2. Substrates included in Biolog EcoPlates™, grouped according to molecular guilds (Sala et al. 2010).

Amines	**Carbohydrates**	**Carboxylic Acids**	**Phenolic Compounds**
Phenylethylamine	D-Cellobiose	D-Galacturonic Acid	2-Hydroxy Benzonic Acid
Putrescine	D-Galactonic Acid y-Lactone	D-Glucosaminic Acid	4-Hydroxy Benzonic Acid
	D-Mannitol	D-Malic Acid	
Amino Acids	D-Xylose	Glycyl-L-Glutamic Acid	**Polymers**
L-Arginine	D,L-α-Glycerol Phosphate	Itaconic Acid	Glycogen
L-Asparagine	Glucose-1-Phosphate	Pyruvic Acid Methyl Ester	Tween 40
L-Phenylalanine	i-Erythritol	α-Ketobutyric Acid	Tween 80
L-Serine	N-Acetyl-D-Glucosamine	γ-Hydroxybutyric Acid	α-Cyclodextrin
L-Threonine	α-D-Lactose		
	β-Methyl-D-Glucoside		

Table A3. Sediment samples used for Biolog EcoPlates™. One replicate site was used for each station from June through September. In May, only intertidal and fjord samples were collected, and only results from the fjord sediments plate are included in this study for comparison to the melt season samples..

Station	May	June	July	August	September
River		6.River.x	7.River.y	8.River.z	9.River.z
Intertidal	5.Intertidal.x	6.Intertidal.z	7.Intertidal.x	8.Intertidal.y	9.Intertidal.x
Subtidal		6.Subtidal.y	7.Subtidal.y	8.Subtidal.y	9.Subtidal.y
Fjord	5.Fjord.y	6.Fjord.x	7.Fjord.y	8.Fjord.y	9.Fjord.x

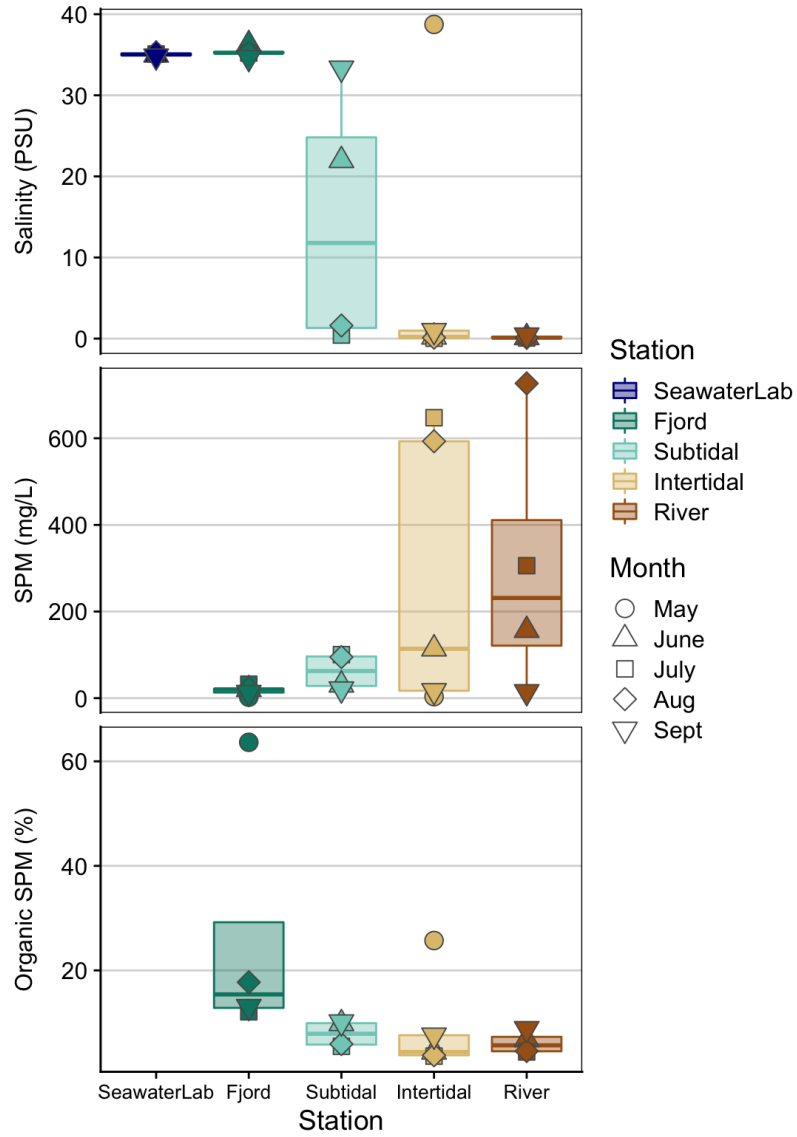

Figure A2. Boxplots showing **(A)** salinity, **(B)** total SPM, and **(C)** organic content of SPM of adjacent water from each station from all months and Seawater Lab water (used in sediment suspensions for EcoPlates). Points represent individual water samples, with shape displaying month. Particulates were not analyzed in Seawater Lab water as it was pre-filtered.

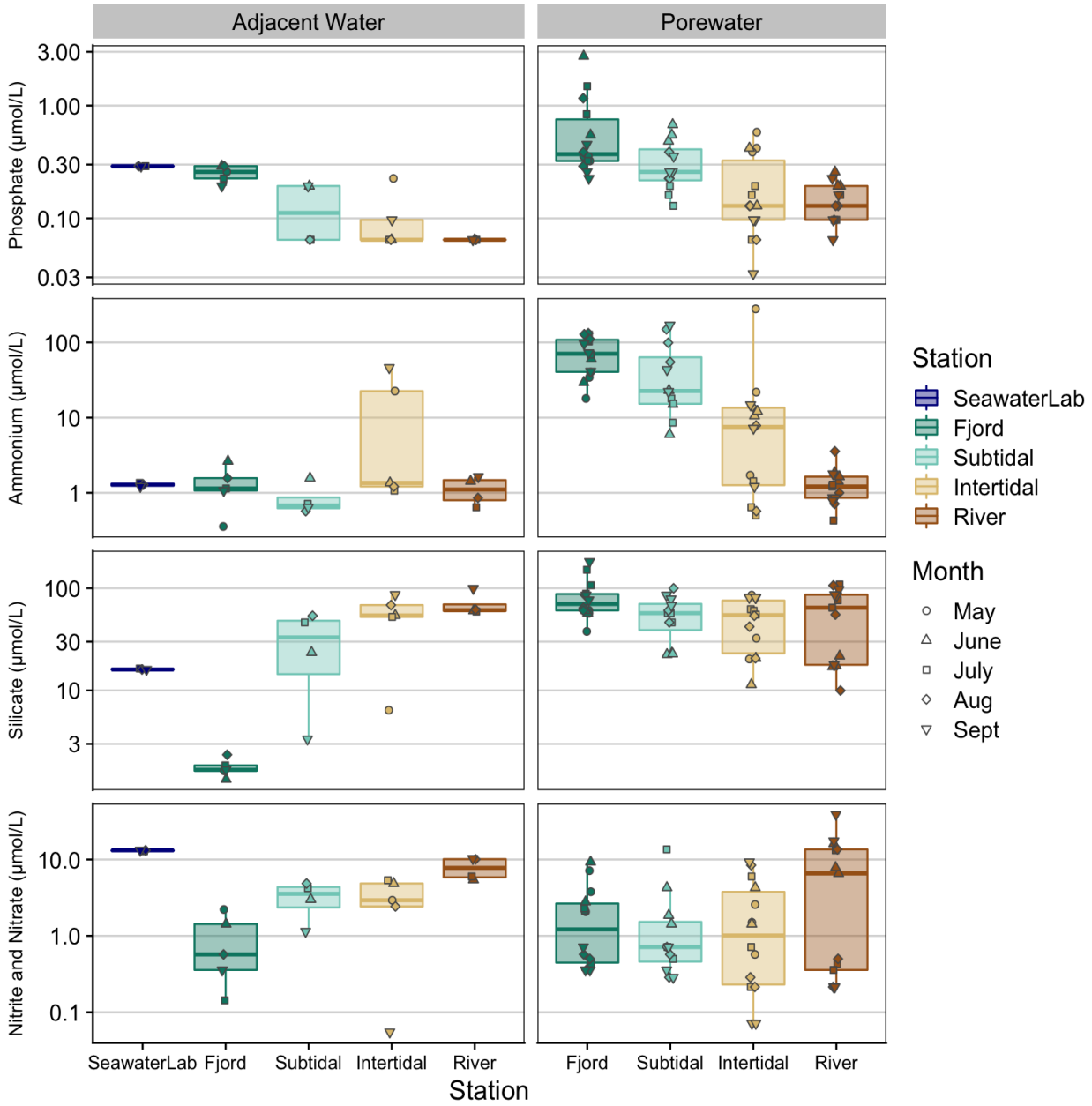

Figure A3. Boxplots showing inorganic nutrient concentrations from **(A)** adjacent water samples and **(B)** porewater samples. Points represent individual samples, with shape showing the month. Phosphate, ammonium, silicate, and nitrate are all shown in µmol/L, on log-scaled y-axes. Seawater Lab water was used in sediments suspensions for EcoPlates.

Table A4. Read counts for each sample following processing steps. Bolded samples were removed from downstream analyses due to low read counts. In *Sample*, F denotes fjord, S subtidal, I intertidal, R river, and B extraction blanks.

Sample	*Input*	*Remove seq. w/ ambig. nucleo.*	*Primers clipped (remove w/ out primers)*	*Quality filter and truncate*	*Denoise Forward*	*Denoise Reverse*	*Merge*	*Remove chim.*	*Remove euk., chloro., mitochon.*	*Remove contam.*	*Remove singls.*
5-F-x	83030	66715	66274	55623	52007	53403	47059	45295	44290	44290	39429
5-F-y	67228	53873	53509	44647	41586	42688	37643	36242	35637	35637	32570
5-F-z	37625	30224	29966	24926	23339	23924	21574	20954	20086	20086	19133
5-I-x	**741**	**593**	**557**	**361**	**303**	**320**	**286**	**282**	**186**	**186**	**169**
5-I-y	26632	21362	21208	17553	16885	17081	16149	15973	13321	13321	12646
5-I-z	14527	11669	11562	9610	9124	9263	8677	8556	7743	7742	7457
6-S-x	37019	29626	29385	24711	23956	24197	23133	22866	22388	22385	21127
6-S-y	56548	45508	45188	38063	35437	36588	31371	30450	29325	29325	28373
6-S-z	59745	48117	47768	39803	37219	38173	33166	32291	31508	31508	30523
6-F-x	54020	43954	43585	35233	33767	34510	30548	28008	26861	26861	26517
6-F-y	79069	63551	63173	53251	51434	52299	47497	43401	40735	40735	40079
6-F-z	63531	50920	50593	42489	41496	42105	39541	37321	34762	34762	34299
6-R-x	71950	57727	57317	47284	44369	45179	39215	37917	37194	37194	34010
6-R-y	52779	42509	42188	34921	32644	33189	28784	27787	26922	26916	25509
6-R-z	48705	39266	38975	32429	30102	30652	26314	25405	24658	24657	23560
6-I-x	16130	12953	12838	10444	9880	9991	9169	8981	8820	8820	8476
6-I-y	22503	18149	17996	14928	13878	14166	12771	12494	12370	12370	11813
6-I-z	45397	36467	36183	30026	28158	28724	25760	25133	24824	24824	22786
7-S-x	24517	19652	19480	16306	15506	15764	14497	14205	13806	13806	13528
7-S-y	30145	24295	24079	20080	19258	19509	18173	17825	17372	17372	17059
7-S-z	**1965**	**1528**	**1478**	**1173**	**1073**	**1099**	**1005**	**988**	**972**	**971**	**925**
7-F-x	77070	62042	61583	52108	49137	50790	42753	40972	40277	40277	38715
7-F-y	89484	71972	71440	60522	57979	59418	51795	47415	44957	44957	44043
7-F-z	54998	44374	44000	36790	34899	35818	30910	29246	28389	28385	27792
7-R-x	31109	24899	24681	20324	19088	19415	17116	16549	15994	15994	15466
7-R-y	39173	31382	31153	25381	23650	24173	21078	20420	19339	19339	18392
7-R-z	40384	32494	32235	26396	25028	25272	22319	21727	21490	21490	20126
7-I-x	45355	36305	36042	29284	28224	28551	26383	25821	25007	25007	24303
7-I-y	24615	19633	19450	15831	15235	15359	14188	13948	13418	13417	13113
7-I-z	8197	6584	6508	5268	4925	5009	4492	4387	4256	4256	4130
8-S-x	51215	41017	40612	33739	32076	32783	29322	28422	28215	28214	27698
8-S-y	52303	42039	41722	34292	32699	33441	29987	29233	28818	28818	28238
8-S-z	67490	54239	53817	44864	42485	43426	39179	38207	37832	37831	36592
8-F-x	44897	36258	35934	30176	28602	29289	26106	25420	25200	25196	24619
8-F-y	75978	61215	60788	51475	49023	50019	44186	42931	42470	42470	41428
8-F-z	46483	37338	37074	31167	29832	30356	27844	27205	26941	26941	26508
8-R-x	31608	25400	25159	20804	19681	19911	17882	17411	16958	16958	16234
8-R-y	26187	21076	20853	16888	15919	16217	14340	13955	13681	13679	13257
8-R-z	18365	14865	14685	12183	11517	11677	10627	10282	9727	9727	9354
8-I-x	22185	17874	17715	14519	13830	14031	12850	12598	12180	12180	11880
8-I-y	30719	24631	24412	20317	19250	19582	17870	17378	15807	15807	15295
8-I-z	41241	33191	32844	26999	25669	26031	23892	23372	20732	20732	19404
9-S-x	43457	34838	34544	28873	27828	28256	26244	25618	25488	25488	25052
9-S-y	47028	37957	37636	31702	30417	30931	28184	27460	27311	27311	26927
9-S-z	44378	35567	35265	29565	28068	28702	25737	25167	24655	24655	24068
9-F-x	43882	35334	35063	29398	27586	28507	24094	23200	22756	22756	22311
9-F-y	30259	24293	24074	20077	18885	19465	16762	16268	16037	16037	15668
9-F-z	44694	35868	35560	29857	28265	28993	25499	24656	24361	24361	23690
9-R-x	27339	21904	21717	17914	17102	17368	15800	15388	14905	14905	14478
9-R-y	20397	16375	16212	13251	12628	12806	11673	11356	10953	10953	10650
9-R-z	33456	26837	26594	21862	21026	21203	19476	19005	18478	18478	18089
9-I-x	42417	33790	33499	27776	26829	27110	25249	24722	23350	23350	22791
9-I-y	44573	35838	35569	29699	28484	28890	26389	25748	24406	24406	23756
9-I-z	51106	40837	40482	34050	32790	33244	30817	30195	27054	27054	26079
B-1	202	145	122	34	16	7	6	6	6	NA	NA
B-2	119	93	78	16	4	3	1	1	1	NA	NA
B-3	89	62	52	17	4	3	3	3	3	NA	NA
B-4	132	107	92	36	19	20	18	18	18	NA	NA
B-5	4818	3919	3873	3157	2236	2545	1225	1225	1225	NA	NA

Table A5. KO genes or enzymes related to KEGG reactions or pathways of interest, as defined by the KEGG database, used to investigate targeted functions.

Metabolic Function	Kegg Orthologs
Denitrification	K00370, K00371, K00374, K02567, K02568, K00368, K15864, K04561, K02305, K00376
Nitrification	K10944, K10945, K10946, K10535
Nitrogen Fixation	K02588, K02586, K02591, K00531, K22896, K22897, K22898, K22899
Phosphate utilization (organic)	K01514, K01524
Sulfate reduction (dissimilatory and assimilatory)	K00958, K00394, K00395, K11180, K11181, K13811, K00958, K00860, K00955, K00957, K00956, K00957, K00860, K00390, K00380, K00381, K00392
Iron oxidation	K03594, K13624, K14735, K19054, K22336, K22552

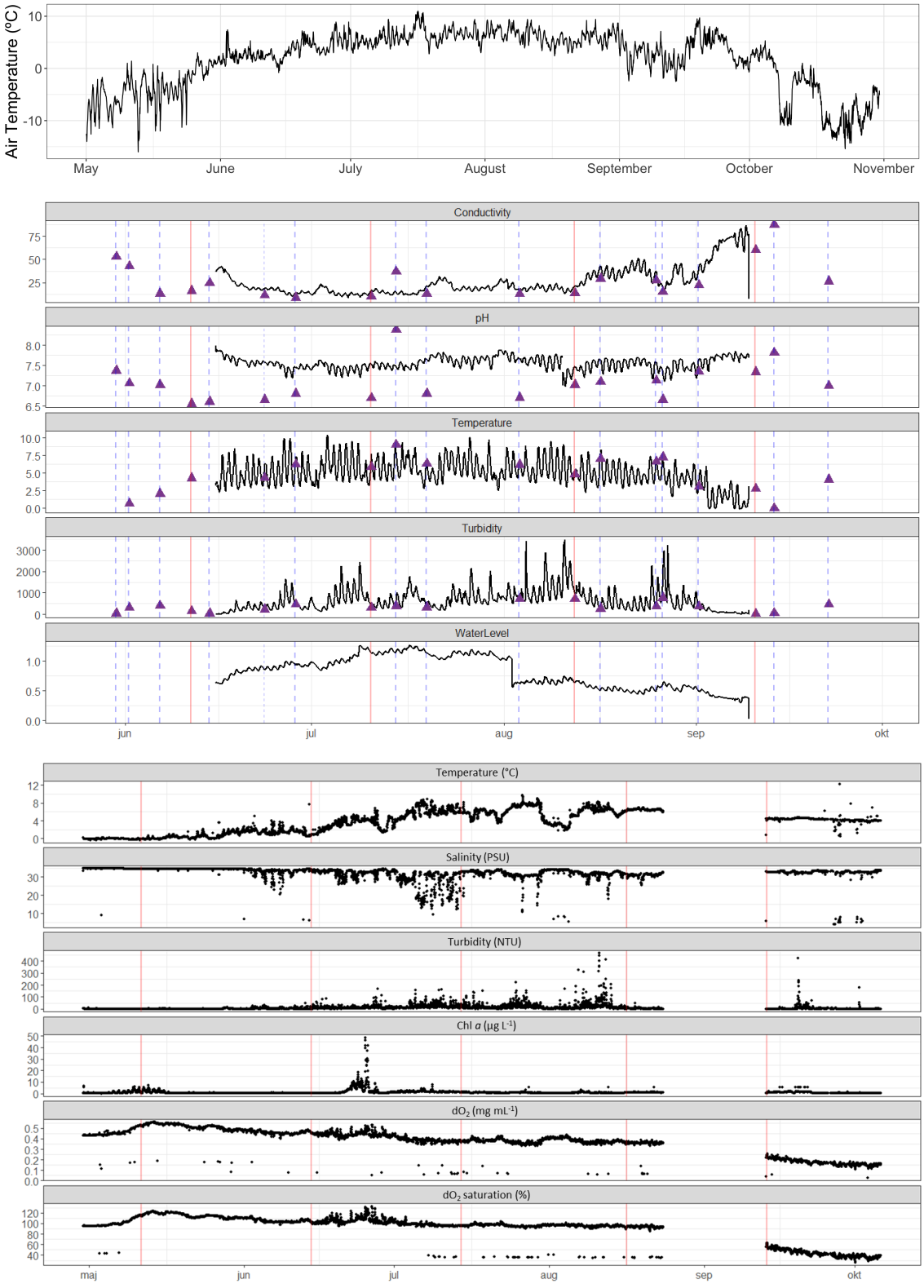

Figure A4. (A) Hourly air temperature from May through October in Adventdalen (station SN99870) retrieved from the Norwegian Meteorological Institute (MET Norway). **(B)** Sensor data from the NIVA operated mooring in Adventelva (A. Poste/NIVA, unpublished data). Solid red lines show dates of main sampling campaigns in the river and intertidal while dashed blue lines show dates of higher frequency monitoring. Purple triangles are values measured with hand-held sensors (Andersen in press). **(C)** Sensor data from the NIVA operated bouy in Adventfjord (A. Poste/NIVA, unpublished data). Solid red lines show dates of main sampling campaigns in the fjord. Missing data is due to electronic failures.

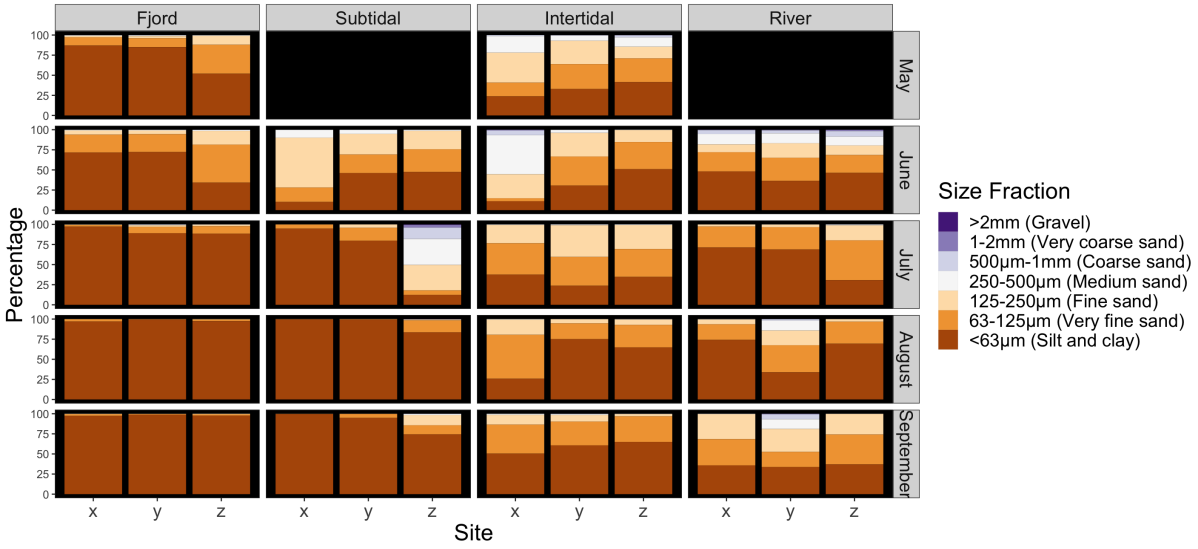

Figure A5. Distribution of grain size fractions in each sample, as determined through wet sieving. Each bar shows the distribution of a single sediment sample.

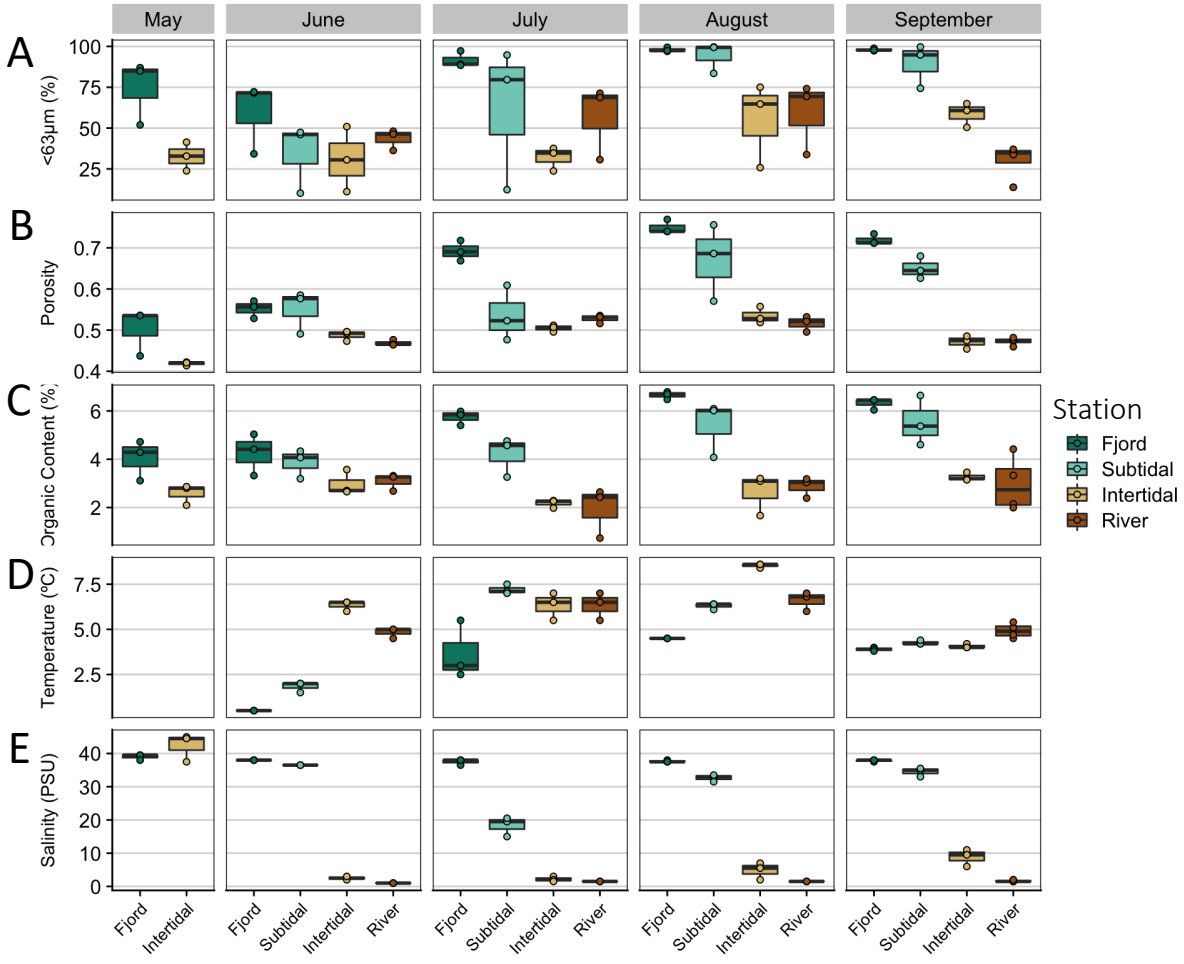

Figure A6. Boxplots displaying environmental variables for each sediment sampling site, grouped by station and month. **(A)** Percent by mass of the sediment less than 63µm. **(B)** Porosity of the sediment (water content by volume). **(C)** Organic matter content of sediments as determine by LOI. **(D)** Sediment temperature, not recorded in May. **(E)** Salinity of the porewater.

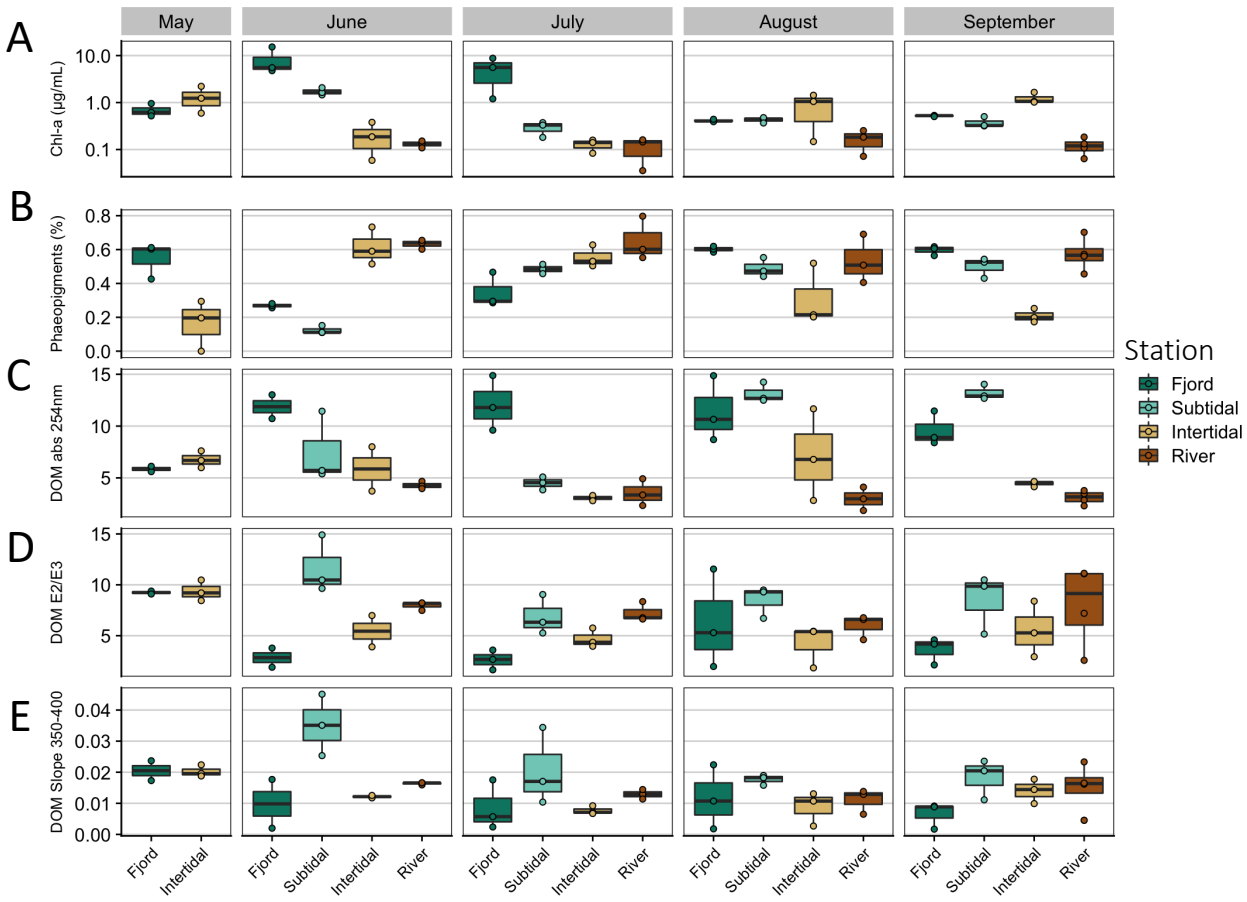

Figure A7. Boxplots displaying indicators of organic matter quality for each sediment sampling site, grouped by station and month. Colors show stations. **(A)** Chl-*a* concentration. The y-axis is log-scaled for increased resolution. **(B)** Percentage of phaeopigments out of total sediment pigments. **(C)** cDOM absorbance coefficient at 245 nm. **(D)** cDOM E2/E3 ratio. **(E)** cDOM spectral slope from 350 to 400 nm.

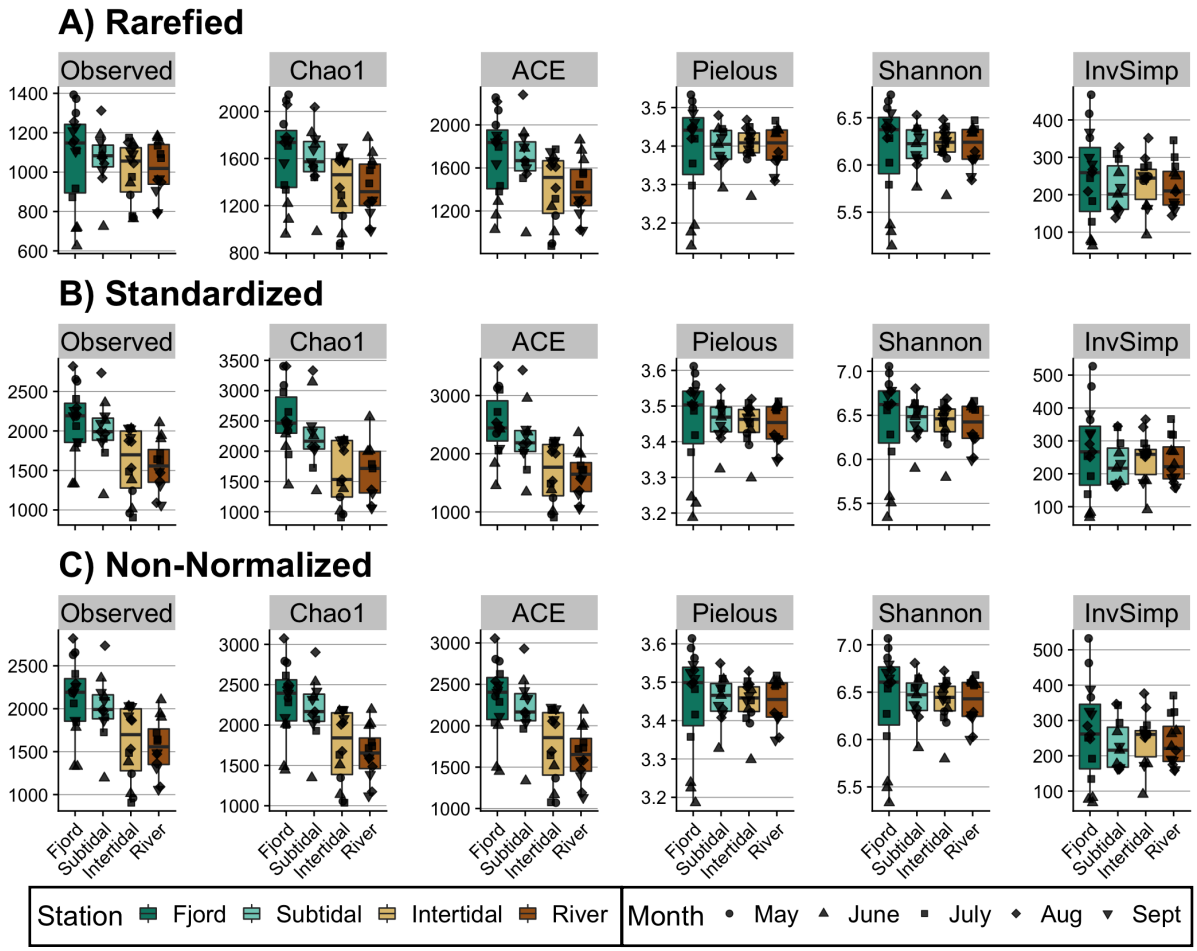

Figure A8. Boxplots displaying alpha diversity metrics for all samples from each station using **(A)** the rarefied community dataset, **(B)** the standardized community dataset, and **(C)** the non-normalized community dataset. Points represent individual samples, and their shape displays month.

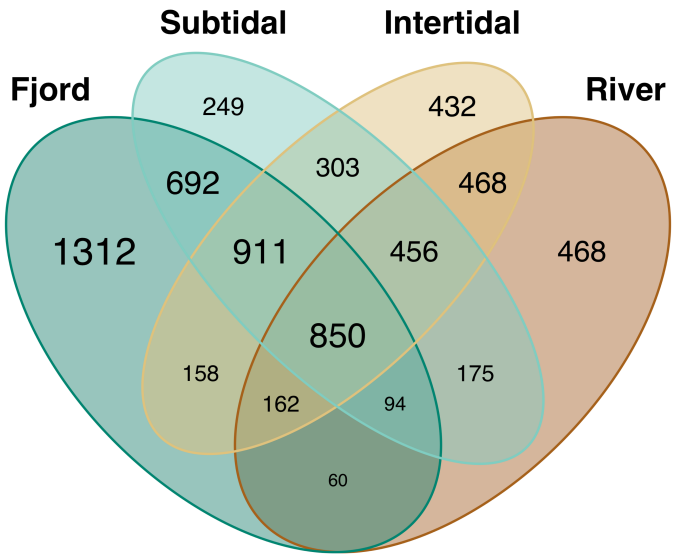

Figure A9. Venn Diagram displaying shared and unique ASVs from each station across all sampling months as evaluated on the rarefied dataset to remove artefacts of differential read counts for samples.

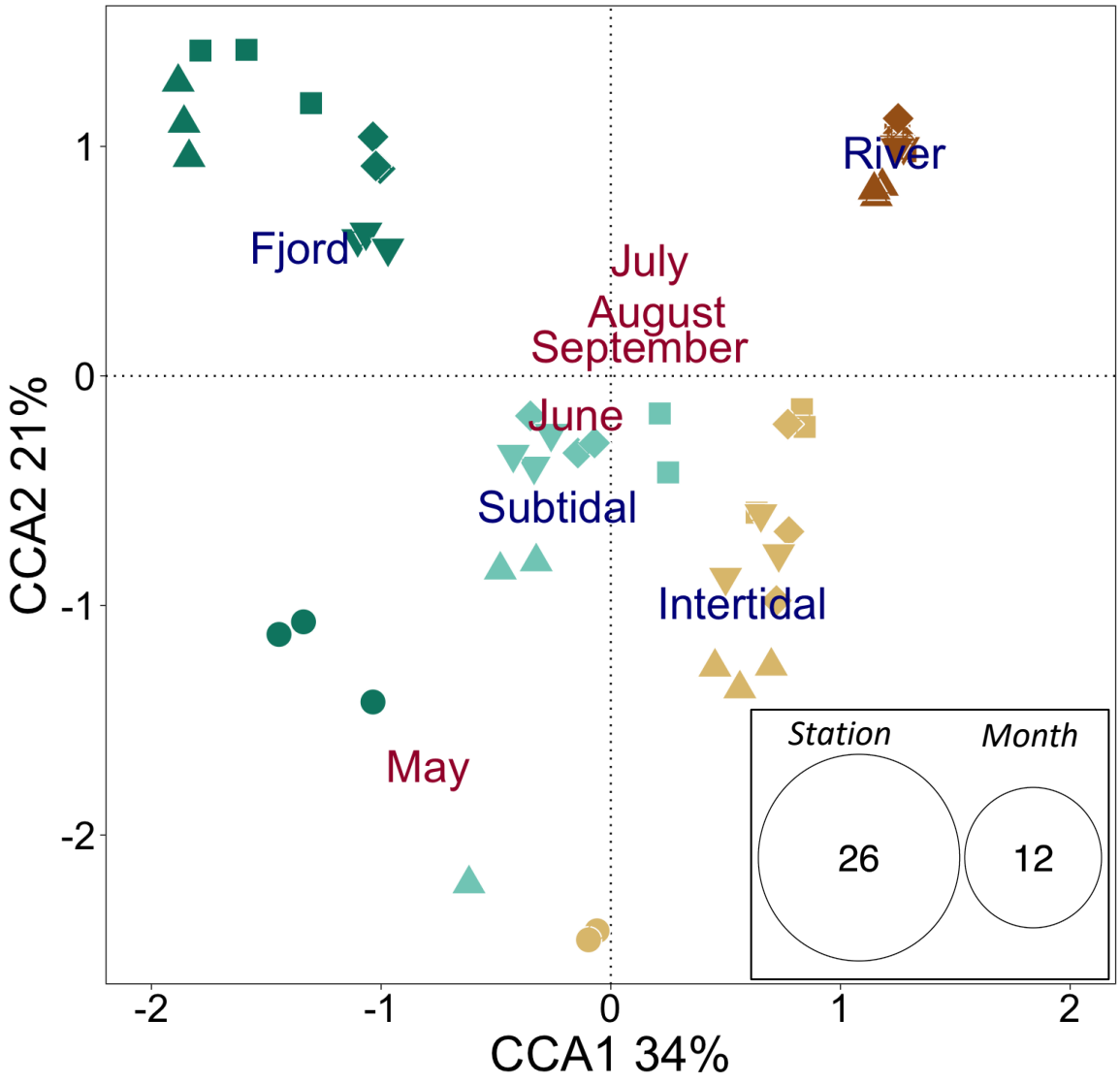

Figure A10. CCA with community composition constrained by station and month. Community composition was transformed to proportions before ordination. Centroids of each factor are displayed, months in red and stations in blue. Together, station and month explained 44% of the variation in community composition. **(Inset)** Variance partitioning on the model showed that station explained 26% of the variation in community composition and month explained 12%, with no overlap between the two.

Table A6. Results of Dunn's post-hoc test comparing sediment characteristics between clusters. Adjusted *p*-values (Benjamini-Hochberg 1995) less than 0.025 are in bold.

		>250µm (%)		125-250µm (%)		63-125µm (%)		<63µm (%)		Porosity		Organic (%)	
Group1	Group2	Z	*p*	Z	*p*	Z	*p*	Z	*p*	Z	*p*	Z	*p*
Intertidal	Late-Marine	2.45	**0.02**	4.08	**0.00**	4.65	**0.00**	-4.37	**0.00**	-4.35	**0.00**	-4.58	**0.00**
Intertidal	Post-Bloom	-0.20	0.42	1.70	0.09	1.64	0.10	-1.78	0.07	-2.50	**0.01**	-2.73	**0.01**
Late-Marine	Post-Bloom	-2.12	0.04	-1.55	0.09	-2.06	0.05	1.69	0.08	0.98	0.23	0.95	0.19
Intertidal	Pre-Melt	-1.90	0.06	-0.23	0.45	0.91	0.26	-0.09	0.46	-0.02	0.49	-0.99	0.20
Late-Marine	Pre-Melt	-3.95	**0.00**	-3.75	**0.00**	-3.12	**0.00**	3.67	**0.00**	3.73	**0.00**	2.99	**0.00**
Post-Bloom	Pre-Melt	-1.37	0.14	-1.73	0.10	-0.73	0.29	1.54	0.09	2.25	**0.02**	1.65	0.08
Intertidal	River	-0.89	0.23	0.07	0.47	0.29	0.39	0.19	0.47	0.46	0.40	0.60	0.27
Late-Marine	River	-3.22	**0.00**	-3.87	**0.00**	-4.20	**0.00**	4.39	**0.00**	4.63	**0.00**	5.00	**0.00**
Post-Bloom	River	-0.51	0.34	-1.61	0.09	-1.37	0.14	1.89	0.07	2.80	**0.01**	3.13	**0.00**
Pre-Melt	River	1.07	0.20	0.29	0.48	-0.64	0.29	0.25	0.50	0.42	0.38	1.48	0.10

Table A7. Results of Dunn's post-hoc test comparing porewater chemistry between clusters. Adjusted *p*-values (Benjamini-Hochberg 1995) less than 0.025 are in bold.

		Salinity (PSU)		PO4 (µmol/L)		NH4 (µmol/L)		SiO2 (µmol/L)		NO3/NO2 (µmol/L)	
Group1	Group2	Z	*p*	Z	*p*	Z	*p*	Z	*p*	Z	*p*
Intertidal	Late-Marine	-2.78	**0.00**	-3.31	**0.00**	-4.27	**0.00**	-2.44	0.04	0.82	0.30
Intertidal	Post-Bloom	-3.28	**0.00**	-4.09	**0.00**	-3.01	**0.00**	-2.23	0.03	-1.44	0.15
Late-Marine	Post-Bloom	-1.01	0.19	-1.55	0.09	0.24	0.41	-0.37	0.39	-2.04	0.10
Intertidal	Pre-Melt	-3.50	**0.00**	-3.97	**0.00**	-2.25	**0.02**	0.35	0.36	-1.65	0.12
Late-Marine	Pre-Melt	-1.00	0.18	-1.01	0.19	1.53	0.09	2.48	0.06	-2.34	0.10
Post-Bloom	Pre-Melt	0.09	0.46	0.64	0.29	1.00	0.18	2.34	0.03	0.03	0.49
Intertidal	River	2.08	0.03	-0.18	0.43	1.06	0.18	-0.54	0.37	-1.05	0.25
Late-Marine	River	4.68	**0.00**	3.06	**0.00**	5.22	**0.00**	1.86	0.06	-1.83	0.11
Post-Bloom	River	4.83	**0.00**	3.90	**0.00**	3.77	**0.00**	1.80	0.06	0.64	0.29
Pre-Melt	River	5.19	**0.00**	3.75	**0.00**	3.14	**0.00**	-0.82	0.30	0.70	0.30

Table A8. Results of Dunn's post-hoc test comparing indicators of organic matter between clusters. Adjusted *p*-values (Benjamini-Hochberg 1995) less than 0.025 are in bold.

		Chl-a (µg/L)		Phaeo (%)		a254 nm		E2/E3		Slope 350-400	
Group1	Group2	Z	*p*	Z	*p*	Z	*p*	Z	*p*	Z	*p*
Intertidal	Late-Marine	-0.64	0.26	-1.64	0.08	-3.95	**0.00**	-1.44	0.08	-0.86	0.24
Intertidal	Post-Bloom	-3.40	**0.00**	1.23	0.14	-3.11	**0.00**	1.61	0.08	0.34	0.37
Late-Marine	Post-Bloom	-2.82	**0.01**	2.49	**0.02**	-0.11	0.46	2.68	**0.01**	0.98	0.23
Intertidal	Pre-Melt	-2.57	**0.01**	1.29	0.14	-1.48	0.09	-3.55	**0.00**	-3.57	**0.00**
Late-Marine	Pre-Melt	-1.95	0.03	2.67	**0.01**	1.87	0.05	-2.29	**0.02**	-2.80	**0.01**
Post-Bloom	Pre-Melt	0.96	0.19	-0.05	0.48	1.62	0.08	-4.29	**0.00**	-3.16	**0.00**
Intertidal	River	2.29	**0.02**	-2.22	0.03	1.23	0.12	-2.35	0.02	-1.22	0.18
Late-Marine	River	2.82	**0.00**	-0.57	0.32	5.09	**0.00**	-0.90	0.18	-0.36	0.40
Post-Bloom	River	5.11	**0.00**	-2.95	**0.01**	4.01	**0.00**	-3.37	**0.00**	-1.25	0.21
Pre-Melt	River	4.47	**0.00**	-3.17	**0.01**	2.49	**0.01**	1.51	0.08	2.49	**0.02**

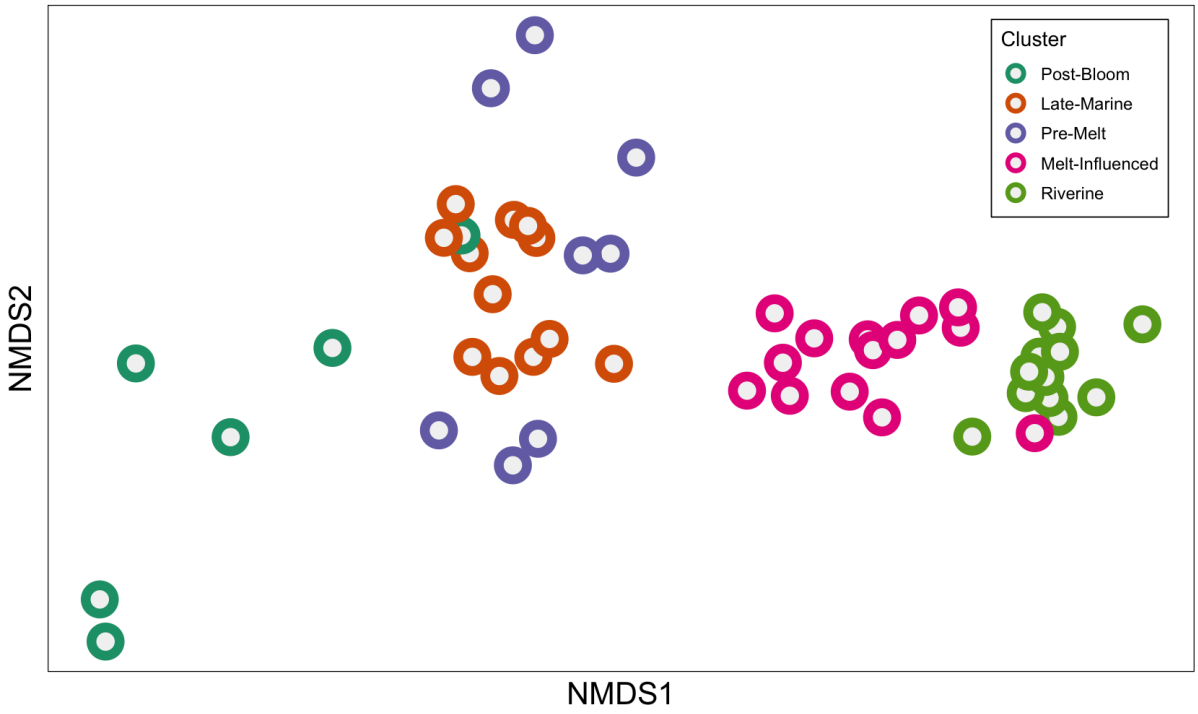

Figure A11. Non-metric multidimensional scaling (NMDS) ordinations using Bray-Curtis dissimilarities of community functional potential based on KEGG metabolic pathways predicted with Tax4Fun (stress = 0.05). Colors show clusters, as defined from hierarchical clustering analysis (see Figure 7A).

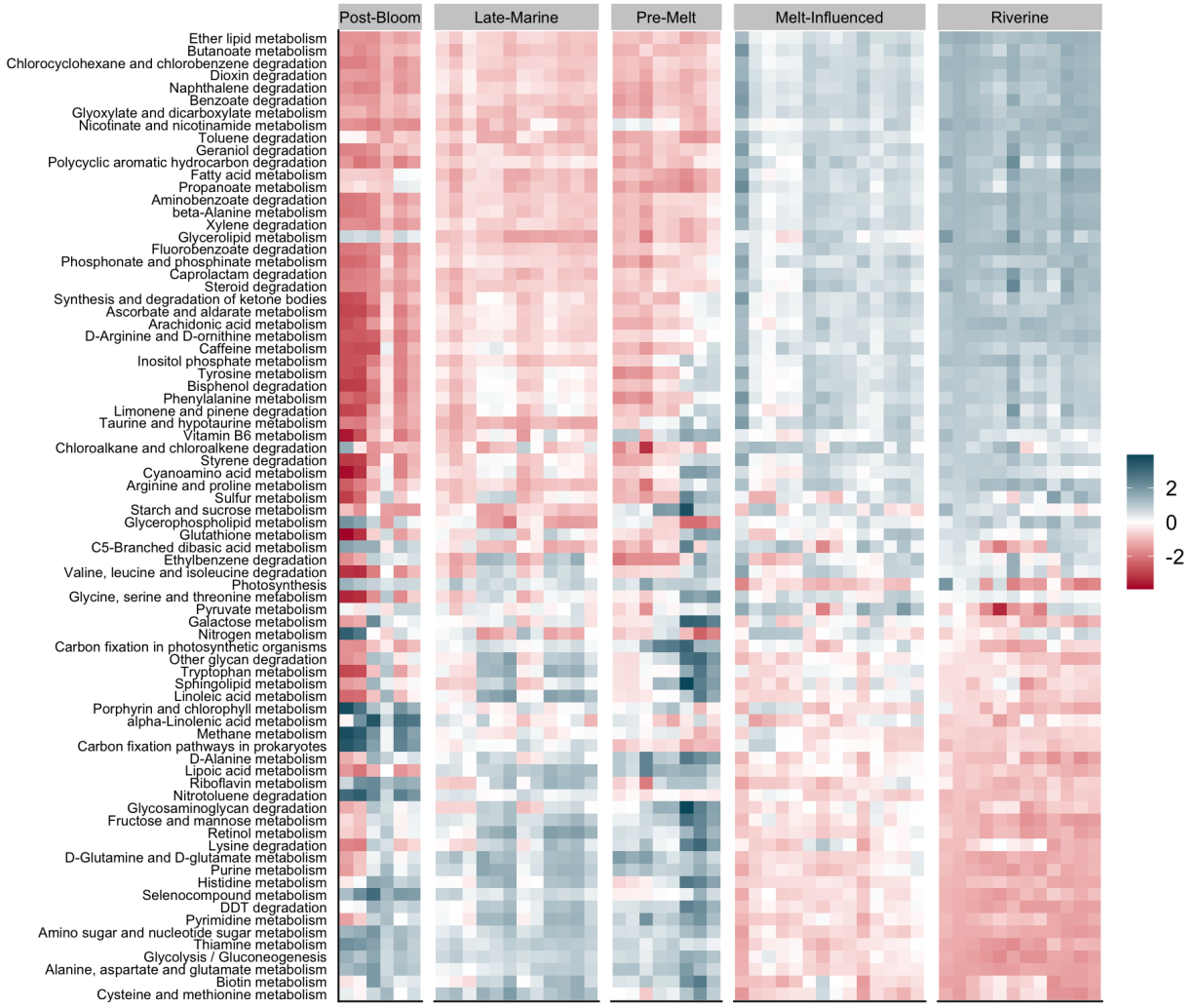

Figure A12. Heatmap displaying differential abundances of metabolic and degradation potential functional capacities predicted with Tax4Fun as based on taxonomic assignment. Potential functions were z-scaled for comparison across samples, and samples are grouped by cluster. Blue indicates a relatively high abundance while red indicates a relatively low abundance.

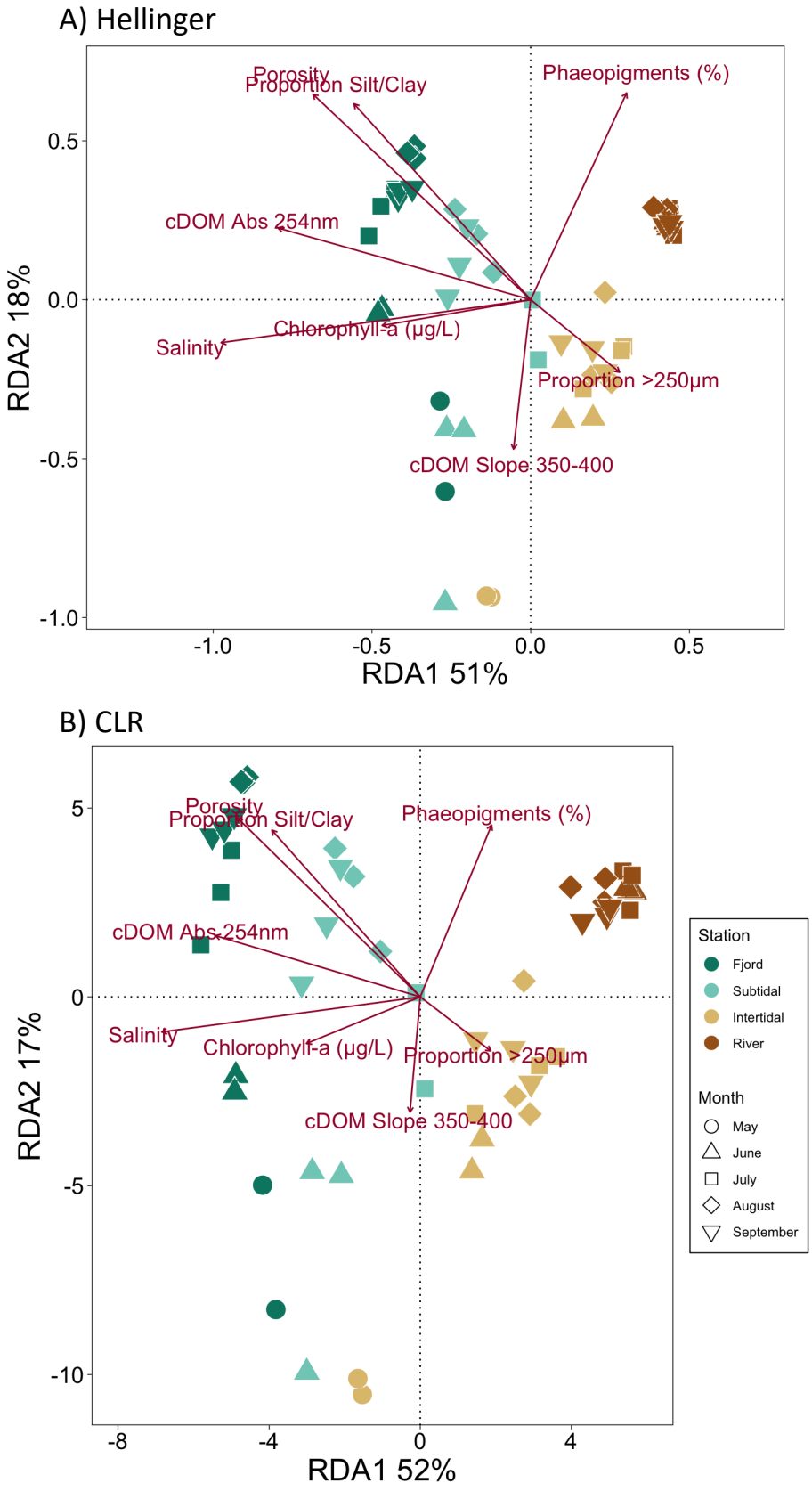

Figure A13. Redundancy analyses (RDA) on community composition and environmental variables. Community composition was **(A)** Hellinger-transformed and **(B)** centered-log-ratio (CLR) transformed prior to ordination. Environmental variables were z-scaled. The same legend applies to both figures.

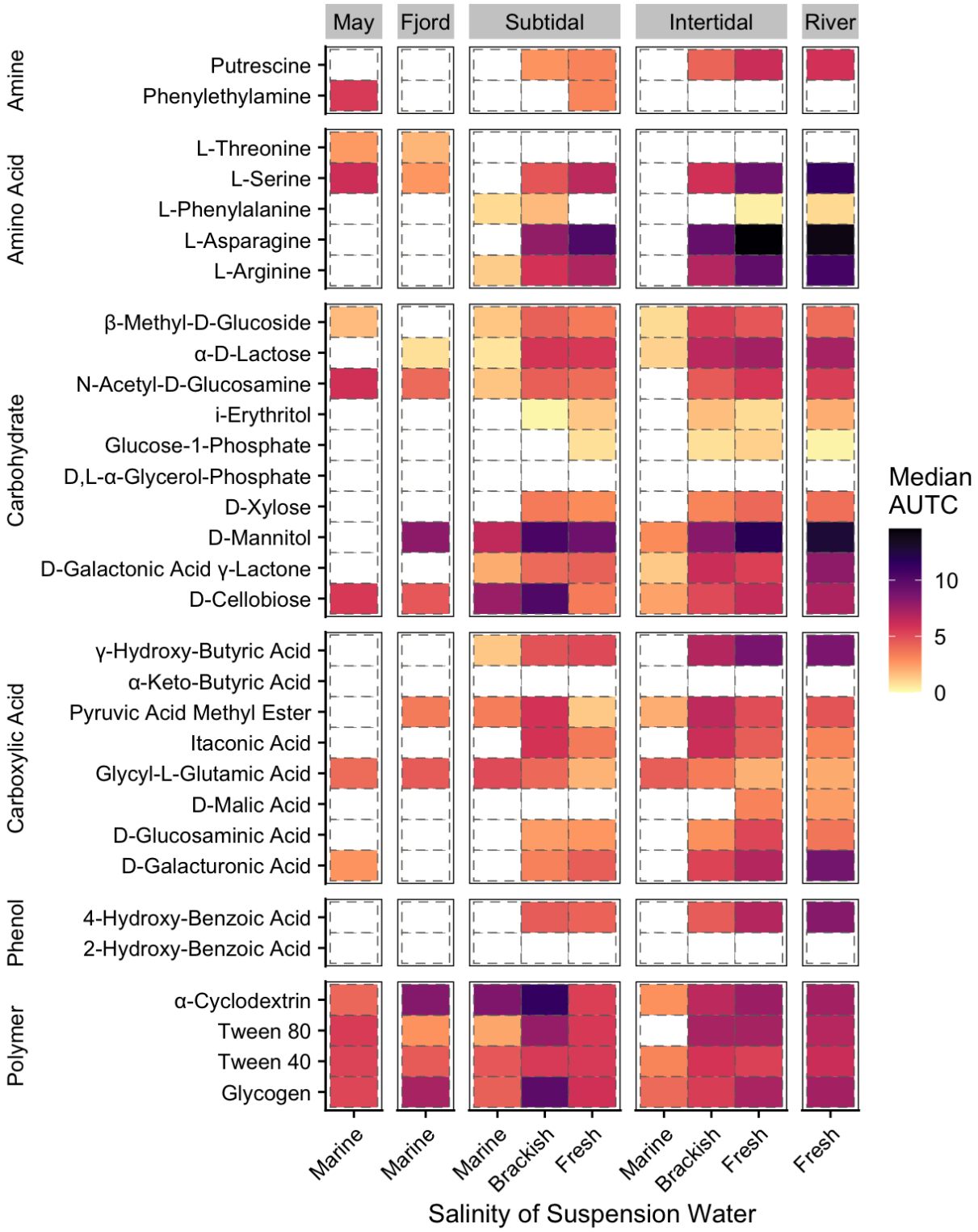

Figure A14. Heatmap displaying median area under the curve (AUTC) for each substrate on Biolog EcoPlates, with plates grouped by station and salinity of suspension water (n=4). *May* presents results from only one plate with fjord sediments suspended in deep fjord water and incubated at 4ºC for comparison. Substrates are grouped by molecular guild, according to Sala et al. (2010). Dark purple to black indicates rapid and high uptake of a substrate while light yellow indicates slower and lower uptake. Substrates that were not utilized are displayed in white.

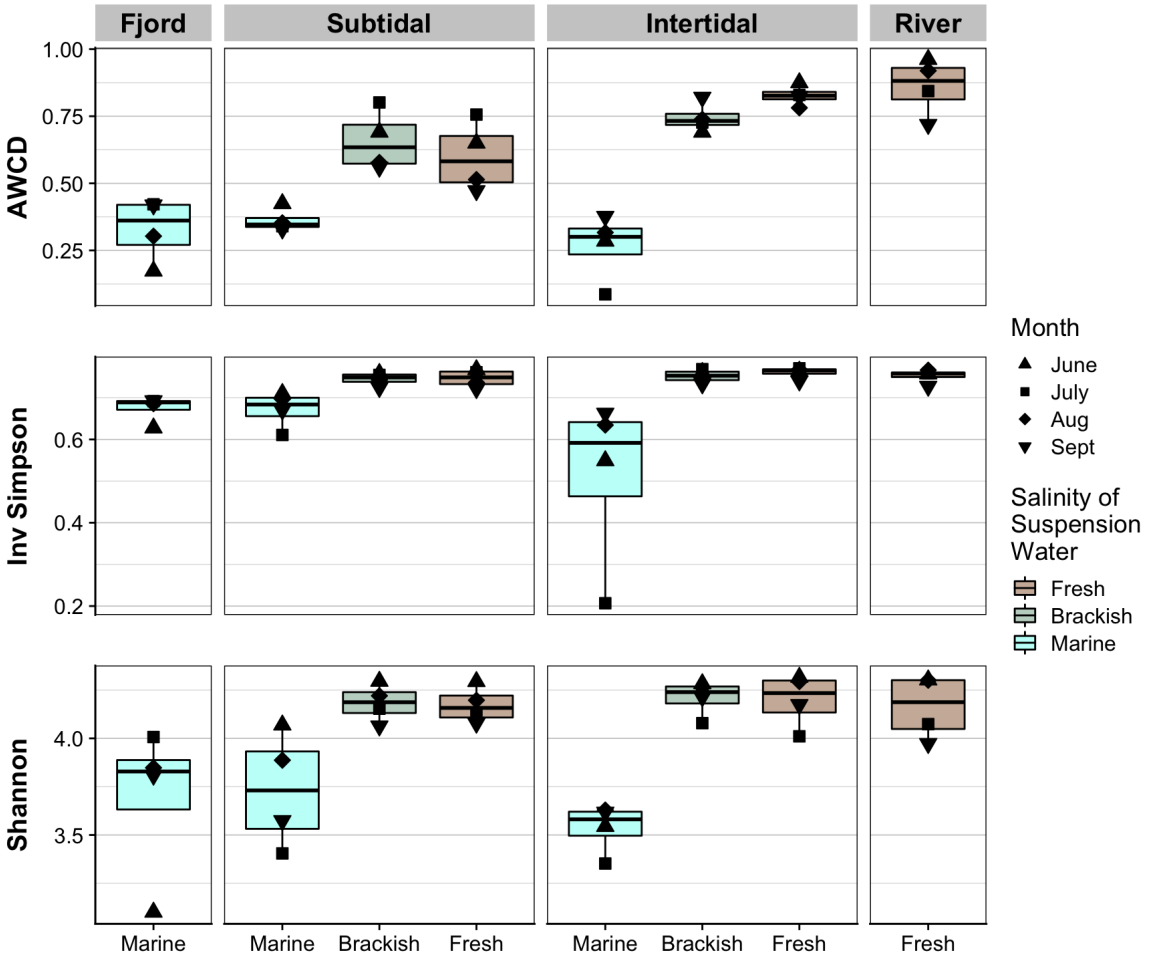

Figure A15. Boxplot showing **(A)** average well color development (AWCD), **(B)** Inverse Simpson's diversity index, and **(C)** Shannon's diversity index from Biolog EcoPlates. Plates are grouped by sediment sampling location and type of water used for sediment suspensions. Black points represent single plates, with shape depicting the sampling month.

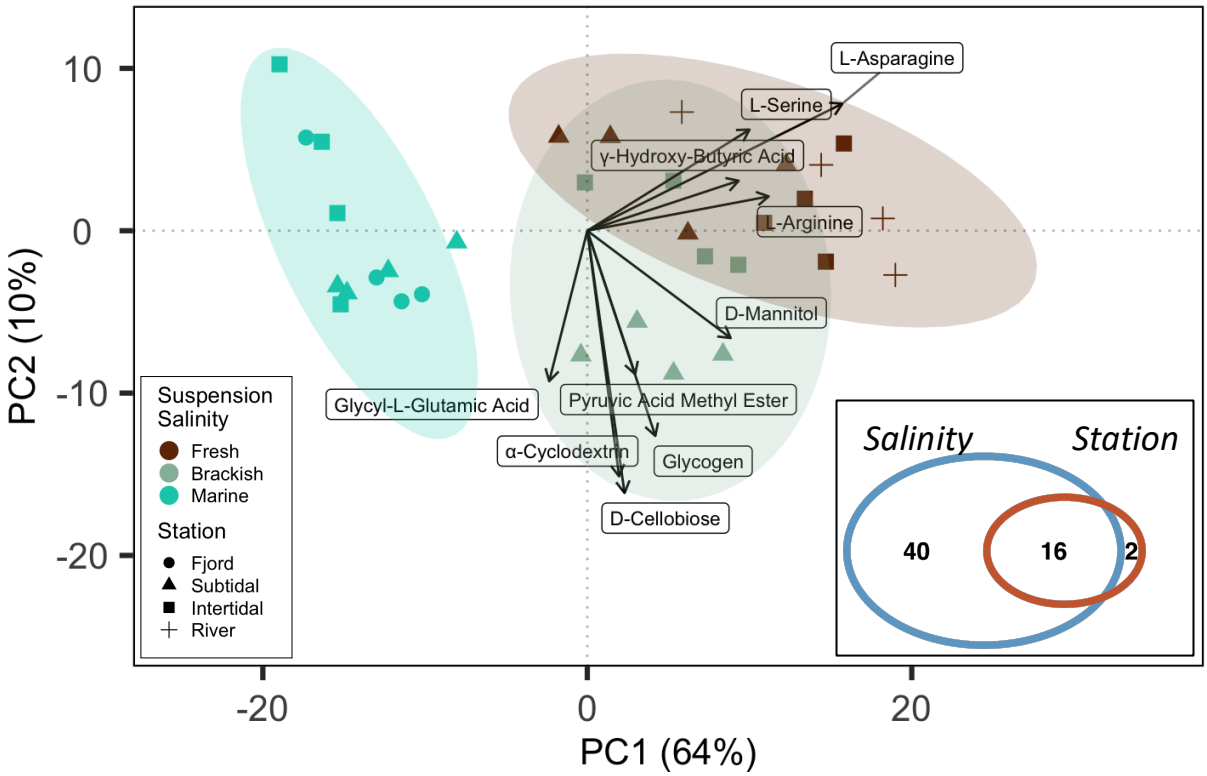

Figure A16. Principal component analysis (PCA) using area under the curve (AUTC) for each substrate on each Biolog EcoPlate. Individual points are plates, colored by salinity treatment with shape showing sampling station. Brackish suspensions were only used for tidal flat sediments (intertidal and subtidal stations). **(Inset)** Variance partitioning on the model showed that individually salinity explained 40% of the variation in community level physiological profile and sampling station explained 2%, with 16% of the variation explained by both.